

Quantification of Supramolecular Complexes Involving Charged Species in Non-Aqueous Solvents: Theory and Application

Jason William Jones

Dissertation submitted to the Faculty of the Virginia Polytechnic Institute
and State University in partial fulfillment of the requirements for the degree of

*Doctor of Philosophy
in
Chemistry*

Dr. Harry W. Gibson, Chair

Dr. Alan R. Esker

Dr. Timothy E. Long

Dr. Herve Marand

Dr. James E. McGrath

On May 13, 2004

Blacksburg, VA

Keywords: supramolecular chemistry, equilibrium constants, ion pairing, secondary ammonium, pseudorotaxane, pseudocryptand

Copyright 2004, Jason W. Jones

Quantification of Supramolecular Complexes Involving Charged Species in Non-Aqueous Solvents: Theory and Application

Jason William Jones

Professor Harry W. Gibson, Committee Chair
Department of Chemistry
Virginia Polytechnic Institute and State University
Blacksburg, VA 24061-0212

(ABSTRACT)

We report for the first time a broad equilibrium model describing the complexation of ionic species in non-aqueous media that explicitly includes ion pairing for one of the components and that relies upon activities rather than molar concentrations. This model directly contradicts existing commonplace equilibrium treatments, which were shown to be incomplete, often invalid, and misleading. Experimental validation of our model was achieved through studies of pseudorotaxane formation between dibenzylammonium salts (DBAm-X) and dibenzo-24-crown-8 (DB24C8) in $\text{CDCl}_3:\text{CD}_3\text{CN}$ (3:2). In that particular case, we showed that fluctuations in the apparent $K_{a,\text{exp}}$ values as usually reported are attributable to ion pairing, with a dissociation constant K_{ipd} , and that the constant K_{assoc} for pseudorotaxane complexation is independent of the counterion, a result of the complex existing in solution as a free cation. In accord with this model, we further described a straightforward and simple method to increase the extent of complexation by using either a ditopic cation and anion host, or adding to the charged host/guest solution a molecularly separate host capable of complexing the dissociated counterion. Also in accord with this model, we investigated the influence of the solvent's dielectric constant on K_{ipd} and K_{assoc} . On the basis of competing condensation reactions between amines and ketones which were shown to occur within the timescale of host/guest recognition, we also challenged the commonly employed use of acetone in similar complexation studies involving 2° ammonium ions.

Because a major goal of this work was to ultimately increase binding efficiency and selectivity, we explored new methods to drive complexation in related pseudorotaxane systems. We noted that addition of di- or tri-topic hydrogen bond

accepting anions to solutions of bis(5-hydroxymethyl-1,3-phenylene)-32-crown-10 or bis(5-carboxy-1,3-phenylene)-32-crown-10 and paraquat di(hexafluorophosphate) served to significantly enhance host/guest interaction. The addition of $\text{Et}_4\text{N}^+\text{TFA}^-$ to an acetone solution of diacid crown and paraquat 2PF_6 effectively boosted $K_{a,\text{exp}}$ 40-fold, as estimated by ^1H NMR studies. Similar increases in the apparent $K_{a,\text{exp}}$ were observed upon the addition of $n\text{-Bu}_4\text{N}^+\text{OTs}^-$. Evidenced by crystal structures, the increase in association resulted from chelation of the OH moieties of the crown by the di- or tri-topic anions, forming supramolecular bicyclic macrocycles (pseudocryptands) and stabilizing the complex in a cooperative manner. Significantly, $K_{a,\text{exp}}$ of one of the pseudocryptands was shown to equal that determined in the corresponding cryptand complex.

Table of Contents

I	Supramolecular Interactions in Non-Aqueous Solvents: Historical Perspectives	
I.1	Introduction.....	1
I.2	Threading Influences on Supramolecular Chemistry	3
I.3	Improvement in Threading Efficiencies.....	5
I.4	Modern Pseudorotaxanes	10
I.5	Pseudorotaxanes and Material Applications.....	12
I.6	Quantifying Host/Guest Association Constants and Material Applications	14
I.7	References	16
II	Supramolecular Interactions in Non-Aqueous Solvents: Development of an Equilibrium Model	
II.1	Host/Guest Interactions.....	22
II.2	Ionic Strength Considerations in Host/Guest Complexes Involving Electrolyte Components in Non-Aqueous Solvents.....	25
II.3	Quantification of Host/Guest Complexes Involving a Singularly Charged Component in Non-Aqueous Solvents: Comprehensive Model...	32
II.4	Quantification of Host/Guest Complexes Involving a Singularly Charged Component in Non-Aqueous Solvents: A Pre-equilibrium Model.....	36
II.5	Conclusions and Modifications.....	41
II.6	References.....	42
III	Supramolecular Interactions in Non-Aqueous Solvents: Testing of an Equilibrium Model	
III.1	Quantification of Pseudorotaxane Complexation and Error Analysis.....	45
III.2	Probing Inconsistencies From the Literature.....	48

III.3	Piecing Together the Puzzle: Application of the Pre-Equilibrium Model to Pseudorotaxane 1•2-X	58
III.4	Determination of Activity Coefficients	61
III.5	Non-Linear Least-Squares Fit of the Pre-Equilibrium Model	64
III.6	Approximation of the Pre-Equilibrium Model	67
III.7	Comparison of Three Pre-Equilibrium Treatments.....	70
III.8	Utilization of the Model as a Predictive Tool.....	72
III.9	Comparisons Between Hosts for Any Given Guest.....	77
III.10	Acknowledgement of Assumptions Used to Derive K_{ipd} and K_{assoc}	78
III.11	Experimental.....	83
III.12	References.....	86
IV	Formation of Iminium Ions by Acetone Condensation with Secondary Ammonium Salts	
IV.1	Exploring Influence of Dielectric Constant on K_{ipd} and K_{assoc}	91
IV.2	Byproducts from 2° Ammonium Salts in Acetone.....	91
IV.3	Refocusing Our Efforts: Byproduct Identification.....	95
IV.4	Indirect Proof of Iminium Ion Formation.....	98
IV.5	Lessons From Acetone Studies.....	98
IV.6	Experimental.....	99
IV.7	References.....	100
V	Cooperative Host/Guest Interactions via Counterion Assisted Chelation: Pseudorotaxanes from Pseudocryptands	
V.1	Inclusion Efficiency and General Trends.....	102

V.2	Contributions to Improved Binding Efficiencies: Model Studies.....	105
V.3	Contributions to Improved Binding Efficiencies: Discovery of a Pseudocryptand.....	109
V.4	Versatility of Pseudocryptands and Comparison to Covalent Cryptands...	115
V.5	Experimental.....	119
V.6	References.....	120
VI	Conclusions and Areas of Future Work.....	122
AI	Preliminary Investigations into the Calculation of K_{ipd} For 2-X salts Based on NMR Spectroscopy	
AI.1	Justification for Independent Calculations.....	124
AI.2	Benesi-Hildebrand Analysis and Ion Pairing.....	124
AI.3	Basis for Analysis of Fast Exchanged Events.....	126
AI.4	Basis for Ion Pair Dissociation Constants.....	129
AI.5	Application to 2-TFA.....	130
AI.6	References.....	137

Table of Figures

I	Supramolecular Interactions in Non-Aqueous Solvents: Historical Perspectives	
Figure I-1	Cartoon representations of a pseudorotaxane and a rotaxane.....	3
Figure I-2	Complexation of <i>t</i> -butylamine by 2-carboxy-1,3-phenylene-19-crown-6	4
Figure I-3	Various conformations of 18-crown-6.....	7
Figure I-4	Molecular structures of 18-crown-6, valinomycin, and [2.2.2]cryptand.....	8
Figure I-5	Influence on association constants by donor atoms around 18-membered crown ether hosts upon complexation with <i>t</i> -butylammonium thiocyanate in MeOH.....	9
Figure I-6	Main- and side- chain polypseudorotaxane architectures.....	12
Figure I-7	Theoretical relationship between the degree of polymerization (log DP) versus log K_a for a system a) 1.0 M, solid line or b) 10 M, dotted line, in homoditopic monomer.....	15
II	Supramolecular Interactions in Non-Aqueous Solvents: Development of an Equilibrium Model	
Figure II-1	Two commonly encountered spectroscopic exchange rate regimes in supramolecular assembly formation: a) slow exchange, b) fast exchange.....	24
Figure II-2	Relative error in the spectroscopic determination of concentrations for single site binding studies as a function of percent binding.....	25
Figure II-3	^1H NMR spectra (400 MHz) of solutions of a) 2 -PF ₆ , b) a 1:1 mixture of 1 and 2 -PF ₆ (2 mM in each component initially), and c) 1 (3.82 mM initially) in CDCl ₃ :CD ₃ CN (3:2), 295 K.....	27
Figure II-4	$K_{a,\text{exp}}$ vs. [1], [2 -PF ₆] in CDCl ₃ :CD ₃ CN (3:2), 295 K.....	28
Figure II-5	Limiting Debye-Hückel slopes for three solvents at 298 K.....	29
Figure II-6	a) Percent dissociation versus $[\text{G}^+\text{X}^-]_0$ and b) $[\text{G}^+\text{X}^-]_0$ versus $[\text{G}^+]$ for three values of K_{ipd}	31

Figure II-7	$[G^+X^-]_0 / K_{ipd}$ versus $[G^+]$ for three values of K_{ipd}	31
III	Supramolecular Interactions In Non-Aqueous Solvents: Testing of An Equilibrium Model	
Figure III-1	1H NMR spectra (400 MHz) of a) 1 , b) 1 (0.657 mM initially) and $(n-Bu)_4N^+BF_4^-$ (0.627 mM initially), c) 1 (0.657 mM initially) and $(n-Bu)_4N^+BF_4^-$ (2.50 mM initially), d) 1 (0.657 mM initially) and $(n-Bu)_4N^+BF_4^-$ (6.20 mM initially), and e) $(n-Bu)_4N^+BF_4^-$ in $CDCl_3:CD_3CN$ (3:2), 295 K.....	49
Figure III-2	Influence of $Bu_4N^+PF_6^-$ on $K_{a,exp}$ when added at various concentrations to equimolar (1.67 mM initially) solutions of 1/2-PF₆ in $CDCl_3:CD_3CN$ (3:2), 295 K.....	50
Figure III-3	Influence of component concentration on $K_{a,exp}$ for equimolar solutions of 1 and 2-PF₆ in $CDCl_3:CD_3CN$ (3:2), 299 K.....	51
Figure III-4	1H NMR spectra (400 MHz) of solutions of 1 (3.82 mM initially) and 2-TFA [initially a) 20.0 mM, b) 15.4 mM, c) 7.71 mM, and d) 3.85 mM] in $CDCl_3:CD_3CN$ (3:2), 295 K.....	52
Figure III-5	1H NMR spectra (400 MHz) of equimolar solutions (4.00 mM initially) of 1 and a) 2-PF₆ , b) 2-BF₄ , c) 2-OTs , and d) 2-TFA in $CDCl_3:CD_3CN$ (3:2), 295 K.....	53
Figure III-6	Published crystal structures showing the charge separation between cation and anion centers for complexes with 1 and a) 2-PF₆ (7.808 Å), b) ammonium-PF ₆ (7.423 Å), c) bis(4-chlorobenzyl)ammonium-PF ₆ (7.866 Å), and d) bis(3-nitrobenzyl) ammonium-PF ₆ (8.246 Å).....	55
Figure III-7	Crystal packing diagrams of 2-TFA	57
Figure III-8	Crystal packing diagrams of 2-OTs	57
Figure III-9	Crystal packing diagrams of 2-CF₃SO₃	58
Figure III-10	Plots of Eq. 7m ($K_{assoc}[H] \gg 1$) for solutions of 1 and a) 2-PF₆ , b) 2-BF₄ , c) 2-OTs , and d) 2-TFA in $CDCl_3:CD_3CN$ (3:2), 295 K.....	60
Figure III-11	Plots of Eq. 7o ($K_{assoc}[H] \ll 1$) for solutions of 1 and a) 2-PF₆ , b) 2-BF₄ , c) 2-OTs , and d) 2-TFA in $CDCl_3:CD_3CN$ (3:2), 295 K.....	61

Figure III-12	γ_{\pm} as calculated according to Eq. 7m ($K_{\text{assoc}}[\text{H}] \gg 1$, top dotted curve) and Eq. 7o ($K_{\text{assoc}}[\text{H}] \ll 1$, bottom solid curve) vs. $[\text{G}^+\text{X}^-]_0$ for solutions of 1 and a) 2 -PF ₆ , b) 2 -BF ₄ , c) 2 -OTs, and d) 2 -TFA in CDCl ₃ :CD ₃ CN (3:2), 295 K.....	63
Figure III-13	$\{[\text{H}\cdot\text{G}^+]/[\text{G}^+\text{X}^-]^{1/2}\}^2$ versus $[\text{H}]$ for solutions of 1 and a) 2 -PF ₆ , b) 2 -BF ₄ , c) 2 -OTs, and d) 2 -TFA in CDCl ₃ :CD ₃ CN (3:2), 295 K.....	66
Figure III-14	$\{[\text{H}\cdot\text{G}^+]/[\text{G}^+\text{X}^-]^{1/2}\}^2$ versus $[\text{H}]$ for solutions of 1 and a) 2 -PF ₆ , b) 2 -BF ₄ , c) 2 -OTs, and d) 2 -TFA in CDCl ₃ :CD ₃ CN (3:2), 295 K, amended.....	67
Figure III-15	Plots of Eq. 9c for solutions of 1 and a) 2 -PF ₆ , b) 2 -BF ₄ , c) 2 -OTs, and d) 2 -TFA, $[\text{H}] \leq 3.00$ mM in CDCl ₃ :CD ₃ CN (3:2), 295 K.....	69
Figure III-16	Plots of $[\text{H}\cdot\text{G}^+]/[\text{G}^+\text{X}^-]^{1/2}$ calculated according to Eq. 7k versus $[\text{H}\cdot\text{G}^+]/[\text{G}^+\text{X}^-]^{1/2}$ as determined by experiment for solutions of 1/2 -PF ₆ , in CDCl ₃ :CD ₃ CN (3:2), 295 K.....	73
Figure III-17	Plots of $-\log \gamma_{\pm}$ versus $[\mathbf{1}\cdot\mathbf{2}^+]$ for solutions of 1 and a) 2 -PF ₆ , b) 2 -BF ₄ , c) 2 -OTs, and d) 2 -TFA in CDCl ₃ :CD ₃ CN (3:2), 295 K, $K_{\text{assoc}}[\text{H}] \gg 1$	74
Figure III-18	Plots of $-\log \gamma_{\pm}$ versus $[\mathbf{2}\text{-X}]_0$ for solutions of 1 and a) 2 -PF ₆ , b) 2 -BF ₄ , c) 2 -OTs, and d) 2 -TFA in CDCl ₃ :CD ₃ CN (3:2), 295 K, $K_{\text{assoc}}[\text{H}] \ll 1$	75
Figure III-19	Plots of Eq. 7o ($K_{\text{assoc}}[\text{H}] \ll 1$, assuming $[\text{'G'}]_{\text{observed}} \approx [\text{G}^+\text{X}^-]$) for solutions of 1 and a) 2 -PF ₆ , b) 2 -BF ₄ , c) 2 -OTs, and d) 2 -TFA in CDCl ₃ :CD ₃ CN (3:2), 295 K.....	82
IV	Formation of Iminium Ions by Acetone Condensation with Secondary Ammonium Salts	
Figure IV-1	¹ H NMR spectra (400 MHz, 295K, acetone- <i>d</i> ₆) of a) 2.00 b) 4.00 c) 8.00 and d) 16.0 mM equimolar solutions of 1 and 2 -BF ₄ , initially.....	92
Figure IV-2	¹ H NMR spectra (400 MHz, 295K, acetone- <i>d</i> ₆) of 2 -PF ₆ , 16.0 mM, collected after a) 5 minutes and b) 24 hours of solvation.....	93
Figure IV-3	¹ H NMR spectra (400 MHz, 295K, acetone- <i>d</i> ₆) of 3 -PF ₆ collected after a) 5 minutes and b) 24 hours of solvation.....	94
Figure IV-4	¹ H NMR spectra (400 MHz, 295K, acetone- <i>d</i> ₆) of 4 -2PF ₆ collected after a) 5 minutes and b) 24 hours of solvation.....	94

Figure IV-5	^1H NMR spectra (400 MHz, 295K, acetone- d_6) of 5 - BF_4 collected after a) 5 minutes and b) 24 hours of solvation.....	95
Figure IV-6	^1H NMR spectra (400 MHz, 295K, acetone- d_6) of 2 - PF_6 a) 24 hours after solvation in dry acetone stirring over molecular sieves and b) sample from a) to which a drop of H_2O has been added.....	97
V	Cooperative Host/Guest Interactions via Counterion Assisted Chelation: Pseudorotaxanes from Pseudocryptands	
Figure V-1	Published ORTEP diagrams of a) 2a b) the taco-complex 2b/1a - 2PF_6 and c) the cryptand complex 3/1a - 2PF_6	104
Figure V-2	^1H NMR spectra (400 MHz, 295K, acetone- d_6) of a) 2b ; b) 3.00 mM 2b + 6.95 mM (<i>n</i> -Bu) $_4\text{N}$ - PF_6 ; c) (<i>n</i> -Bu) $_4\text{N}$ - PF_6	105
Figure V-3	^1H NMR spectra (400 MHz, 295K, acetone- d_6) of a) 3.00 mM 1b - 2PF_6 + 6.95 mM (<i>n</i> -Bu) $_4\text{N}$ - PF_6 and b) (<i>n</i> -Bu) $_4\text{N}$ - PF_6	106
Figure V-4	^1H NMR spectra (400 MHz, 295 K, acetone- d_6) of a) 2b ; b) 2.00 mM 2b + 2.00 mM 1b - 2PF_6 ; c) 2.00 mM 2b + 2.00 mM 1b - 2PF_6 + 4.63 mM (<i>n</i> -Bu) $_4\text{N}$ - PF_6	107
Figure V-5	^1H NMR spectra (400 MHz, 295 K, acetone- d_6) of a) 0.9 mM 2b + 1.0×10^2 mM 1b - 2PF_6 and b) 0.9 mM 2b + 1.0×10^2 mM 1b - 2PF_6 + 1.0×10^2 mM (<i>n</i> -Bu) $_4\text{N}$ - PF_6	108
Figure V-6	^1H NMR spectra (400 MHz, 295 K, acetone- d_6) of a) 2b ; b) 3.01 mM 2b + 3.52 mM (CH_3CH_2) $_4\text{N}$ -TFA; c) (CH_3CH_2) $_4\text{N}$ -TFA.....	110
Figure V-7	^1H NMR spectra (400 MHz, 295K, acetone- d_6) of a) 2.95 mM 1b - 2PF_6 + 3.52 mM (CH_3CH_2) $_4\text{N}$ -TFA and b) (CH_3CH_2) $_4\text{N}$ -TFA.....	110
Figure V-8	^1H NMR spectra (400 MHz, 295 K, acetone- d_6) of a) 2b ; b) 2.00 mM 2b + 2.00 mM 1b - 2PF_6 ; c) 2.00 mM 2b + 2.00 mM 1b - 2PF_6 + 2.35 mM (CH_3CH_2) $_4\text{N}$ -TFA; d) 2.00 mM 2b + 2.00 mM 1b - 2PF_6 + 4.70 mM (CH_3CH_2) $_4\text{N}$ -TFA.....	111
Figure V-9	ORTEP diagram of 1a - 2TFA with 50% probability ellipsoids.....	112
Figure V-10	^1H NMR spectra (400 MHz, 295 K, acetone- d_6) of a) 3.00 mM 2b + 3.00 mM 1a - 2PF_6 and b) 2.00 mM 2b + 2.00 mM 1a - 2PF_6 + 6.60 mM (CH_3CH_2) $_4\text{N}$ -TFA.....	112
Figure V-11	^1H NMR spectra (400 MHz, 295 K, acetone- d_6) of a) 3.00 mM 2a + 3.00 mM 1a - 2PF_6 and b) 2.00 mM 2a + 2.00 mM 1a - 2PF_6 + 2.50 mM (CH_3CH_2) $_4\text{N}$ -TFA.....	113

Figure V-12	^1H NMR spectra (400 MHz, 295 K, acetone- d_6) of a) 3.00 mM 2a + 3.00 mM 1b -2PF ₆ ; b) 2.00 mM 2a + 2.00 mM 1b -2PF ₆ + 2.50 mM (CH ₃ CH ₂) ₄ N-TFA; c) 2.00 mM 2a + 2.00 mM 1b -2PF ₆ + 7.50 mM (CH ₃ CH ₂) ₄ N-TFA.....	113
Figure V-13	ORTEP diagram of 2b/1a -PF ₆ /TFA with 50% probability ellipsoids.....	115
Figure V-14	^1H NMR spectra (400 MHz, 295 K, acetone- d_6) of a) 2.00 mM 2b + 2.00 mM 1b -2PF ₆ and b) 2.00 mM 2b + 2.00 mM 1b -2PF ₆ + 2.50 mM (<i>n</i> -Bu) ₄ N-OTs.....	116
Figure V-15	^1H NMR spectra (400 MHz, 295 K, acetone- d_6) of a) 2.00 mM 2b + 2.00 mM 1b -2PF ₆ and b) 2.00 mM 2b + 2.00 mM 1b -2PF ₆ + 4.10 mM (<i>n</i> -Bu) ₄ N-BF ₄	116
Figure V-16	^1H NMR spectra (400 MHz, 295 K, acetone- d_6) of a) 2.00 mM 2b + 2.00 mM 1b -2PF ₆ ; b) 2.00 mM 2b + 2.00 mM 1b -2PF ₆ + 2.00 mM (<i>n</i> -Bu) ₄ N-CF ₃ SO ₃ ; c) 2.00 mM 2b + 2.00 mM 1b -2PF ₆ + 4.00 mM (<i>n</i> -Bu) ₄ N-CF ₃ SO ₃	117
A1	Preliminary Investigations into the Calculation of K_{ipd} For 2-X Salts Based on NMR Spectroscopy	
Figure A1	Typical spectrum of a fast exchanged complexation event between bound and free states.....	125
Figure A2	Chemical shift of H ₁ of 2 -TFA versus concentration (297 mM \geq [2 -TFA] \geq 0.500 mM) in CDCl ₃ :CD ₃ CN (3:2) at 295 K.....	131
Figure A3	Chemical shift of H ₁ versus [2 -TFA] ₀ ⁻¹ ([2 -TFA] > 60 mM) in CDCl ₃ :CD ₃ CN (3:2) at 295 K.....	132
Figure A4	1 / [2 -TFA] ₀ versus chemical shift of H ₁ (10.0 \geq [2 -TFA] \geq 0.5 mM) in CDCl ₃ :CD ₃ CN (3:2) at 295 K.....	133
Figure A5	Plot of Eq. A4a for 300 mM \geq [2 -TFA] ₀ \geq 0.6 mM) in CDCl ₃ :CD ₃ CN (3:2) at 295 K showing deviation from linearity beyond [G ⁺ X ⁻] > 10 mM, assuming $\epsilon_{\text{mixture}} = 17.5$	135
Figure A6	Plot of Eq. A4a for 10 mM \geq [2 -TFA] ₀ \geq 0.6 mM) in CDCl ₃ :CD ₃ CN (3:2) at 295 K, assuming $\epsilon_{\text{mixture}} = 17.5$	136

Table of Schemes

I	Host/Guest Interactions in Non-Aqueous Solvents: Historical Perspectives	
Scheme I-1	Binding of alkali ions by dibenzo-18-crown-6.....	2
Scheme I-2	A) “Slippage” and B) reversible capping approaches to rotaxane Formation.....	3
Scheme I-3	Pseudorotaxane formation from bis- <i>p</i> -phenylene-34-crown-10 and bis- <i>m</i> -phenylene-32-crown-10 with dimethylparaquat bis(hexafluorophosphate).....	10
Scheme I-4	X-ray structures of pseudorotaxanes formed between bis- <i>p</i> -phenylene-34-crown-10 and dibenzo-24-crown-10 with dibenzylammonium hexafluorophosphate.....	11
Scheme I-5	Cartoon representation of supramolecular polymers fashioned via pseudorotaxane interactions, and the monomers used by Gibson et al. to assemble linear arrays.	13
Scheme I-6	Cartoon of the self-assembly of dendritic supermolecules and the components used to prepare self-assembled dendrimers.....	14
IV	Formation of Iminium Ions by Acetone Condensation with Secondary Ammonium Salts	
Scheme IV-1	Proposed mechanism for formation of observed byproduct.....	96
V	Cooperative Host/Guest Interactions via Counterion Assisted Chelation: Pseudorotaxanes from Pseudocryptands	
Scheme V-1	Cartoon representation of a cooperative host/guest interaction via pseudocryptand formation.....	114

Table of Tables

I	Host/Guest Interactions in Non-Aqueous Solvents: Historical Perspectives	
Table I-1	Potassium cation binding strengths and rates for various ligands in water at 298K.....	8
II	Supramolecular Interactions in Non-Aqueous Solvents: Development of an Equilibrium Model	
Table II-1	$K_{a,exp}$ of 1 / 2 -PF ₆ as a function of [1] ₀ and [2 -PF ₆] ₀ [CDCl ₃ :CD ₃ CN (3:2), 295 K].....	28
III	Supramolecular Interactions In Non-Aqueous Solvents: Testing of An Equilibrium Model	
Table III-1	Percentage of host occupied by guest (θ) for twelve independently prepared solutions, initially 4.0 mM in both 1 and 2 -TFA, CDCl ₃ :CD ₃ CN (3:2), 295 K.....	47
Table III-2	Percentage of host occupied by guest (θ) for 5 independent Fourier transformations of a randomly chosen sample from Table 2 ([1] ₀ = [2 -TFA] ₀ = 4.00 mM, CDCl ₃ :CD ₃ CN (3:2), 295 K).....	48
Table III-3	K_{assoc} and K_{ipd} values for 2 -X salts with 1 in CDCl ₃ :CD ₃ CN (3:2), 295 K, as calculated according to Eqs. 6l and 6n.....	59
Table III-4	Percentage of host occupied by guest (θ) as a function of [1] ₀ and [2 -X] ₀ , CDCl ₃ :CD ₃ CN (3:2), 295 K.....	65
Table III-5	K_{assoc} and K_{ipd} values for 2 -X salts with 1 in CDCl ₃ :CD ₃ CN (3:2), 295 K, as calculated from non-linear least-square fitting treatments....	65
Table III-6	Percentage of host occupied by guest (θ) as a function of [1] ₀ and [2 -X] ₀ in the limit [H] ≤ 3.00 mM, CDCl ₃ :CD ₃ CN (3:2), 295 K.....	68
Table III-7	K_{assoc} and K_{ipd} values for 2 -X salts with 1 in CDCl ₃ :CD ₃ CN (3:2), 295 K, as calculated according to Eq. 9c.....	69
Table III-8	K_{assoc} and K_{ipd} values for 2 -X salts with 1 in CDCl ₃ :CD ₃ CN (3:2), 295 K, as calculated according to three independent pre-equilibrium treatments.....	70

Table III-9	Percentage of host occupied by guest (θ) and $K_{a,exp}$ of 1/2-Cl as a function of added anion host 3 [$CDCl_3:CD_3CN$ (3:2), 22 °C].....	76
Table III-10	Uncorrected $[X^-]$ and $[G^+X^-]$ values, calculated as a function of K_{ipd} as well as “corrected” values, calculated as a function of K_{ipd} and γ_{\pm} at 298 K with $\epsilon = 17.5$	80
V	Cooperative Host/Guest Interactions via Counterion Assisted Chelation: Pseudorotaxanes from Pseudocryptands	
Table V-1	Comparison of various pseudocryptand and cryptand systems in acetone- d_6 at 295 K.....	118
AI	Preliminary Investigations into the Calculation of K_{ipd} For 2-X salts Based on NMR Spectroscopy	
Table A1	Concentration dependence of H_1 of 2-TFA in $CDCl_3:CD_3CN$ (3:2) at 295 K.....	130
Table A2	Experimental concentrations and activity coefficients calculated assuming $\delta_{paired} = 3.950$ ppm and $\delta_{dissociated} = 4.175$ ppm, for 2-TFA in $CDCl_3:CD_3CN$ (3:2) at 295 K.....	134
Table A3	γ_{\pm} for 16 mM > [2-TFA] > 5 mM calculated according to Eq. 3 [13] from experimental concentrations of 2⁺ in $CDCl_3:CD_3CN$ (3:2) at 295 K, assuming $\epsilon_{mixture} \approx 17.5$	136

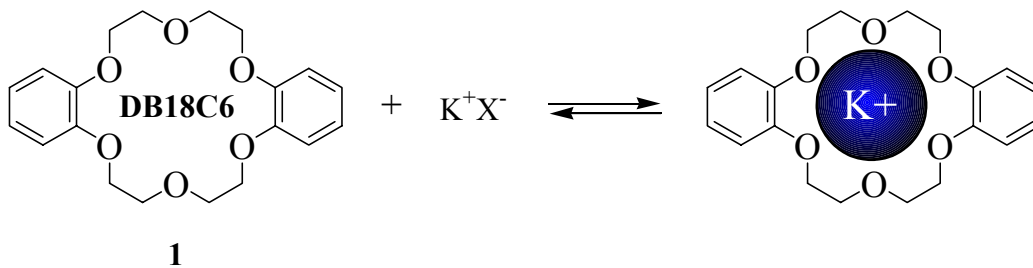
Chapter I

Supramolecular Interactions in Non-Aqueous Solvents: Historical Perspectives

I.1 Introduction

Over the past half-century, the enormously broad field of supramolecular chemistry has emerged and grown into an important segment of our overall understanding of the natural world. [1] At the forefront of this movement, the elucidation of the molecular structure of nucleic acids and their importance in information transfer among living materials, for which Watson and Crick [2] shared the 1962 Noble prize in Medicine, paved the way for numerous studies into intermolecular recognition motifs. Most impressively, the Pandora's Box of Mother Nature's genetic sequencing has recently and simultaneously been unleashed by two independent groups of researchers. [3] In order to more fully understand and realize the ramifications of such an awe-inspiring scientific revolution, great strides are continually being made in small molecule molecular recognition under the general umbrella of host-guest chemistry.

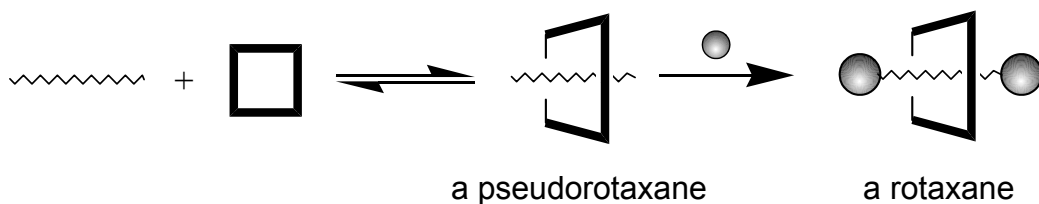
Acknowledging the discovery that enzymatic catalysis is enabled as a result of highly selective complex formation between reactants and catalyst, Cram coined the term host-guest chemistry in 1974, [4] wherein a large host molecule recognizes a smaller guest species by "complexing best those guest molecules that contain the array of binding sites and steric features that complement those of the host." This coinage was not without impetus: in 1967 Pedersen discovered that dibenzo-18-crown-6 (DB18C6, **1**) formed a complex with alkali ions in a selective manner (see Scheme I-1), [5] an important finding as the alkali and alkaline earth metals are involved in many physiological processes, thereby imparting potentially useful pharmaceutical applications to the crown ether. [6] It is widely recognized that the field of supramolecular chemistry emanated directly from Pedersen's discovery. It is therefore not surprising that the supramolecular properties of macrocyclic hosts have been at the forefront of the host/guest movement.

Scheme I-1. Binding of alkali ions by dibenzo-18-crown-6 (**1**).

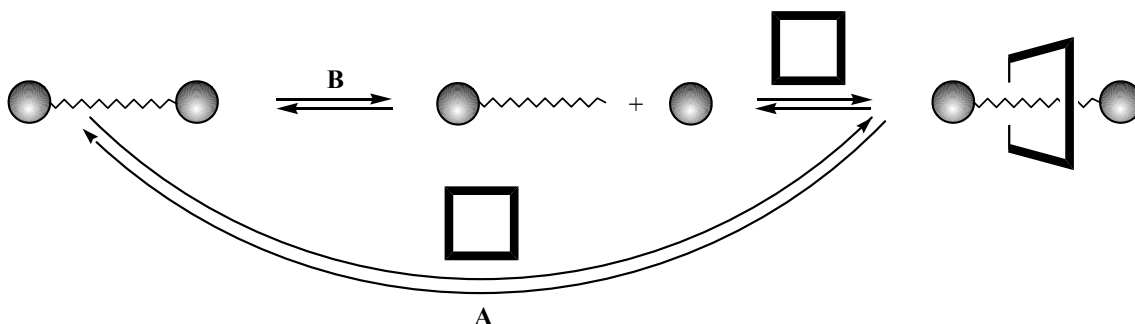
While the search for physiological applications of crown ethers is still on-going nearly four decades later, [7] the macrocyclic literature has experienced a major shift towards material applications, predominately in the form of rotaxane or rotaxane-like interactions (Figure I-1) between cyclic host and linear guest species. [8] It is a scientific oddity that such a shift actually predates Pedersen's discovery, as Frisch and Wasserman conceptually extended the idea of non-covalent polymer topologies to the area of rotaxanes as early as 1961. [9] This conceptual visualization was made a reality in 1967 when the first experimental evidence of rotaxane formation was shown by two independent research groups: Schill and Zöllenkopf examined rotaxane formation by a multi-step and tedious chemical conversion method, [10] while Harrison and Harrison prepared rotaxanes [11] in a 6% yield using a polymeric support. [12] Harrison later went on to modify this approach by showing the formation of rotaxanes via a) "slippage," a kinetic process, [13] and b) reversible capping equilibria, a thermodynamic process (Scheme I-2). [14] In both cases, an unspecified mixture of cyclic hydrocarbons was introduced to 1,10-bis-(triphenylmethoxy)decane at 120 °C. It was shown that for rotaxanes formed by slippage, the "wheel" component required a macrocycle composed of exactly 29 methylene units: macrocycles of less than 29 units lacked the thermal expansion requirements to slip over the endgroups, while macrocycles of greater than 29 units were not sufficiently hindered to retain a mechanical linkage. Upon addition of a catalytic amount of trichloroacetic acid to enable reversible detachment of the bulky triphenylmethyl end groups, Harrison determined that a minimum ring size of 23 methylene units was required for the threading of a straight chain alkane. Further work in

this area established blocking group effectiveness and the influence of linear chain length on the formation of rotaxane complexes. [15]

Figure I-1. Cartoon representations of a pseudorotaxane and a rotaxane.



Scheme I-2. A) “Slippage” and B) reversible capping approaches to rotaxane formation.

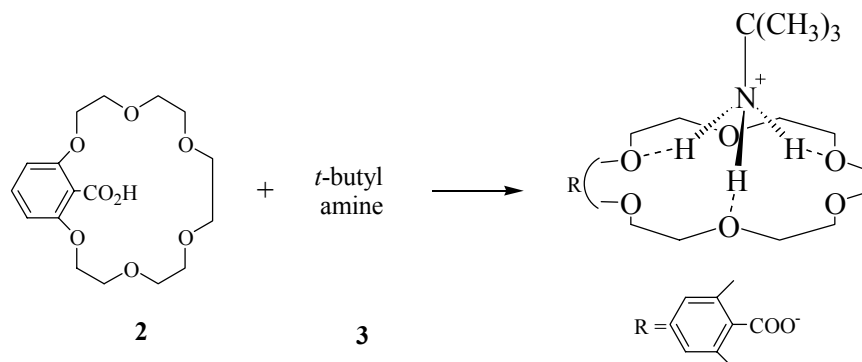


I.2 Threading Influences on Supramolecular Chemistry

While Schill's and Harrison's studies were revolutionary with regard to the rotaxane literature, the lack of specific interaction between the macrocyclic “wheel” and the linear “axle” did little to pique the curiosity of many in the adolescent field of supramolecular chemistry. All of this changed in 1972, when Frensdorff reported on the ability of crown ethers to recognize ammonium and alkylammonium salts, [16] work which was further extended by Goldberg in 1975 (Figure I-2). [17] Though not pseudorotaxanes in the sense that the ammonium ion does not extend through the cavity of the crown ether, [18] it was nonetheless clear that building the attribute of recognition

into the “wheel” and “axle” components might be a viable technique for preparing rotaxanes in greater than statistical, and possibly quantitative, yields.

Figure I-2. Complexation of *t*-butylamine (**3**) by 2-carboxy-1,3-phenylene-19-crown-6 (**2**).



The first group to exploit this predisposition of crown ethers to adopt rotaxane formations with suitable guests was Zilkha et al., who published two papers describing the formation of rotaxanes from benzo-crown ethers and oligo(ethylene glycol)s. [19] It is of historical interest that Zilkha’s group did not intentionally set out to exploit host/guest chemistry to prepare their rotaxanes. In fact, they believed their complexes to be formed by statistical means despite isolated yields (up to 63%) which said otherwise. Their results indicated that pseudorotaxane formation was increased until the ratio of macrocycle to linear diol reached two and then remained constant. It was further shown that the degree of threading increased with crown ether cavity size, while threading was independent of linear chain length. All of these factors led the discerning reader to one conclusion: dipole-dipole attractions, here in the form of hydrogen bonding between the acidic hydrogens of the alcohol and the electron rich oxygen atoms of the macrocycle, can be applied and utilized as a major driving force for rotaxane formation, known as a templated approach.

Subsequent investigations into this newly defined templated approach to rotaxane formation support Zilkha’s experimental work: Cram and others manipulated the N-H···O interaction between 27-crown-9 and guanidinium to form stoichiometric 1:1 complexes;

[20] Metcalf et al. published a manuscript detailing the perching complexes fashioned between *N,N'*-dimethyldiaza-12-crown-4 with various secondary ammonium ions; [21] Stoddart and co-workers bound ammonia to a transition metal cation, thereby acidifying the N-H bonds and allowing the transition metal complex to be readily associated to a crown ether, in this case, 18-crown-6; [22] Gibson et al. have synthesized polyamide, [23] polyurethane, [24] and polyester [25] rotaxanes utilizing aliphatic crown ethers as the host moiety. Each study confirms the importance of hydrogen bonding in the formation of diol- and amine-based rotaxanes and polyrotaxanes, as implied by the results of Zilkha decades ago.

1.3 *Improvement in Threading Efficiencies*

As the rationale behind template directed rotaxane formation is to drive threading efficiency to near quantitative values, a consistent and pervasive theme throughout the four decades of rotaxane research has been in the enhancement of host/guest recognition, a focus which is shared with the more general field of supramolecular chemistry. To address this issue two questions must be asked: first) what approaches can one take to enhance non-covalent interactions, and second) how does one quantify such interactions? This latter question will be addressed in Chapter II. As to the former, one must first consider the forces involved in self-assembly before moving forward.

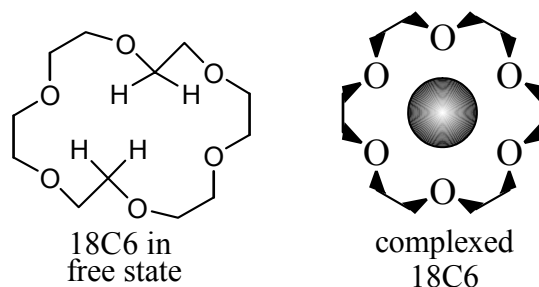
The process of self-assembly might be well described as the process wherein two otherwise fully independent molecules spontaneously recognize each other and become intimately associated through non-covalent interactions in response to external stimuli. The idea of selectivity, wherein two molecules *preferentially* recognize each other in a self-assembly process, has been intentionally left out of the above definition as selectivity is not a requirement of self-assembly. Because self-assembly is a diffusion limited process (in other words, two molecules must be located within a proximity close enough to enable the non-covalent forces to perform their work), a vast majority of self-assembly events occur in solution, but this is also not a rigid requirement as demonstrated by a number of processes, including the self-assembled ordering of block copolymers. [26]

Such spontaneous processes are primarily driven by hydrogen bonding, van der Waals forces (which include induced dipole, charge-fluctuation forces, dispersion forces, and electrodynamic forces), electrostatic interactions and/or hydrophobic-hydrophilic interactions.

Because of the electrodynamic nature of such non-covalent interactions, the disadvantage of performing a self-assembly process in solution becomes obvious when one considers solvent polarity: any medium that can participate in competing non-covalent interactions will hinder self-assembly. As a result, relatively low dielectric constant media (i.e., $\epsilon < 30$) have become the solvents of choice where possible due to the lack of competition from the relatively non-polar media. However, use of low dielectric constant solvents carries its own limitations, which will be addressed in detail in Chapters II and III.

While solvent choice is one approach to control non-covalent interactions, the largest gains in binding efficiencies have been realized by supramolecular chemists who have looked to the work of Fischer. In 1894 Fischer discovered that sugar metabolizing enzymes had the unique ability to recognize various sugars of specific shape. [27] This discovery led to the template hypothesis, which states that binding efficiency and selectivity is maximized by a host whose cavity is pre-formed in a shape to accommodate a specific guest ligand, and whose binding sites are well matched to that of the guest. A simple analogy is that of a “lock and key,” wherein only matched keys are able to unlock the tumbler; ill-fitting keys do not provide entry.

Applying the same analogy to the supramolecular chemistry of crown ethers, early efforts involving 18-crown-6 showed that the structure of uncomplexed 18-crown-6 varies dramatically in structure from that of 18-crown-6 complexed by an alkali metal (Figure I-3). [28] In the free state, two methylene groups occupy what would otherwise be a void. While the barrier to inversion may be sufficiently small to allow complexation to occur within the simple crown ether macrocycles, it necessarily follows that the 18-crown-6 ‘lock’ was not custom-made for the alkali metals, and is therefore not optimized for inclusion of guest species.

Figure I-3. Various conformations of 18-crown-6.

In an impressive series of experiments designed to study optimization of 18-crown-6 and related hosts around the potassium cation, the rigid [2.2.2]-cryptand (so named because of guest trapping within the three armed, bridged macrocycle) and flexible 36-membered natural antibiotic valinomycin were pitted head to head with simple 18-crown-6 (Figure I-4). [29] Assessment of potassium cation binding constants ($K_{a,exp}$) from Table I-1 suggests that association is strongest in the inflexible cryptand, just as one may expect due to entropic reasoning: a molecule that does not require rearrangement will be a better host than one that does. Interestingly, association of potassium by the relatively large and conformationally flexible valinomycin dwarfs that by the smaller 18-crown-6. Further investigation of potassium release rates provides consistent insight. Again just as one might expect, release rates vary according to strength of binding: 18-crown-6 more readily gives up the potassium cation than does the [2.2.2]-cryptand. Keeping in mind that valinomycin is a flexible molecule, it becomes obvious that a host molecule that can bind the cation in a three-dimensional array of donor groups will demonstrate strong binding ability, while offering the potential to shield the guest from its environment. On the other hand, a host that is permanently set in the three-dimensional array does not readily give up the complexed guest. The guest is trapped within a cage, so to speak, whereas compounds that can encapsulate guest moieties by conformational rearrangements have the unique ability to open up their cavities to allow cation transport. As an example, valinomycin adopts a three-dimensional “tennis ball seam” arrangement about the cation by utilizing intramolecular hydrogen bonding and can open up these seams in the proper environment. [30] At the other extreme, simple crown ethers are not large enough to fully encapsulate most guest molecules, thereby ensuring a weaker binding constant than the three-dimensional array

permits. The smaller crown also exposes more of the bound guest's surface area to the environment, enabling a facile releasing mechanism. It follows from these arguments that hosts which fully encapsulate charged guest molecules have the unique capability of separating the guest ligand from its counterion; hosts which do not fully encapsulate the guest permit contact ion pairs to form, the degree to which depends on the solvent dielectric constant. [31] There are advantages and disadvantages of each binding arrangement.

Table I-1. Potassium cation binding strengths and rates for various ligands in water at 298 K. [32]

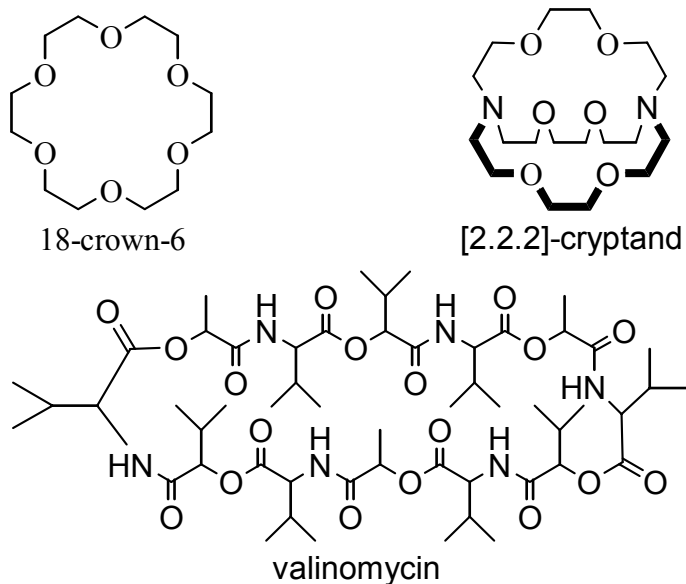
Ligand	$K_{a,exp}$ (M^{-1})	k_1^a ($M^{-1}s^{-1}$)	k_{-1}^b (s^{-1})
18-crown-6	115	4.3×10^8	7.5×10^6
[2.2.2]-cryptand	200,000	7.5×10^6	380
valinomycin ^c	31,000	4.0×10^7	1.3×10^3

^a binding rate constant

^b decomplexation rate constant

^c values determined in anhydrous methanol

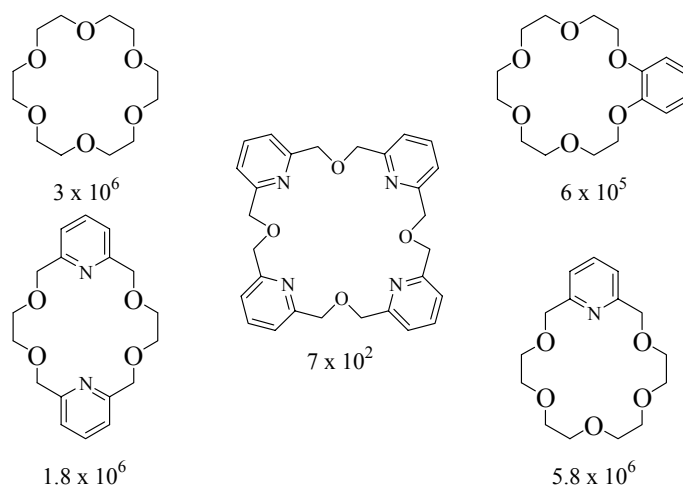
Figure I-4. Molecular structures of 18-crown-6, [2.2.2]-cryptand, and valinomycin.



In addition to host size and shape, gains in binding efficiencies have been realized by researchers who have explored substituent effects on both host and guest species. The pioneering work of Pedersen and Frensdorff [33] provided a basis for observation of guest substituent effects. In particular, the effect of R on the binding constants for complexes of 18-crown-6 and R-NH₃⁺ was dramatic. In methanol, the binding constants ($\log K_{a,\text{exp}}$) of 18-crown-6 with MeNH₃⁺, EtNH₃⁺, PhNH₃⁺, and *t*-BuNH₃⁺ were shown to be 4.25, 3.99, 3.80, and 2.90, respectively. [34] Three N-H···O hydrogen bonds stabilize the complex; the binding constants decrease as a function of steric influences.

Host substituent effects have been explored by Gokel and others, who looked at the effect of varying donor atoms around the 18-membered crown ether hosts upon complexation with *t*-butylammonium thiocyanate (see Figure I-5). [35] It had been shown as early as 1979 that azacrown ethers, crown ethers containing at least one nitrogen donor atom within the crown, form stronger complexes with primary ammonium ions than do the corresponding simple crown ethers. [32,35] Varying the crown ether ring size also had dramatic effects on complexation with cationic guests (see Figure I-5). Several researchers demonstrated that 18-membered rings more readily bind ammonium ions than do 12-, 15-, and 24-membered rings. [36]

Figure I-5. Influence on association constants (as listed under each host; values given in units of M⁻¹) by donor atoms around 18-membered crown ether hosts upon complexation with *t*-butyl-ammonium thiocyanate in MeOH.

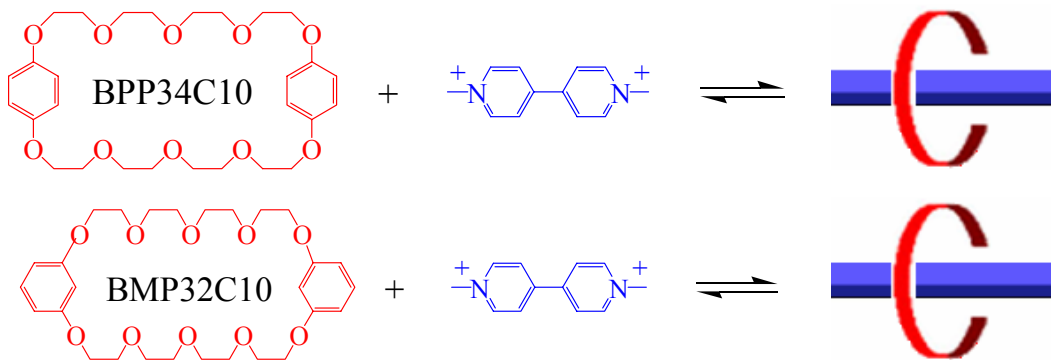


I.4 Modern Pseudorotaxanes

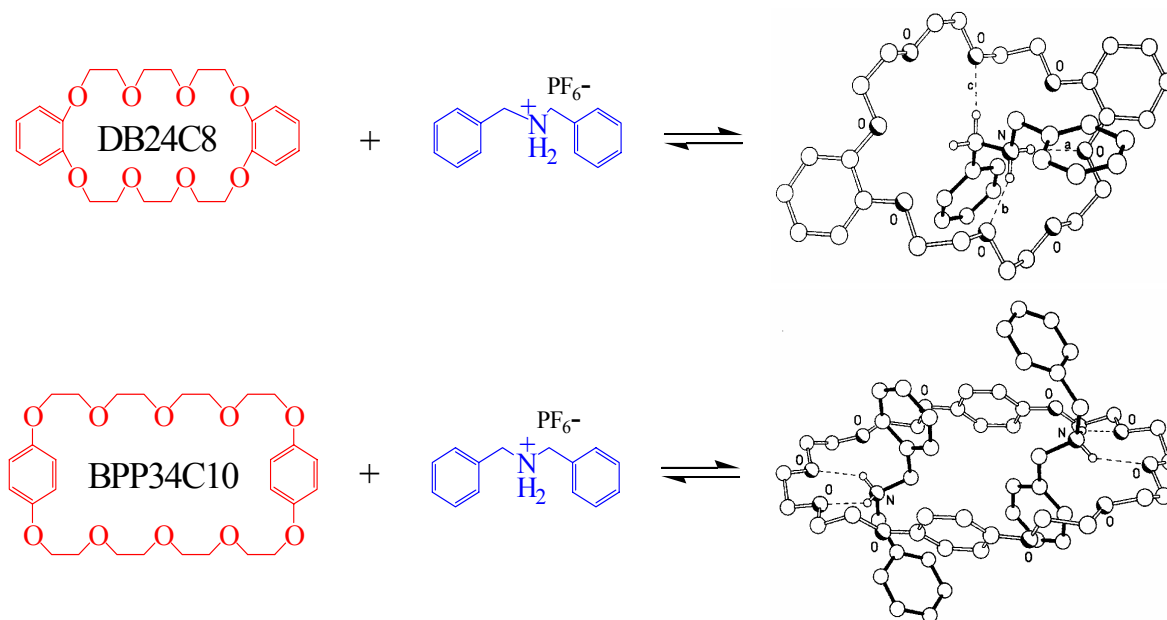
While all of the above studies greatly influenced the field of supramolecular chemistry, the modern face of self-assembly, particularly the field of rotaxanes and pseudorotaxanes, has been predominately sculpted by the work of Stoddart. In fact, it is largely this work that has enabled the shift from physiological applications of macrocyclic hosts towards the exploration of material applications of similar hosts.

In 1987, Stoddart and coworkers studied the complexation of paraquat dications with two larger crown ethers, bis *para*-phenylene-34-crown-10 (BPP34C10) and bis *meta*-phenylene-32-crown-10 (BMP32C10), to form pseudorotaxanes (Scheme I-3). [37] Stoddart and coworkers later demonstrated the synthesis of rotaxanes from crown ethers and secondary ammonium ions, namely dibenzo-24-crown-8 (DB24C8) and BPP34C10 with dibenzylammonium hexafluorophosphate (Scheme I-4). [38] In the case of BPP34C10, two 2° ammonium salts were found to thread through the host cavity, giving rise to the coining of the descriptor [*n*]pseudorotaxane, where *n* establishes the total number of components involved in a single binding unit, i.e., the BPP34C10 complex incorporating two guests is a [3]pseudorotaxane (Scheme I-4).

Scheme I-3. Pseudorotaxane formation between bis-*p*-phenylene-34-crown-10 and bis-*m*-phenylene-32-crown-10 with dimethylparaquat bis(hexafluorophosphate). [37]



Scheme I-4. X-ray structures of pseudorotaxanes formed between bis-*p*-phenylene-34-crown-10 and dibenzo-24-crown-10 with dibenzylammonium hexafluorophosphate. [38]



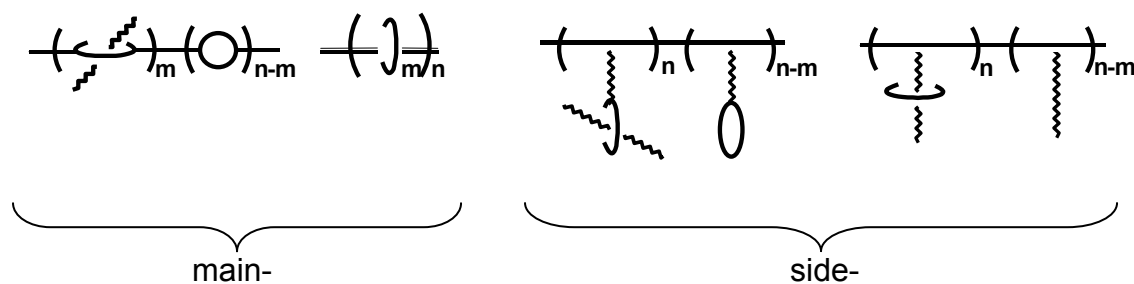
Stoddart went on to finely tune the stability of such complexes by substitution of the dibenzylammonium phenyl rings [39] as well as controlled manipulation of the crown ether structure: one, two, and four fused benzo-rings, as well as macrocycles with 25-crown-8 constitution have been studied. [40] Not unexpectedly, the researchers qualitatively determined that experimental stability constants increase when an electron-withdrawing substituent is placed on the dibenzylammonium guest, while electron-donating substituents reduce experimental association constants. [39] The opposite trend holds for host substituents effects: experimental association constants decrease upon the addition of electron withdrawing substituents and increase with electron donating substituents. [39,41] In addition, as aromatic units are appended into the macrocyclic framework or as the macrocycle's cavity is extended from 24 to 25 interior atoms, the affinity of the crown ether towards the ammonium salt decreases. [40]

While this dissertation will focus specifically on pseudorotaxane formation via crown ethers and charged species, as described above, it is informative to note that these binding motifs have been extended to many other macrocyclic species, including but not limited to cyclodextrins, [42] cucurbiturils, [43] calixarenes, [44] and porphyrins. [45]

I.5 Pseudorotaxanes and Material Applications

With the discovery that organic building blocks can be readily utilized to yield stable host/guest assemblies in the form of pseudorotaxanes came multiple reports manipulating such interaction for the construction of novel materials. The earliest reports detailed the use of pseudorotaxane self-assembly with macromolecules, as pioneered by Gibson. In general, there are three broad families of polymeric pseudorotaxane architectures: main- and side- chain polypseudorotaxanes (Figure I-6) as well as self-assembled polymers (scheme I-5). These macromolecules are of interest because the architectural changes in going from simple, non-complexed homopolymers to polypseudorotaxanes result in vastly different properties and behaviors. [46]

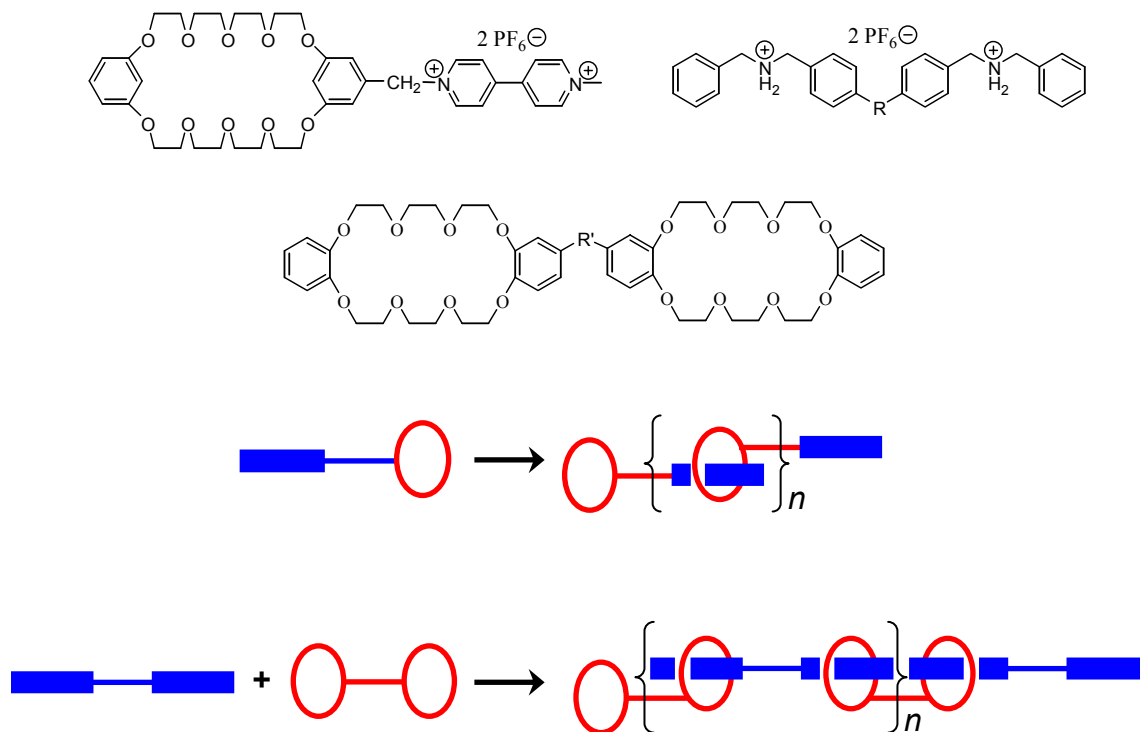
Figure I-6. Main- and side- chain polypseudorotaxane architectures.



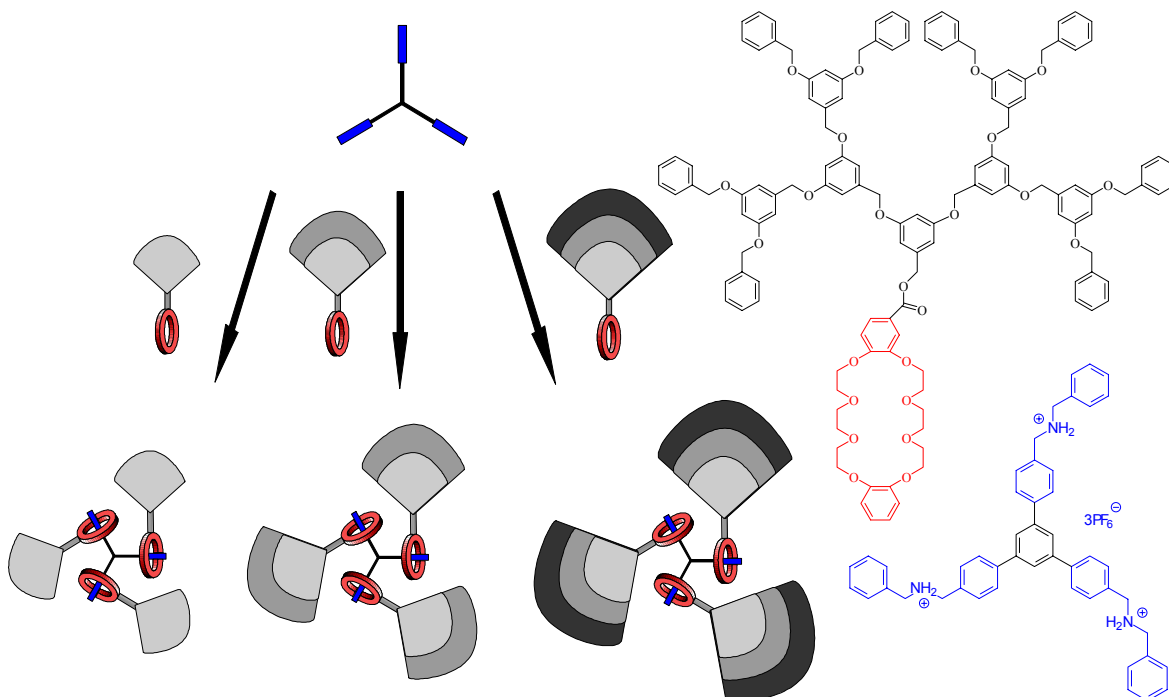
Gibson et al. and others have exhaustively detailed numerous approaches to the synthesis of a variety of polypseudorotaxanes. [46] More recently, the complexes described by Stoddart et al. above, namely pseudorotaxanes fashioned between DB24C8 with dibenzylammonium salts, as well as BMP32C10 with paraquat salts, have been used

to prepare self-assembled dendrimers, hyperbranched polymers, and linear polymers. [47] In these studies, the polymeric backbone is grown in a non-covalent fashion (see Schemes I-5 and I-6), which is possible due to the modest strength of association found in such pseudorotaxanes; the modest strength of association also limits the ultimate degree of polymerization, as described in the final section of this chapter.

Scheme I-5. Cartoon representation of supramolecular polymers fashioned via pseudorotaxane interactions, and the monomers used by Gibson et al. to assemble linear arrays. [47a,d]



Scheme I-6. Cartoon of the self-assembly of dendritic supermolecules and the components used to prepare self-assembled dendrimers. [47b,c,e]



In addition to self-assembled polymers, within the past half decade, pseudorotaxanes have been applied to such diverse areas as sensors, molecular electronics, and molecular machines. [48] The current focus of this research is in the construction of future computers, which require a significant reduction in size, weight, and power use over today's machines. Pseudorotaxanes and related structures have been shown to be leading candidates in memory devices, [49] and molecular switches. [50]

1.6 *Quantifying Host/Guest Association Constants and Material Applications*

For a majority of material applications, the strength of binding carries enormous consequences, and is perhaps the single most important aspect in determining ultimate

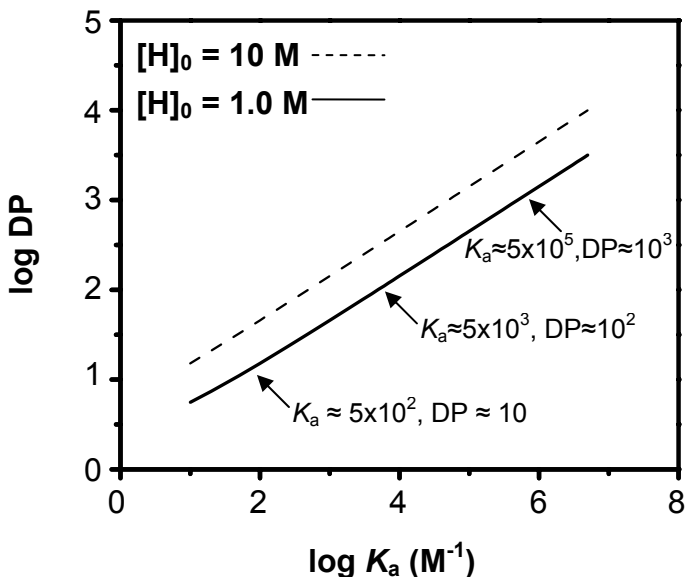
supramolecular polymer properties and uses. In the area of self-assembled polymers, Meijer has calculated the degree of polymerization (i.e., the number of self-assembled repeat units) to be inversely related to the square root of the binding constant for linear chain extensions via homoditopic AB building blocks (Eq. 1); the degree of polymerization is also dependent upon the initial homoditopic monomer concentration, $[H]_0$. [51] The ramifications of these studies are readily apparent upon inspection of Figure I-7, which shows a log-log plot of the degree of polymerization versus K_a , for 1.0 and 10 M homoditopic AB systems. In order to extend chains to appreciable length, a large K_a (on the order of 10^5 M^{-1} and greater) is required; for the 1.0 M case, a moderate K_a of 10^3 M^{-1} yields a maximum of only 46 repeat units, ignoring the presence of cyclic species.

$$DP = \frac{2 K_a [H]_0}{(1 + 2 K_a [H]_0)^{1/2} - 1} \quad \text{Eq. 1}$$

When $2K_a[H]_0 \gg 1$, and $(2K_a[H]_0)^{1/2} \gg 1$,

$$DP \approx (2 K_a [H]_0)^{1/2} \quad \text{Eq. 1b}$$

Figure I-7. Theoretical relationship between the degree of polymerization (log DP) versus log K_a for a system a) 1.0 M (solid fit) or b) 10 M (dashed fit) in homoditopic monomer. K_a values given in units of M^{-1} .



In the area of moletronics and other device applications, knowledge of K_a is imperative in order to predict and control the reversible associations which form the application basis. In addition, specific knowledge of these values enables the researcher to determine the limits of such a system, while providing insight into potential means of application improvement.

As a result of the necessity of establishing accurate and reproducible K_a values, a number of reports have surfaced which explicitly describe experimental methods to measure the equilibrium constant and values for standard enthalpy and entropy changes in a myriad of systems using multiple analytical techniques. These techniques form the content of Chapter II.

I.7 References

- [1] a) Vögtle, F. *Supramolecular Chemistry*; Wiley: Chichester, 1991. b) Lehn, J. – M. *Supramolecular Chemistry*; VCH: Weinheim, 1995. c) *Comprehensive Supramolecular Chemistry*; Atwood, J. L.; Davies, J. E. D.; MacNicol, D. D.; Vögtle, F., Eds.; Pergamon: Oxford, 1996.
- [2] a) Watson, J. D.; Crick, F. H. C. *Nature* **1953**, *171*, 737-738. b) Watson, J. D.; Crick, F. H. C. *Nature* **1953**, *171*, 964-967.] and Wilkins[a] Langridge, R.; Wilson, H. R.; Hooper, C. W.; Wilkins, M. H. F.; Hamilton, L. D. *J. Mol. Biol.* **1960**, *2*, 19-37. b) Spencer, M.; Fuller, W.; Wilkins, M. H. F.; Brown, G. L. *Nature* **1962**, *194*, 1014-1020.
- [3] a) The Genome International Sequencing Consortium *Nature* **2001**, *409*, 860-921. b) Venter, J. C. et al. *Science* **2001**, *291*, 1304-1351.
- [4] Cram, D. J.; Cram, D. J. *Science* **1974**, *183*, 803-809.
- [5] For a discussion on the nomenclature of “crown ethers”, see Pedersen, C. J. *J. Am. Chem. Soc.* **1967**, *89*, a.) 2495-2496 b.) 7017-7036.
- [6] Ball, P. *Designing the Molecular World: Chemistry at the Frontier*. Princeton University Press: Princeton, **1994**, 159.

- [7] see for example a) Jansen, B. A. J.; Wielaard, P.; den Dulk, H.; Brouwer, J.; Reedijk, J. *Eur. J. Inorg. Chem.* **2002**, *9*, 2375-2379. b) Ueshige, T.; Nishioka, R.; Nakamura, T.; Hirose, K.; Tobe, Y. *Chromatography* **2000**, *21*, 368-369. c) Katsu, T.; Mori, Y.; Furuno, K.; Gomita, Y. *J. Pharm. Biomed. Anal.* **1999**, *19*, 585-593. d) Darwish, I. A.; Uchegbu, I. F. *Int. J. of Pharm.* **1997**, *59*, 207-213.
- [8] The term rotaxane derives from the Latin roots for wheel and axle, which provides an semi-accurate visual description of the complexation event: a linear guest “axle” is threaded through the vacuous cavity of a cyclic host “wheel,” effectively forming a reversible complex known as a “pseudorotaxane” (Figure I-1). The distinction between pseudorotaxane and rotaxane is an important one: if both ends of the threaded guest are end-capped with a substituent bulky enough to hinder slipping off of the “wheel”, threading is no longer reversible and the mechanical linkage is thus known as a rotaxane (Figure I-1).
- [9] Frisch, H. L.; Wasserman, E. *J. Am. Chem. Soc.* **1961**, *83*, 3789-3895.
- [10] a) Schill, G.; Zöllenkopf, H. *Nachr. Chem. Techn.* **1967**, *79*, 149. b) Schill, G.; Zöllenkopf, H. *Justus Liebigs Annalen der Chemie* **1969**, *721*, 53-74.
- [11] In their report, Harrison and Harrison suggested the term “hooplane” to describe the mechanical linkage.
- [12] Harrison, I. T.; Harrison, S. J. *J. Am. Chem. Soc.* **1967**, *89*, 5723-5724.
- [13] Ashton, P. R.; Belohradsky, M.; Philp, D.; Stoddart, J. F. *J. Chem. Soc., Chem. Comm.* **1993**, *16*, 1269-74.
- [14] Harrison, I. T. *J. Chem. Soc. Chem. Comm.* **1972**, 231-232.
- [15] a) Harrison, I. T. *J. Chem. Soc. Perk. Trans. I* **1974**, 301. b) Schill, G.; Beckmann, W.; Schweickert, N.; Fritz, H. *Chem. Ber.* **1986**, *119*, 2647.
- [16] a) Frensdorff, H. K. *J. Am. Chem. Soc.* **1971**, *93*, 4684-4688. b) Pedersen, C. J.; Frensdorff, H. K. *Angew. Chem. Int. Ed. Engl.* **1972**, *11*, 16-25.
- [17] Goldberg, I. *Acta Crystallogr., Sect. B* **1975**, *31*, 2592-2600.
- [18] Such a formation is often referred to as a perching, or ‘exo’, complex.
- [19] a) Agam, G.; Graiver, D.; Zilkha, A. *J. Am. Chem. Soc.* **1976**, *98*, 5206-5214. b) Agam, G.; Zilkha, A. *J. Am. Chem. Soc.* **1976**, *98*, 5214-5216.

- [20] Timko, J. M.; Helgeson, R. C.; Newcomb, M.; Gokel, G. W.; Cram, D. J. *J. Am. Chem. Soc.* **1974**, *96*, 7097-7079.
- [21] Metcalf, J. C.; Stoddart, J. F.; Jones, G. *J. Am. Chem. Soc.* **1977**, *99*, 8317-8319.
- [22] Colquhoun, H. M.; Stoddart, J. F. *J. Chem. Soc., Chem. Commun.* **1981**, 612-613.
- [23] Shen, Y. X.; Zie, D.; Gibson, H. W. *J. Am. Chem. Soc.* **1994**, *116*, 537-548.
- [24] a) Gibson, H. W.; Liu, S.; Lecavalier, P.; Wu, C.; Shen, Y. X. *J. Am. Chem. Soc.* **1995**, *117*, 852-874. b) Gong, C.; Gibson, H. W. *J. Am. Chem. Soc.* **1997**, *119*, 8585-8591. c) Gong, C.; Gibson, H. W. *Angew. Chem. Int. Ed.* **1997**, *36*, 2331-2333. d) Gong, C.; Subramanian, C.; Ji Q.; Gibson, H. W. *Macromolecules* **1998**, *31*, 1814-1818.
- [25] a) Gibson, H. W.; Marand, H.; Liu, S. *Adv. Mater.* **1993**, *5*, 11-21. b) Gibson, H. W.; Liu, S.; Gong, C.; Joseph, E. *Macromolecules* **1997**, *30*, 3711-3727. c) Gong, C.; Gibson, H. W. *Angew. Chem. Int. Ed.* **1998**, *37*, 310-314.
- [26] see for example: a) Riess, G. *Prog. Poly. Sci.* **2003**, *28*, 1107-1170. b) Klok, H. – A.; Lecommandoux, S. *Adv. Mater.* **2001**, *13*, 1217-1229. c) Pitsikalis, M.; Pispas, S.; Mays, J. W.; Hadjichristidis, N. *Adv. Poly. Sci.* **1998**, *135*, 1-137.
- [27] Fischer, E. *Ber. Dtsch. Chem. Ges.* **1894**, *27*, 2985-2993.
- [28] Gokel, G. W. *Crown Ethers and Cryptands*. The Royal Society of Chemistry: Cambridge, 1991.
- [29] Gokel, G. W.; Nakano, A. *Crown Compounds: Toward Future Applications*. Cooper, S. R.; Ed. VCH Publishers, Inc.: New York, NY, 1992; Ch. 1, p. 5.
- [30] Truter, M. R. *Structure and Bonding* **1973**, *16*, 71-111.
- [31] Davlieva, M. G.; Lü, J. –M.; Lindeman, S. V.; Kochi, J. *J. Am. Chem. Soc.* **2004**, *126*, 4557-4565.
- [32] Bovill, M. J.; Chadwick, D. J.; Johnson, M. R.; Jones, N. F.; Sutherland, I. O.; Newton, R. F. *J. Chem. Soc., Chem. Commun.* **1979**, 1065-1066.
- [33] a) Pedersen, C. J.; Frensdorff, H. K. *Angew. Chem. Int. Ed. Engl.* **1972**, *11*, 16-25. b) Frensdorff, H. K. *J. Am. Chem. Soc.* **1971**, *93*, 4684-4688.
- [34] a) Izatt, R. M.; Lamb, J. D.; Rossiter, B. E.; Christensen, J. L.; Haymore, B. L. *J. Am. Chem. Soc.* **1979**, *101*, 6273-6276. b) Lehn, J. -M.; Vierling, P. *Tetrahedron Lett.* **1980**, 1323-1326.

- [35] Gokel, G. W.; Abel, E. *Complexation of Organic Cations*. Gokel, G. W.; Abel, E.; Eds. Pergamon: Oxford, UK, 1997; Vol. 1, 511.
- [36] a) Johnson, M. R.; Sutherland, I. O.; Newton, R. F. *J. Chem. Soc., Perkin. Trans. I* **1979**, 357-371. b) Leigh, S. J.; Sutherland, I. O. *J. Chem. Soc., Perkin. Trans. I* **1979**, 1089-1103. c) Hodgkinson, L. C.; Johnson, M. R.; Leigh, S. J.; Spencer, N.; Sutherland, I. O.; Newton, R. F. *J. Chem. Soc., Perkin. Trans. I* **1979**, 2193-2202. d) Pearson, D. P. J.; Leigh, S. J.; Sutherland, I. O. *J. Chem. Soc., Perkin. Trans. I* **1979**, 3113-3126. e) Chadwick, D. J.; Cliffe, I. A.; Newton, R. F.; Sutherland, I. O. *J. Chem. Soc., Perkin. Trans. I* **1984**, 1707-1717. f) Johnson, M. R.; Jones, N. F.; Sutherland, I. O. *J. Chem. Soc., Perkin. Trans. I* **1985**, 1637-1643.
- [37] Allwood, B. L.; Shahriarizavareh, H. Stoddart, J. F.; Williams, D. J. *J. Chem. Soc., Chem. Commun.* **1987**, 1058-1061.
- [38] Ashton, P. R.; Campbell, P. J.; Chrystal, E. J. T.; Glinke, P. T.; Menzer, S.; Philp, D.; Spencer, N.; Stoddart, J. F.; Tasker, P. A.; Williams, D. J. *Angew. Chem. Int. Ed.* **1995**, *34*, 1865-1869.
- [39] Ashton, P. R.; Fyfe, M. C. T.; Hickingbottom, S. K.; Stoddart, J. F.; White, A. J. P.; Williams, D. J. *J. Chem. Soc., Perkin. Trans. 2* **1998**, 2117-2128.
- [40] a) Ashton, P. R.; Bartsch, R. A.; Cantrill, S. J.; Hanes, R. E. Jr.; Hickingbottom, S. K.; Lowe, J. N.; Preece, J. A.; Stoddart, J. F.; Talanov, V. S.; Wang, Z.- H. *Tetrahedron Lett.* **1999**, *40*, 3661-3664. b) For a thorough review of the various complexes prepared prior to 1999, see Fyfe, M. C. T.; Stoddart, J. F. *Adv. Supramol. Chem.* **1999**, *5*, 1-53.
- [41] Jones, J. W. Masters Thesis, VPI&SU Department of Chemistry, 2000.
- [42] a) Li, J.; Ni, X.; Leong, K. *Angew. Chem. Int. Ed. Eng.* **2003**, *42*, 69-72. b) Harada, A. *Acc. Chem. Res.* **2001**, *34*, 456-464. c) Nepogodiev, S. A.; Stoddart, J. F. *Chem. Rev.* **1998**, *98*, 1959-1976. d) Isnin, R.; Kaifer, A. E. *Pure & Appl. Chem.* **1993**, *65*, 495-498.
- [43] a) Moon, K.; Kaifer, A. E. *Org. Lett.* **2004**, *6*, 185-188. b) Kim, K. *Chem. Soc. Rev.* **2002**, *31*, 96-107.

- [44] a) Arduini, A.; Calzavacca, F.; Pochini, A.; Secchi, A. *Chem.* **2003**, *9*, 793-799. b) Arduini, A.; Ferdani, R.; Pochini, A.; Secchi, A.; Ugozzoli, F. *Angew. Chem., Int. Ed. Engl.* **2000**, *39*, 3453-3456. c) Kanamathareddy, S.; Gutsche, C. D. *J. Am. Chem. Soc.* **1993**, *115*, 6572-6579.
- [45] a) Bruce, J. I.; Sauvage, J. -P. *Adv. Mol. Struct. Res.* **1999**, *5*, 153-187. b) Chambron, J. -C.; Collin, J. -P.; Dalbavie, J. -O.; Dietrich-Buchecker, C. O.; Heitz, V.; Odobel, F.; Solladie, N.; Sauvage, J. -P. *Coord. Chem. Rev.* **1998**, *178-180*, 1299-1312.
- [46] See a) Gibson, H. W.; Marand, H. *Mater.* **1993**, *5*, 11-21. b) Amabilino, D. B.; Parsons, I. W.; Stoddart, J. F. *Trends Polym. Sci.* **1994**, *2*, 146-152. c) Gibson, H. W.; Bheda, M.; Engen, P. T. *Prog. Polym. Sci.*, **1994**, 843-945. d) Raymo, F. M.; Stoddart, J. F. *Trends Polym. Sci.* **1996**, *4*, 208-211. e) Gong, C.; Gibson, H. W. *Polyrotaxanes - syntheses and properties* in *Molecular Catenanes, Rotaxanes, Knots*. Sauvage, J. -P.; Dietrich-Buchecker, C., Eds. Wiley-VCH, Weinheim, 1999, 277-321.
- [47] a) Gibson, H. W.; Yamaguchi, N.; Jones, J. W. *J. Am. Chem. Soc.* **2003**, *125*, 3522-3533. b) Gibson, H. W.; Yamaguchi, N.; Hamilton, L.; Jones, J. W. *J. Am. Chem. Soc.* **2002**, *124*, 4653-4665. c) Gibson, H. W.; Hamilton, L.; Yamaguchi, N. *Polym. Adv. Technol.* **2000**, *11*, 791-797. d) Yamaguchi, N.; Gibson, H. W. *Angew. Chem., Int. Ed. Eng.* **1999**, *38*, 143-147. e) Yamaguchi, N.; Hamilton, L. M.; Gibson, H. W. *Angew. Chem., Int. Ed. Eng.* **1998**, *37*, 3275-3279.
- [48] see for example a) Paolesse, R.; Di Natale, C.; Nardis, S.; Macagnano, A.; D'Amico, A.; Pinalli, R.; Dalcanele, E. *Chem. Eur. J.* **2003**, *9*, 5388-5395. b) Kwok, K. S. *Materials Today* **2003**, *6*, 20-27. c) Ratner, M. A. *Materials Today* **2002**, *5*, 20-27. d) Kwok, K. S.; Ellenbogen, J. C. *Materials Today* **2002**, *5*, 28-37.
- [49] a) Flood, A. H.; Ramirez, R. J. A.; Deng, W. -Q.; Muller, R. P.; Goddard, W. A., III; Stoddart, J. F. *Aust. J. Chem.* **2004**, *57*, 301-322. b) Chen, Y.; Jung, G. -Y.; Ohlberg, D. A. A.; Li, X.; Stewart, D. R.; Jeppesen, J. O.; Nielsen, K. A.; Stoddart, J. F.; Williams, R. S. *Nanotech.* **2003**, *14*, 462-468. c) Cavallini, M.;

- Biscarini, F.; Leon, S.; Zerbetto, F.; Bottari, G.; Leigh, D. A. *Science* **2003**, *299*, 531.
- [50] a) Pease, A. R.; Jeppesen, J. O.; Stoddart, J. F.; Luo, Y.; Collier, C. P.; Heath, J. R. *Acc. Chem. Res.* **2001**, *34*, 433-444. b) Collier, C. P.; Matterstei, G.; Wong, E. W.; Luo, Y.; Beverly, K.; Sampaio, J.; Raymo, F. M.; Stoddart, J. F.; Heath, J. R. *Science* **2000**, *289*, 1172-1175.
- [51] Sijbesma, R. P.; Beijer, F. H.; Brunsveld, L.; Folmer, B. J. B.; Hirschberg, J. H. K. K.; Lange, R. F. M.; Lowe, J. K. L.; Meijer, E. W. *Science* **1997**, *278*, 1601-1604.

Chapter II
Supramolecular Interactions in Non-Aqueous Solvents:
Development of an Equilibrium Model

II.1 Host/Guest Interactions

In any host/guest system, the degree of complexation may be readily expressed in terms of an equilibrium constant. In a simple supramolecular process involving a neutral host H and a neutral guest G yielding a 1:1 complex H•G, the equilibrium is given by:



and the association constant, K_a , is thus

$$K_a = \frac{[\text{H}\bullet\text{G}]}{[\text{H}][\text{G}]} \quad \text{Eq. 1}$$

As discussed in Chapter 1, the importance of knowing equilibrium constants cannot be understated: K_a values inherently determine the ultimate usefulness of any given host/guest system in a number of material applications, ranging from molecular electronics to self-assembled polymers. The determination of K_a has therefore become a hot topic in the supramolecular literature. A number of reports have surfaced which explicitly describe experimental methods to measure the equilibrium constant and values for standard enthalpy and entropy changes in a myriad of systems using multiple analytical techniques, including calorimetry and various spectroscopic measurements. [1] Most of these techniques are cross-over technologies from the biological sciences, as self-assembly is essential to all known cellular and physiological processes. [2] As a result, when one adopts biological models to describe synthetic self-assembly, one must consider that the biological models are intended for use with aqueous systems. This factor is important because a number of the synthetic systems involve charged species in non-aqueous media and therefore the influences of ionic strength and ion pairing needs to be considered. These issues will be addressed in significant detail below.

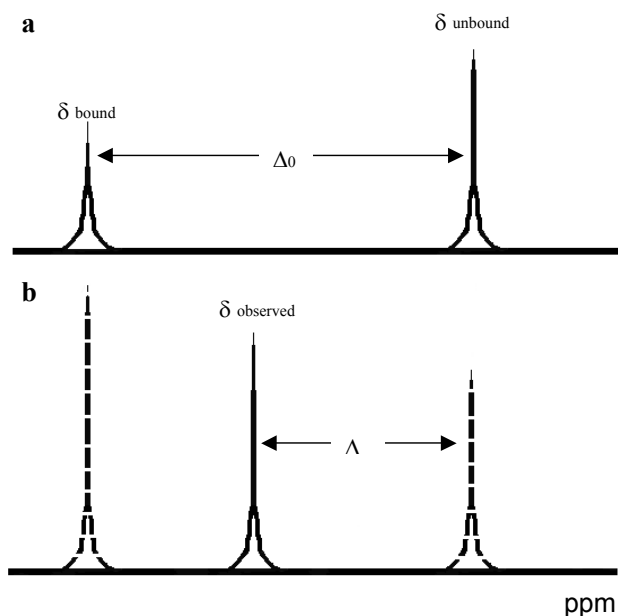
Spectroscopy has become the analytical technique of choice to describe host/guest binding in supramolecular systems. UV-Vis and ^1H NMR are by far the most commonly utilized techniques, predominately due to the widespread availability of both instruments. [3] As spectroscopic techniques have matured, the use of 2-D techniques such as diffusion measurements have recently found their way into the literature. [4] For simplicity, we here consider only the use of 1-D NMR or UV-Vis spectroscopy to describe self-assembled systems. For the simple experiments, there are two extreme exchange regimes commonly encountered in supramolecular assemblies: slow-exchange and fast exchange.

In the slow-exchange regime, two chemically dissimilar environments exist at a single moment in the spectrometer's time scale: one observes *both* the supramolecular complex $\text{H}\cdot\text{G}$ as well as the unbound ligands H and G (Figure II-1a). Utilizing the integration values of complexed (δ_{bound}) versus uncomplexed (δ_{unbound}) components affords a facile means to determine the percentage of complexed guest (or host) species. Coupled with knowledge of the precise concentrations of host and guest moieties added, in the absence of ionic strength issues, one can readily determine both the stoichiometry and association constants from a single NMR experiment; hence its reference as the "single point method."

In the fast-exchange regime, a single, time-averaged peak is observed (Figure II-1b) and it is no longer possible to determine K_a based on the single point method. Instead, one must utilize a multi-point method that takes advantage of the time-averaging of the signal. The Benesi-Hildebrand, [5] Scatchard, [6] Creswell-Allred, [7] and Rose-Drago [8] multi-point methods have been utilized for this purpose, and have been derived under the premise that under fast exchange, $\Delta/\Delta_0 = \text{percentage of guest (or host, depending upon which signal one follows) complexed}$, where $\Delta = \delta_{\text{obs}} - \delta_{\text{unbound}}$ and $\Delta_0 = \delta_{\text{unbound}} - \delta_{\text{bound}}$, as shown in Figure II-1 (see Appendix A for a discussion). δ_{obs} and δ_{unbound} may be determined directly from experiment. In cases where the host signal is being followed, δ_{bound} may be estimated according to the Benesi-Hildebrand method by titrating guest into a constant concentration of host, ultimately overloading the host with at least a 100 fold excess of guest (or titrating host into guest if one wishes to observe the guest resonances). Δ may then be plotted versus $1/[\text{H}]_0$ to yield a linear plot whose slope

and intercept surrender estimated Δ_0 and K_a values, respectively. Gibson et al. have drastically improved this approximation by using an iterative technique in which they first allow $[H]_0$ or $[G]_0$ to approximate $[H]$ or $[G]$, solve for Δ_0 using the Benesi-Hildebrand method and then go on to use the estimated Δ_0 to refine the initial estimate of $[H]$ or $[G]$. [9] This process is repeated until continued iterations result in constant Δ_0 and K_a values. In the absence of ionic strength effects, these simple treatments describe host/guest systems very well.

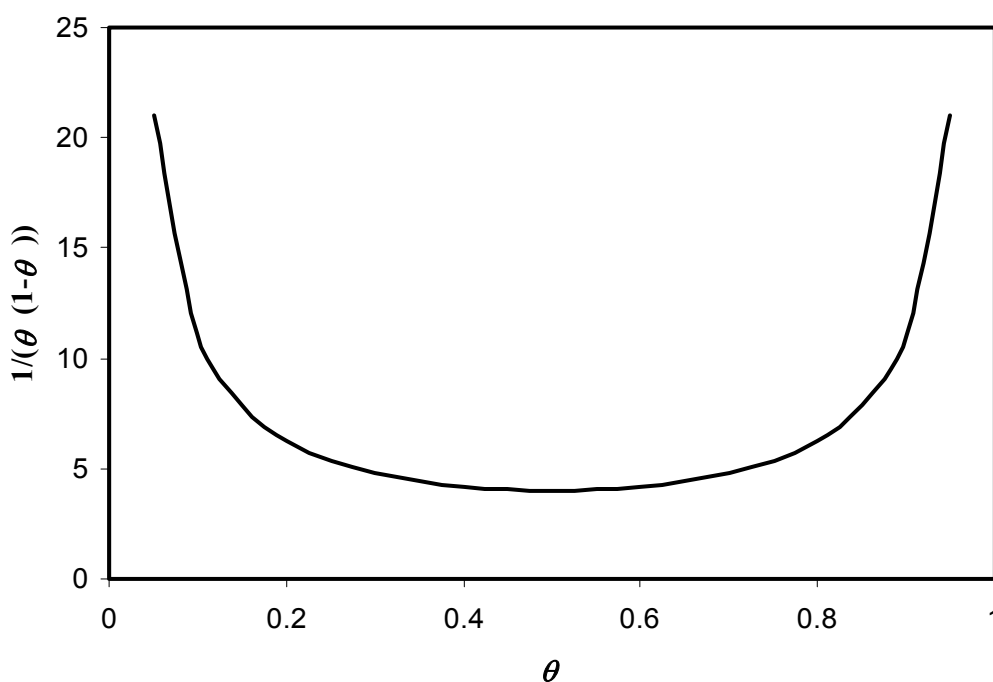
Figure II-1. Two commonly encountered spectroscopic exchange rate regimes in supramolecular assembly formation: a) slow exchange, b) fast exchange.



Regardless of the exchange rate or spectroscopic technique utilized to follow any given supramolecular system, there are inherent errors in estimating experimental concentrations from integration or chemical shift values. Due to solubility limitations, non-ideal binding behavior, and other experimental difficulties [10] these errors become particularly large under the extreme instances of low and high percentages of complexation (Δ/Δ_0); error is minimized at exactly 50% binding. This point is stressed by the experimental work of Weber [11] and corroborated by the theoretical work of Deranleau, [12] who determined the relative error in K_a for systems involving one-site

binding to be described by Figure II-2, which plots the error (ordinate) as a function of percent binding (θ , abscissa). Noting the sharp increase in error under either low or high percent binding, Deranleau concluded that the most meaningful data fall from the 20 to 80% binding range, which agrees well with Weber's observations.

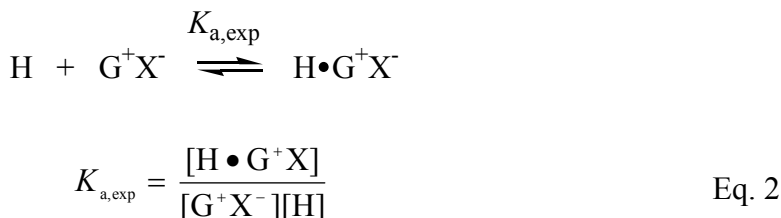
Figure II-2. Relative error in the spectroscopic determination of concentrations for single site binding studies as a function of percent binding.



II.2 *Ionic Strength Considerations in Host/Guest Complexes Involving Electrolyte Components in Non-Aqueous Solvents*

Eq. 1 has been derived for the binding of a neutral guest ligand by a neutral host, a common event in many biological systems. This situation is not the case in the young field of supramolecular chemistry: ionic species have played a dominant role dating to Pedersen's discovery of the alkalai metal templated formation of crown ethers. [13] Ionic components can act as hosts (H) or guests (G), but the latter role is more common. [14]

To maximize attractive intermolecular interactions, many of these complexations have been carried out in low dielectric constant organic solvents (i.e., $\epsilon < 30$). Yet in spite of the known propensity of salts to ion pair in such solvents, [15] this factor has generally not been addressed. [16] On the contrary, as frequently encountered in the literature, association constants for 1:1 complex formation are based strictly on Eq. 2:



An experimentally equivalent expression would apply if the salt and complex were both fully dissociated ionic species.

We have applied Eq. 2 to the determination of formation constants for the pseudorotaxane system fashioned from dibenzo-24-crown-8 (H, DB24C8, **1**) and dibenzylammonium⁺X⁻ (G⁺X⁻, **2-X**), which is a simplified system in that it exhibits slow exchange on the ¹H NMR time scale (see Figure II-3). The single point method may thus be readily used to calculate $K_{a,\text{exp}}$, as has been consistently reported in the literature since Stoddart's discovery of the complex in 1995. [17] In this case, since the concentration of the complex, [**1**•**2**⁺X⁻], can be measured by the single point method, the concentration of the uncomplexed salt, [**2**⁺X⁻], is calculated to be [**2**⁺X⁻]₀ - [**1**•**2**⁺X⁻]; the concentration of the uncomplexed host, [**1**], is [**1**] = [**1**]₀ - [**1**•**2**⁺X⁻]. By definition, this treatment necessarily assumes that a) the slowly exchanging complex peak is the pseudorotaxane complex, as supported by available crystal structures and mass spectroscopy, b) the ion paired ammonium salt is the active guest ligand (or alternatively, that the fully dissociated salt is the active component), and c) the ion paired complex is formed (or alternatively, that the fully dissociated complex is formed).

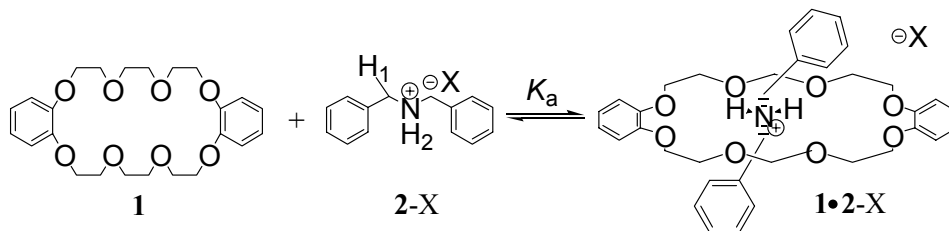
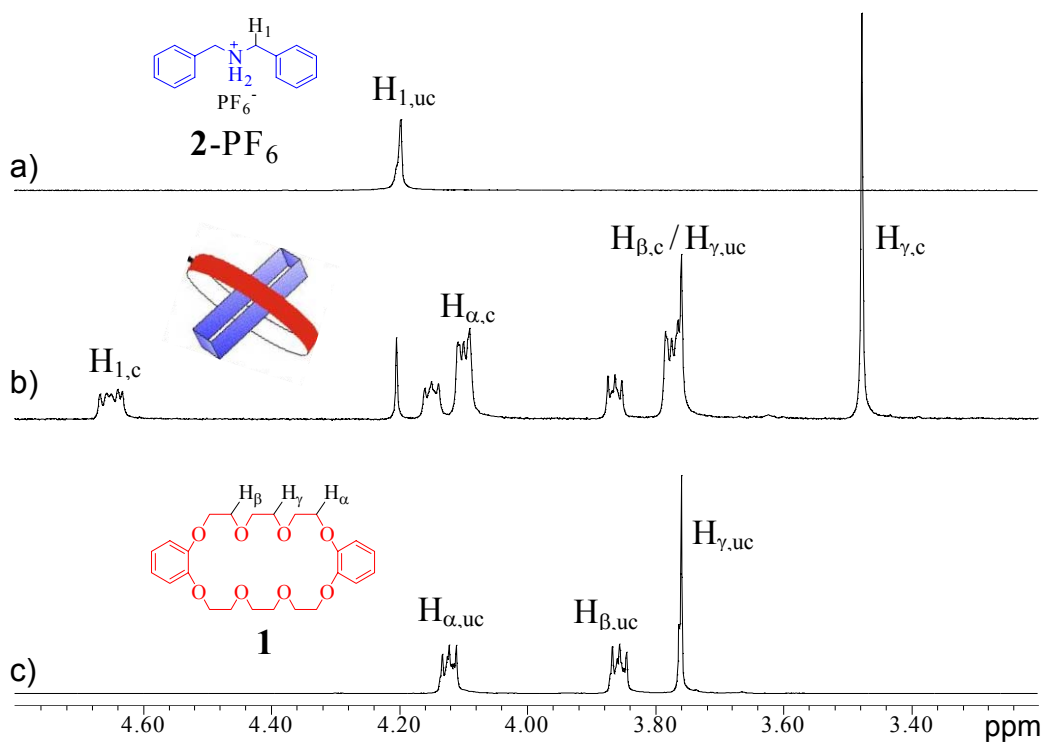
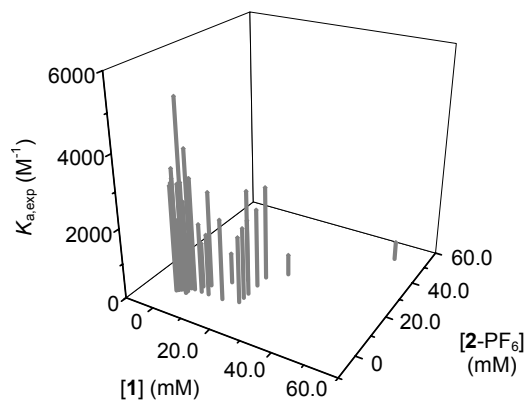


Figure II-3. ^1H NMR spectra (400 MHz) of solutions of a) **2**-PF₆, b) a 1:1 mixture of **1** and **2**-PF₆ (2 mM in each component initially), and c) **1** (3.82 mM initially) in CDCl₃:CD₃CN (3:2), 295 K. The subscripts “uc” and “c” refer to resonances belonging to uncomplexed and complexed host or guest, respectively.



As shown in Figure II-4 and Table II-1, results suggested that application of Eq. 2 to this system is not valid: the “apparent association constant” $K_{a,\text{exp}}$ was found to be highly concentration dependent, displaying a significant 16-fold variation of $K_{a,\text{exp}}$ under the concentrations studied. This observation was a troublesome result in light of the vast amount of literature reporting K_a values for this and like systems based on the single point method, values which we were not able to reproduce.

Figure II-4. $K_{a,\text{exp}}$ vs. $[1]$, $[2\text{-PF}_6]$ in $\text{CDCl}_3:\text{CD}_3\text{CN}$ (3:2), 295 K.**Table II-1.** $K_{a,\text{exp}}$ of $1/2\text{-PF}_6$ as a function of $[1]_0$ and $[2\text{-PF}_6]_0$ [$\text{CDCl}_3:\text{CD}_3\text{CN}$ (3:2), 295 K].

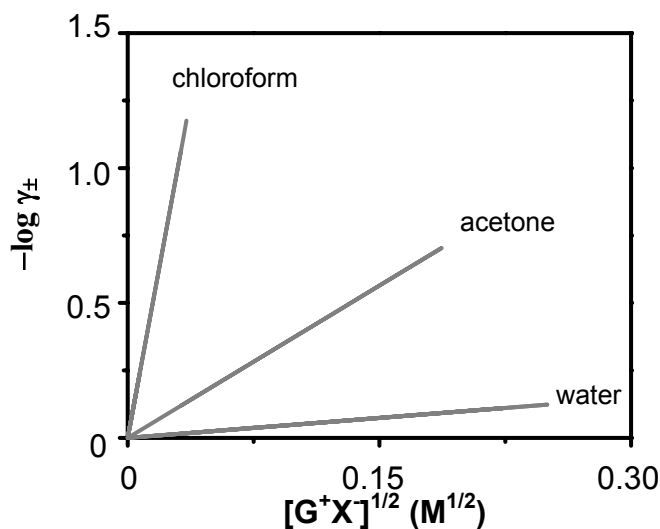
$[1]_0$ (mM)	$[2\text{-PF}_6]_0$ (mM)	fraction 1 complexed	$K_{a,\text{exp}}$ (M^{-1})	$[1]_0$ (mM)	$[2\text{-PF}_6]_0$ (mM)	fraction 1 complexed	$K_{a,\text{exp}}$ (M^{-1})
1.57	1.57	0.576	2.04×10^3	0.950	3.73	0.616	5.10×10^2
3.13	3.13	0.643	1.61×10^3	0.880	3.73	0.589	4.46×10^2
6.25	6.25	0.705	1.29×10^3	0.750	3.73	0.535	3.46×10^2
12.5	12.5	0.739	8.68×10^2	0.600	3.73	0.485	2.74×10^2
25.0	25.0	0.772	5.93×10^2	3.73	5.00	0.850	3.10×10^3
50.0	50.0	0.823	5.27×10^2	3.73	3.80	0.646	1.31×10^3
3.73	3.73	0.771	3.94×10^3	3.73	1.93	0.437	2.59×10^3
1.89	3.73	0.710	1.03×10^3	3.73	1.19	0.285	3.14×10^3
1.20	3.73	0.644	6.12×10^2	3.73	0.918	0.231	5.33×10^3

In fact, this is not a surprising result: by definition, Eq. 2 assumes ideal conditions, a fair assumption for the aqueous biological system from which the equilibrium model was derived, but a poor assumption for systems in low dielectric constant solvents (i.e., $\epsilon < 30$). These errors are highlighted by the work of Debye and Hückel, [18] who established as early as 1923 that the log of the mean ionic activity coefficient of a solution, $\log\gamma_{\pm\text{av}}$, is inversely proportional to $\epsilon^{3/2}$ at constant temperature, in which ϵ represents the dielectric constant of the solvent:

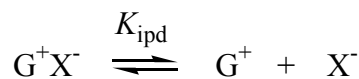
$$\log\gamma_{\pm\text{av}} = -1.823 \times 10^6 \frac{z_i^2}{(\epsilon T)^{3/2}} \sqrt{\mu} \quad \text{Eq. 3}$$

A plot of Eq. 3 for three solvents of differing dielectric constant (chloroform, $\epsilon = 4.81$; acetone, $\epsilon = 20.7$; water, $\epsilon = 80.2$) at 298 K for monovalent ions is shown in Figure II-5; note that the mean activity coefficient in solvents of dielectric constant less than 30, such as those solvents typically used in supramolecular assemblies, dramatically deviates from unity even at very low ionic strengths. For example, at an ionic strength of 0.01 M, $\gamma_{\pm\text{av}} = 0.46$ in chloroform versus $\gamma_{\pm\text{av}} = 0.99$ in water! From this example alone it is clear that one cannot assume ideality in non-aqueous systems involving charged species, as many reports in the supramolecular literature have erroneously proliferated.

Figure II-5. Limiting Debye-Hückel slopes for three solvents at 298 K.



Indeed, early researchers in the field such as Pedersen [19] and Frensdorff [20] explicitly used low concentrations of ionic solutions for that very reason. Recognizing that ion pairing is intimately tied to solution activity, a simple examination of ion pair dissociation clearly shows the error in assuming ideality in non-aqueous solvents of low ϵ relative to H₂O. Consider the salt G⁺X⁻, which dissociates into free cation G⁺ and free anion X⁻ (with the ion pair dissociation constant K_{ipd})



$$K_{\text{ipd}} = \frac{[\text{G}^+][\text{X}^-]}{[\text{G}^+\text{X}^-]} \quad \text{Eq. 4}$$

In the absence of other charged species, $[\text{G}^+] = [\text{X}^-] = x$, and by use of the quadratic formula:

$$x = \frac{-K_{\text{ipd}} \pm (K_{\text{ipd}}^2 + 4K_{\text{ipd}}[\text{G}^+\text{X}^-]_0)^{1/2}}{2} \quad \text{Eq. 5}$$

Solving for x based on various initial salt concentrations for three series of K_{ipd} values ranging from 10^{-2} to 10^{-4} M, values which are typical of organic salts in non-polar media salts, [21] allows for the construction of Figure II-6 and II-7. It is evident that ion pairing is an important consideration under these conditions.

Figure II-6. a) Degree of dissociation versus $[G^+X^-]_0$ and b) $[G^+X^-]_0$ versus $[G^+]$ for three values of K_{ipd} .

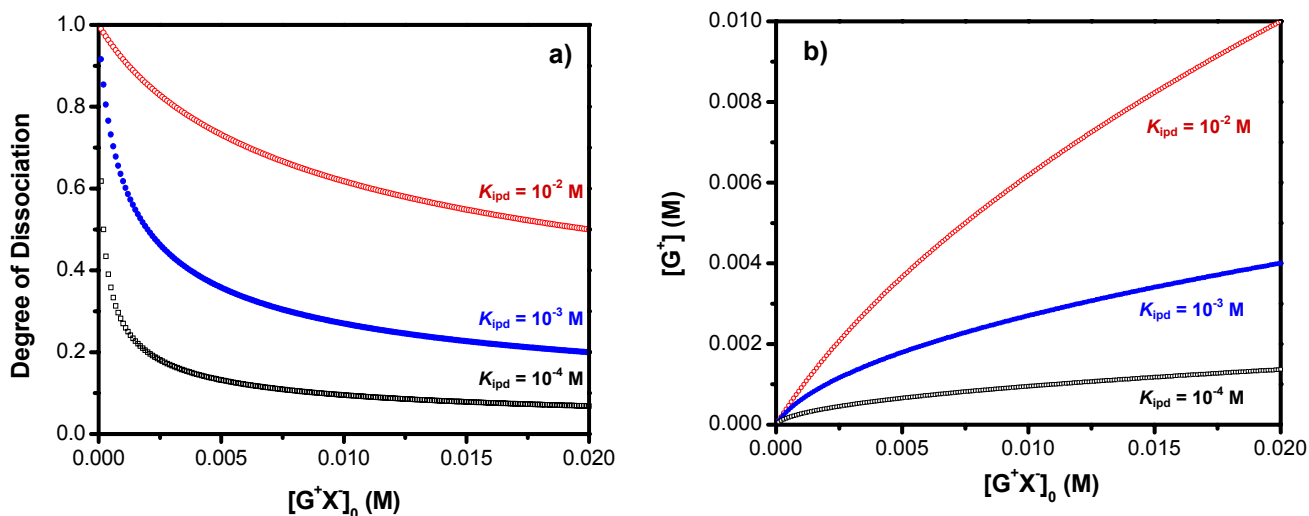
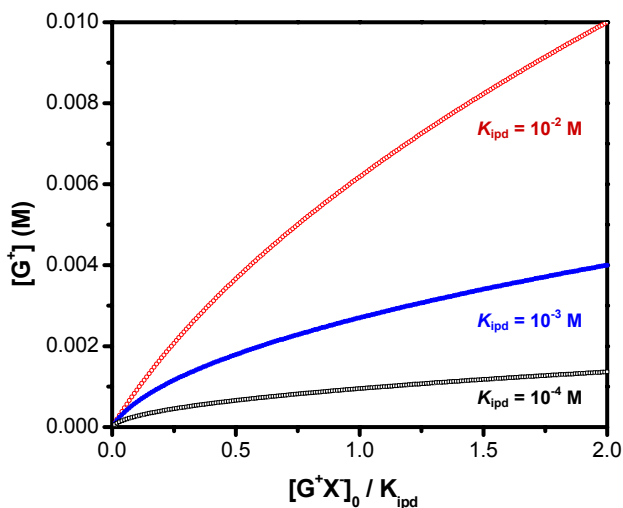


Figure II-7. $[G^+X^-]_0 / K_{ipd}$ versus $[G^+]$ for three values of K_{ipd} .

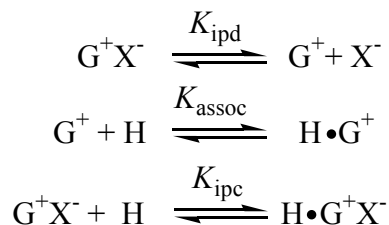


Unless operating in extremely dilute conditions in which the salt is nearly completely ionized (Figure II-6) and thus Eq. 1 is valid, one may not assume that concentration approximates activity for charged species in non-aqueous media, as the supramolecular literature has been wont to do. As a result from using models originally derived for aqueous systems, incomplete descriptions of association constants in non-

aqueous media have become commonplace, [22] the description of pseudorotaxane binding being one example.

II.3 *Quantification of Host/Guest Complexes Involving a Singularly Charged Component in Non-Aqueous Solvents: Comprehensive Model*

To account for ionic strength effects, [23] we consider the possibility that both the ion paired guest and the free guest ion may form a complex with the host (with the equilibrium constant K_{ipc} for complexation of the ion pair, and the equilibrium constant K_{assoc} for association of free guest ion) and assume that a) the electrolyte exists in solution as a monomer and b) there are no other species present. Recognizing that this treatment is amenable to either guest cation or guest anion binding, we here follow the specific case of cation binding for derivation purposes.



$$K_{ipd} = \frac{a_{G^+} a_{X^-}}{a_{G^+X^-}} = \frac{\gamma_+[G^+]\gamma_-[X^-]}{[G^+X^-]} = \frac{\gamma_{\pm}^2[G^+][X^-]}{[G^+X^-]} \quad \text{Eq. 6a}$$

Solving for $[G^+]$:

$$[G^+] = \frac{K_{ipd}[G^+X^-]}{\gamma_{\pm}^2[X^-]} \quad \text{Eq. 6b}$$

And

$$K_{assoc} = \frac{[H \cdot G^+]}{[G^+][H]} \quad \text{Eq. 6c}$$

Solving for $[H \cdot G^+]$:

$$[\text{H} \cdot \text{G}^+] = K_{\text{assoc}} [\text{H}][\text{G}^+] \quad \text{Eq. 6d}$$

Substituting Eq. 6b into 6d

$$[\text{H} \cdot \text{G}^+] = \frac{K_{\text{ipd}} K_{\text{assoc}} [\text{H}][\text{G}^+ \text{X}^-]}{\gamma_{\pm}^2 [\text{X}^-]} \quad \text{Eq. 6e}$$

Also,

$$K_{\text{ipc}} = \frac{[\text{H} \cdot \text{G}^+ \text{X}^-]}{[\text{G}^+ \text{X}^-][\text{H}]} \quad \text{Eq. 6f}$$

Solving for $[\text{H} \cdot \text{G}^+ \text{X}^-]$:

$$[\text{H} \cdot \text{G}^+ \text{X}^-] = K_{\text{ipc}} [\text{H}][\text{G}^+ \text{X}^-] \quad \text{Eq. 6g}$$

Focusing on analysis by spectroscopic methods, if slow exchange exists between $\text{H} \cdot \text{G}^+$ and $\text{H} \cdot \text{G}^+ \text{X}^-$, the two signals may be independently analyzed to determine K_{assoc} and K_{ipc} ; K_{ipd} may be determined in a similar fashion if slow exchange between $\text{G}^+ \text{X}^-$ and G^+ exists. When fast exchange between two species is noted, a more likely scenario in practice, the observed signal will represent both species. Thus, from Eq. 6e and Eq. 6g

$$[\text{H} \cdot \text{G}^+] + [\text{H} \cdot \text{G}^+ \text{X}^-] = \frac{K_{\text{ipd}} K_{\text{assoc}} [\text{H}][\text{G}^+ \text{X}^-]}{\gamma_{\pm}^2 [\text{X}^-]} + K_{\text{ipc}} [\text{H}][\text{G}^+ \text{X}^-] \quad \text{Eq. 6h}$$

In the case of fast exchange, $K_{\text{a,exp}}$ will be equal to

$$K_{\text{a,exp}} = \frac{([\text{H} \cdot \text{G}^+] + [\text{H} \cdot \text{G}^+ \text{X}^-])}{[\text{G}^+ \text{X}^-][\text{H}]} \quad \text{Eq. 6i}$$

and

$$K_{\text{a,exp}} = \frac{K_{\text{ipd}} K_{\text{assoc}}}{\gamma_{\pm}^2 [\text{X}^-]} + K_{\text{ipc}} \quad \text{Eq. 6j}$$

Conservation of charge requires that

$$[\text{X}^-] = [\text{G}^+] + [\text{H} \cdot \text{G}^+] \quad \text{Eq. 6k}$$

Substitution of Eqs. 6b and 6e into Eq. 6k

$$[X^-] = \frac{K_{\text{ipd}}[G^+X^-]}{\gamma_{\pm}^2[X^-]} + \frac{K_{\text{ipd}}K_{\text{assoc}}[H][G^+X^-]}{\gamma_{\pm}^2[X^-]} \quad \text{Eq. 6l}$$

with collection of terms and rearrangement

$$[X^-] = \left[\frac{K_{\text{ipd}}[G^+X^-]}{\gamma_{\pm}^2} (1 + K_{\text{assoc}}[H]) \right]^{1/2} \quad \text{Eq. 6m}$$

Substituting Eq. 6m into Eq. 6j:

$$K_{\text{a,exp}} = \frac{K_{\text{ipd}}^{1/2}K_{\text{assoc}}}{\gamma_{\pm} \{ [G^+X^-] (1 + K_{\text{assoc}}[H]) \}^{1/2}} + K_{\text{ipc}} \quad \text{Eq. 6n}$$

The first term of Eq. 6n represents the fraction of complex that exists as the free ion pair, and the second term results from ion paired pseudorotaxane formation.

Recalling that $K_{\text{a,exp}}$ is based on concentrations that may be determined spectroscopically, Eq. 6n yields an experimentally solvable equation. In the likely event that fast exchange between G^+X^- and G^+ is noted, the observable quantity, $[G^+]_{\text{observed}}$, is equal to $[G^+X^-] + [G^+]$. As a result, all solution sets based on Eq. 6n in which $[X^-]$ may not be determined directly must assume that all of the free guest exists as the fully ion paired salt, i.e., $[G^+]_{\text{observed}} \approx [G^+X^-]$. In fact, this assumption is only approximately valid in the specific instance that $[G^+X^-]_0 / K_{\text{ipd}}$ is large (Figure II-7), thereby leading to an overestimate of $[G^+X^-]$ in all other cases. If $K_{\text{a,exp}}$ is found to be independent of $[G^+X^-]$ and $[H]$, $K_{\text{total}} = K_{\text{a,exp}} = K_{\text{ipc}}$, e.g., all of the complex is formed as the ion pair $H \cdot G^+X^-$, and Eq. 2 is fully valid.

If $K_{\text{a,exp}}$ is found to be concentration dependent, one may consider two solutions sets. In the first, $K_{\text{assoc}}[H] \gg 1$ and Eq. 6n reduces to

$$K_{\text{a,exp}} = \frac{K_{\text{ipd}}^{1/2}K_{\text{assoc}}^{1/2}}{\gamma_{\pm} \{ [G^+X^-][H] \}^{1/2}} + K_{\text{ipc}} \quad \text{Eq. 6o}$$

Accordingly, the apparent “association constant,” $K_{\text{a,exp}}$, is dependent upon both $[G^+X^-]$ and $[H]$, as observed in Figure II-4 and Table II-1 for pseudorotaxane **1/2**-PF₆. Because a

plot of $K_{a,\text{exp}}$ versus $([G^+X^-][H])^{-1/2}$ will yield K_{ipc} as the y-intercept, this treatment is diagnostic of the nature of the complex, whether existing as an ion pair ($K_{a,\text{exp}}$ does not vary with concentration), a fully dissociated ion ($K_{\text{ipc}} = \text{y-intercept} = 0 \text{ M}^{-1}$), or somewhere in between (positive y-intercept).

Once K_{ipc} is known, a plot of $K_{a,\text{exp}} - K_{\text{ipc}}$ versus $([G^+X^-][H])^{-1/2}$ will yield $K_{\text{ipd}}^{1/2}K_{\text{assoc}}^{1/2}$ as the slope, with an intercept of 0. From $K_{\text{ipd}}^{1/2}K_{\text{assoc}}^{1/2}$, γ_{\pm} may then be calculated for every data point, which, to the best of our knowledge, is a novel approach to the experimental determination of mean activity coefficients of individual solutions. [24]

In the second solution set, $K_{\text{assoc}}[H] \ll 1$ and Eq. 6n reduces to

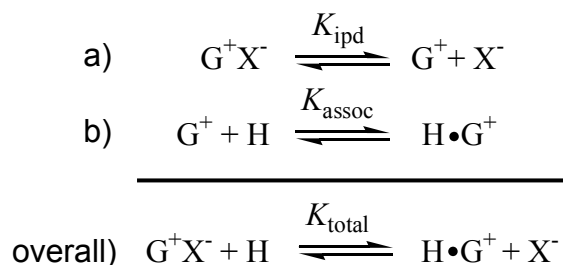
$$K_{a,\text{exp}} = \frac{K_{\text{ipd}}^{1/2}K_{\text{assoc}}^{1/2}}{\gamma_{\pm}[G^+X^-]^{1/2}} + K_{\text{ipc}} \quad \text{Eq. 6p}$$

In this regime, the apparent “association constant” is dependent only upon $[G^+X^-]$. K_{ipc} may be determined from the y-intercept of a plot of $K_{a,\text{exp}}$ versus $[G^+X^-]^{-1/2}$. Once K_{ipc} is known, a plot of $K_{a,\text{exp}} - K_{\text{ipc}}$ versus $[G^+X^-]^{-1/2}$ will yield $K_{\text{ipd}}^{1/2}K_{\text{assoc}}^{1/2}$ as the slope. As before, γ_{\pm} may be calculated for every data point.

Provided both binding regions are experimentally observable, the individual constants may then be determined from the ratio of the slopes. If both regions are not observable, as would be the expected case for complexes of either large K_{assoc} under the condition of low $[H]$ or for singularly charged guests with large K_{ipd} also under the condition of low $[H]$, manipulation of Eq. 6n itself becomes an intensive problem due to the inclusion of four unknown variables, K_{ipd} , K_{assoc} , K_{ipc} , and γ_{\pm} . A much simpler result emerges if $K_{\text{ipc}} = 0 \text{ M}^{-1}$, e.g., the complex exists as a fully dissociated ion. We next consider this special case.

II.4 *Quantification of Host/Guest Complexes Involving a Singularly Charged Component in Non-Aqueous Solvents: A Pre-equilibrium Model*

Allowing for ion pair dissociation as a pre-equilibrium step in the complexation process [25] and assuming that a) the electrolyte exists in solution as a monomer in equilibrium with its component ions, b) it is the free ammonium ion that forms the complex, the latter being fully dissociated, and c) there are no other species present, we derive the following model, again considering the specific case of cation binding for derivation purposes only:



$$K_{\text{total}} = \frac{\gamma_{\pm}^2 [\text{H}\cdot\text{G}^+][\text{X}^-]}{[\text{G}^+\text{X}^-][\text{H}]} = K_{\text{ipd}} K_{\text{assoc}} \quad \text{Eq. 7a}$$

Expressing the overall equilibrium as individual steps:

$$K_{\text{ipd}} = \frac{a_{\text{G}^+} a_{\text{X}^-}}{a_{\text{G}^+\text{X}^-}} = \frac{\gamma_+ [\text{G}^+] \gamma_- [\text{X}^-]}{[\text{G}^+\text{X}^-]} = \frac{\gamma_{\pm}^2 [\text{G}^+][\text{X}^-]}{[\text{G}^+\text{X}^-]} \quad \text{Eq. 7b}$$

Solving for $[\text{G}^+]$:

$$[\text{G}^+] = \frac{K_{\text{ipd}} [\text{G}^+\text{X}^-]}{\gamma_{\pm}^2 [\text{X}^-]} \quad \text{Eq. 7c}$$

And

$$K_{\text{assoc}} = \frac{[\text{H}\cdot\text{G}^+]}{[\text{G}^+][\text{H}]} \quad \text{Eq. 7d}$$

Solving for $[\text{H}\cdot\text{G}^+]$:

$$[\text{H}\cdot\text{G}^+] = K_{\text{assoc}} [\text{H}][\text{G}^+] \quad \text{Eq. 7e}$$

Substituting Eq. 7c into 7e

$$[\text{H}\cdot\text{G}^+] = \frac{K_{\text{ipd}} K_{\text{assoc}} [\text{H}][\text{G}^+\text{X}^-]}{\gamma_{\pm}^2 [\text{X}^-]} \quad \text{Eq. 7f}$$

In this case, the only observable complexed species is the free ion $\text{H}\cdot\text{G}^+$. From the common equilibrium expression:

$$K_{\text{a,exp}} = \frac{[\text{H}\cdot\text{G}^+]}{[\text{G}^+\text{X}^-][\text{H}]} \quad \text{Eq. 7g}$$

It becomes obvious upon inspection of Eq. 7g that the $K_{\text{a,exp}}$ is not based on a balanced chemical reaction. To correct for this oversight, which is clearly the root cause of the concentration dependence seen in Figure II-4, we plug Eq. 7f into Eq. 7g to yield

$$K_{\text{a,exp}} = \frac{K_{\text{total}}}{\gamma_{\pm}^2 [\text{X}^-]} = \frac{K_{\text{ipd}} K_{\text{assoc}}}{\gamma_{\pm}^2 [\text{X}^-]} \quad \text{Eq. 7h}$$

Conservation of charge requires that

$$[\text{X}^-] = [\text{G}^+] + [\text{H}\cdot\text{G}^+] \quad \text{Eq. 7i}$$

Which is identical to Eq. 6k. Thus, plugging Eq. 6m in Eq. 7h yields

$$K_{\text{a,exp}} = \frac{[\text{H}\cdot\text{G}^+]}{[\text{G}^+\text{X}^-][\text{H}]} = \frac{K_{\text{ipd}}^{1/2} K_{\text{assoc}}}{\gamma_{\pm} \{[\text{G}^+\text{X}^-](1 + K_{\text{assoc}}[\text{H}])\}^{1/2}} \quad \text{Eq. 7j}$$

As required, this equation is equivalent to Eq. 6n in the absence of ion pairing. Collection of terms from Eq. 7j yields

$$\frac{[\text{H}\cdot\text{G}^+]}{[\text{G}^+\text{X}^-]^{1/2}} = \frac{K_{\text{ipd}}^{1/2} K_{\text{assoc}} [\text{H}]}{\gamma_{\pm} (1 + K_{\text{assoc}}[\text{H}])^{1/2}} \quad \text{Eq. 7k}$$

which may be solved using concentrations determined by spectroscopic means. If slow exchange exists between G^+X^- and its component ions, one may readily deduce K_{ipd} ; if fast exchange is noted, $[\text{G}^+]_{\text{observed}} = [\text{G}^+\text{X}^-] + [\text{G}^+]$. As before, all solution sets based on

Eq. 7k in which $[X^-]$ may not be determined directly must assume that all of the free guest exists as the fully ion paired salt, i.e., $[G^+]_{\text{observed}} \approx [G^+X^-]$.

Under the pre-equilibrium condition, $K_{a,\text{exp}}$ will vary with $[H]$ and/or $[G^+X^-]$. To solve for the K_{ipd} and K_{assoc} , then, one may proceed as in section II.3, extrapolating the constants under the conditions $K_{\text{assoc}}[H] \gg 1$ and $K_{\text{assoc}}[H] \ll 1$. Alternatively, one may further simplify Eq. 7k by assuming $\gamma_{\pm} = 1$, thereby reducing the number of unknowns to two, which is then solvable by a non-linear least-squares fit. We discuss the former method first.

Much like Eq. 6n, Eq. 7k has two solution sets when solved directly. In the first, when $K_{\text{assoc}}[H] \gg 1$, Eq. 7k reduces to

$$\frac{[H \cdot G^+]}{[G^+X^-]^{1/2}} = \frac{K_{\text{ipd}}^{1/2} K_{\text{assoc}}^{1/2} [H]^{1/2}}{\gamma_{\pm}} \quad \text{Eq. 7l}$$

Under this condition, i.e., when $[H]$ is large, the free counterion essentially results from complex formation, and thus the assumption $[G^+]_{\text{observed}} \approx [G^+X^-]$ is approximately valid because the excess counterion from complexation drives the free guest towards its fully ion paired state. In this regime, the apparent ‘‘association constant’’ (Eq. 7j) is dependent upon both $[G^+X^-]$ and $[H]$. Solving for terms that may be determined experimentally yields

$$\frac{[H \cdot G^+]}{[H]^{1/2} [G^+X^-]^{1/2}} = \frac{K_{\text{ipd}}^{1/2} K_{\text{assoc}}^{1/2}}{\gamma_{\pm}} \quad \text{Eq. 7m}$$

Since at infinite dilution $\gamma_{\pm} = 1$, a plot of the left hand side of Eq. 7m vs. $[G^+X^-]_0$ extrapolated to zero concentration will yield $K_{\text{ipd}}^{1/2} K_{\text{assoc}}^{1/2}$ as the y-intercept. Returning to our consideration of activity coefficients, once $K_{\text{ipd}}^{1/2} K_{\text{assoc}}^{1/2}$ is known, γ_{\pm} may be calculated for every data point.

In the second binding regime, $K_{\text{assoc}}[H] \ll 1$, and

$$\frac{[H \cdot G^+]}{[G^+X^-]^{1/2}} = \frac{K_{\text{ipd}}^{1/2} K_{\text{assoc}} [H]}{\gamma_{\pm}} \quad \text{Eq. 7n}$$

Under this condition, i.e., when $[H]$ is low, the free counterion is essentially generated as a result of ion pair dissociation. Consequently, the assumption $['G']_{\text{observed}} \approx [G^+X^-]$ is not necessarily valid and is heavily dependent upon $[G^+X^-]/K_{\text{ipd}}$ (see Figure II-7). In this regime, the apparent “association constant” (Eq. 7j) is dependent only upon $[G^+X^-]$. Rearrangement yields

$$\frac{[H \cdot G^+]}{[H][G^+X^-]^{1/2}} = \frac{K_{\text{ipd}}^{1/2} K_{\text{assoc}}}{\gamma_{\pm}} \quad \text{Eq. 7o}$$

A plot of the left hand side of Eq. 7o vs. $[G^+X^-]_0$ extrapolated to zero concentration will yield $K_{\text{ipd}}^{1/2} K_{\text{assoc}}$ as the y-intercept. As before, γ_{\pm} may then be calculated for every data point. Provided both binding regions are experimentally observable, [26] the individual constants may then be determined from the ratio of the intercepts.

When both binding regions are not observable, one may estimate K_{assoc} and K_{ipd} by applying a least-squares fit of the non-linear Eq. 7k. However, this requires the assumption of ideal solution behavior, i.e., $\gamma_{\pm} = 1$, which has been previously argued to be an invalid assumption. Nonetheless, we will explore this approximation, noting that the individual constants will be underestimated in this case as the denominator of Eq. 7k contains the γ_{\pm} term.

To derive a non-linear least-squares fit of Eq. 7k, we need to find the minimum of the function ϕ over a range of k

$$\phi(K_{\text{ipd}}, K_{\text{assoc}}) \equiv \sum_k \left[\frac{K_{\text{ipd}} K_{\text{assoc}}^2 [H]_k^2}{(1 + K_{\text{assoc}} [H]_k)} - \frac{[H \cdot G^+]_k^2}{[G^+X^-]_k} \right]^2 \quad \text{Eq. 8a}$$

The values of K_{ipd} and K_{assoc} that minimize ϕ can be found by differentiating Eq. 8a with respect to K_{ipd} and K_{assoc} . Taking the partial derivative of ϕ with respect to K_{ipd}

$$\frac{\partial \phi}{\partial K_{\text{ipd}}} = K_{\text{ipd}} \sum_k \left[\frac{2 K_{\text{assoc}}^4 [H]_k^4}{(1 + K_{\text{assoc}} [H]_k)^2} \right] - \sum_k \left[\frac{2 [H \cdot G^+]_k^2 K_{\text{assoc}}^2 [H]_k^2}{[G^+X^-]_k (1 + K_{\text{assoc}} [H]_k)} \right] = 0 \quad \text{Eq. 8b}$$

Therefore, K_{ipd} becomes

$$K_{\text{ipd}} = \frac{\sum_k \left[\frac{[\text{H} \cdot \text{G}^+]_k^2 K_{\text{assoc}}^2 [\text{H}]_k^2}{[\text{G}^+ \text{X}^-]_k (1 + K_{\text{assoc}} [\text{H}]_k)} \right]}{\sum_k \left[\frac{K_{\text{assoc}}^4 [\text{H}]_k^4}{(1 + K_{\text{assoc}} [\text{H}]_k)^2} \right]} \quad \text{Eq. 8c}$$

Similarly, taking the partial derivative of ϕ with respect to K_{assoc}

Eq. 8d

$$\frac{\partial \phi}{\partial K_{\text{ap}}} = \sum_k 2 \left[\frac{K_{\text{ipd}} K_{\text{assoc}}^2 [\text{H}]_k^2}{(1 + K_{\text{assoc}} [\text{H}]_k)} - \frac{[\text{H} \cdot \text{G}^+]_k^2}{[\text{G}^+ \text{X}^-]_k} \right] \left[\frac{2 K_{\text{ipd}} K_{\text{assoc}} [\text{H}]_k^2}{(1 + K_{\text{assoc}} [\text{H}]_k)} - \frac{K_{\text{ipd}} K_{\text{assoc}}^2 [\text{H}]_k^2}{(1 + K_{\text{assoc}} [\text{H}]_k)^2} [\text{H}]_k \right] = 0$$

yields

$$K_{\text{ipd}} = \frac{\sum_k \left[\frac{2[\text{H} \cdot \text{G}^+]_k^2 K_{\text{assoc}} [\text{H}]_k^2}{[\text{G}^+ \text{X}^-]_k (1 + K_{\text{assoc}} [\text{H}]_k)} - \frac{[\text{H} \cdot \text{G}^+]_k^2 K_{\text{assoc}}^2 [\text{H}]_k^3}{[\text{G}^+ \text{X}^-]_k (1 + K_{\text{assoc}} [\text{H}]_k)^2} \right]}{\sum_k \left[\frac{2 K_{\text{assoc}}^3 [\text{H}]_k^4}{(1 + K_{\text{assoc}} [\text{H}]_k)^2} - \frac{K_{\text{assoc}}^4 [\text{H}]_k^5}{(1 + K_{\text{assoc}} [\text{H}]_k)^3} \right]} \quad \text{Eq. 8e}$$

Setting Eq. 8c equal to Eq. 8e allows one to solve for K_{assoc} using a root finding algorithm; K_{ipd} may then be solved accordingly. It must be remembered, however, the values thus derived are flawed in that γ_{\pm} has been set to unity in this non-linear least-squares fit.

A much simpler approach when both binding regions are not observable involves applying the first two terms of the binomial expansion [27] to the $\{1 + K_{\text{assoc}}[\text{H}]\}^{1/2}$ term of Eq. 7k. Provided $K_{\text{assoc}}[\text{H}]$ is small, i.e., ≤ 1.5 , which gives less than 10% error,

$$\{1 + K_{\text{assoc}}[\text{H}]\}^{1/2} \approx 1 + 0.5 K_{\text{assoc}} [\text{H}] \quad \text{Eq. 9a}$$

Substituting Eq. 9a into Eq. 7k,

$$\frac{[\text{H} \cdot \text{G}^+]}{[\text{G}^+ \text{X}^-]^{1/2}} = \frac{K_{\text{ipd}}^{1/2} K_{\text{assoc}} [\text{H}]}{\gamma_{\pm} (1 + 0.5 K_{\text{assoc}} [\text{H}])} \quad \text{Eq. 9b}$$

Taking the inverse of Eq. 9b and separating terms leads to

$$\frac{[G^+X^-]^{1/2}}{[H \bullet G^+]} = \frac{\gamma_{\pm}}{K_{ipd}^{1/2} K_{assoc}} \left(\frac{1}{[H]} \right) + \frac{\gamma_{\pm}}{2 K_{ipd}^{1/2}} \quad \text{Eq. 9c}$$

A plot of the left hand side of Eq. 9c vs. $1/[H]$ should be linear; limiting values of K_{assoc} and K_{ipd} may then be estimated from the slope and intercept.

II.5 Conclusions and Modifications

The above equilibrium models have been derived for the quantitative determination of association constants. This includes fast exchanged systems on the NMR time scale: once Δ_0 is known, $K_{a,exp}$ may be calculated on a point by point basis and the appropriate model implemented. It should be restated that although the models were derived for the specific case of singularly charged cation complexation, they may be directly applied to the complexation of singularly charged anions as well. In addition, the treatments are amenable to multiply charged species, as we recently reported for a divalent guest complexed by a neutral host. [28] It cannot be understated that all calculated constants for host/guest complexes involving charged component(s) in non-aqueous solvents are highly solvent dependent. Except in cases where $K_{a,exp}$ does not vary with $[G^{m+}X^{n-}]$ and is thus a true constant, i.e., $K_{a,exp} = K_{ipc}$, any comparison between systems in other dielectric media should be used for qualitative purposes only. Any "thermodynamic values" such as ΔH or ΔS derived using $K_{a,exp}$ calculated according to Eq. 2 are meaningless because γ_{\pm} varies with temperature, as shown in Eq. 3.

Finally, it is worth mentioning that current models used to describe binding in polytopic systems [29] such as the Scatchard [6] and Hill [30] treatments have also been derived on the basis of untested and invalid Eq. 2. While the equilibrium models derived in this chapter have been calculated specifically for 1:1 complexes, the protocols can be readily applied to other complex stoichiometries, thereby amending the current polytopic models to allow for ion pairing.

II.6 *References*

- [1] a) Griffey, R. H. *Chem. Biol.* **2002**, *9*, 958-959. b) Hirose, K. *J. Incl. Phenom. Macrocyc. Chem.* **2001**, *39*, 193-209. c) Rundlett, K. L.; Armstrong, D. W. *Electrophoresis* **2001**, *22*, 1419-1427. d) Fielding, L. *Tetrahedron* **2000**, *56*, 6151-6170. e) Connors, K. A. *Binding Constants*, John Wiley & Sons, New York, 1997.
- [2] Michnick, S. W. *Chem. Biol.* **2000**, *7*, R217-221.
- [3] Wilcox, C. S. In *Frontiers of Supramolecular Chemistry and Photochemistry*; Schneider, H. -J.; Durr, H., Eds.; VCH: Weinheim, 1991, p. 123.
- [4] see for example a) Stahl, N. G.; Zuccaccia, C.; Jensen, T. R.; Marks, T. *J. Am. Chem. Soc.* **2003**, *125*, 5256-5257. b) Zhao, T.; Beckham, H. W.; Gibson, H. W. *Macromolecules* **2003**, *36*, 4833-4837. c) Frish, L.; Vysotsky, M. O.; Matthews, S. E.; Böhmer, V.; Cohen, Y. *J. Chem. Soc., Perkin Trans. 2* **2002**, 88-93. d) Frish, L.; Sansone, F.; Casnati, A.; Ungaro, R.; Cohen, Y. *J. Org. Chem.* **2000**, *65*, 5026-5030.
- [5] Benesi, H.; Hildebrand, J. H. *J. Am. Chem. Soc.* **1949**, *71*, 2703-2707.
- [6] Scatchard, G. *Ann. N.Y. Acad. Sci.* **1949**, *51*, 660-672.
- [7] Creswell, C. J.; Allred, M. L. *J. Phys. Chem.* **1962**, *66*, 1469-1472.
- [8] Rose, N. J.; Drago, R. S. *J. Am. Chem. Soc.* **1959**, *81*, 798-799.
- [9] Gong, C.; Balanda, P. B.; Gibson, H. W. *Macromolecules* **1998**, *31*, 5278-5289.
- [10] Connors, K. A. *Binding Constants: The Measurement of Molecular Complex Stability*. John Wiley & Sons: New York, NY, 1987, pp. 46-86.
- [11] Weber noted that in order to minimize error in single site binding studies, the concentration of the species to be observed should remain constant at a value equal to $1/(10K_a)$ while the complementary species should be added at concentrations varying between $1/(10K_a)$ and $10/K_a$. [Weber, G. *Molecular Biophysics*. Pullman, B.; Weissbluth, M., Eds. Academic Press: New York, NY, 1965, 369-367.]
- [12] Deranleau, D. A. *J. Am. Chem. Soc.* **1969**, *91*, 4044-4049.
- [13] Pedersen, C. J. *J. Am. Chem. Soc.* **1967**, *89*, 7017-7036.

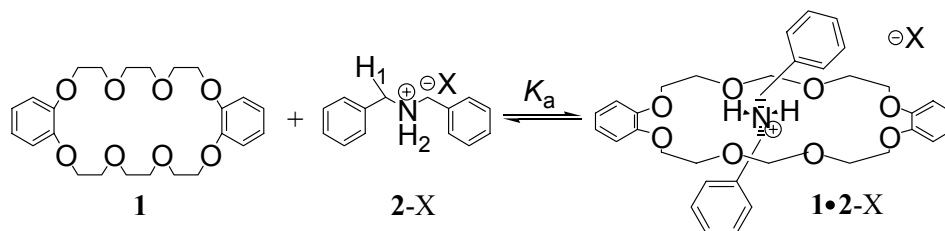
- [14] a) Beer, P. D.; Gale, P. A. *Angew. Chem., Int. Ed.* **2001**, *40*, 486-516. b) Andrews, P. C.; Kennedy, A. R.; Mulvey, R. E.; Raston, C. L.; Roberts, B. A.; Rowlings, R. B. *Angew. Chem., Int. Ed.* **2000**, *39*, 1960-1962. c) Antonisse, M. M. G.; Reinhoudt, D. N. *Chem. Commun.* **1998**, 443-448. d) Izatt, R. M.; Pawlak, K.; Bradshaw, J. S.; Bruening, R. L. *Chem. Rev.* **1995**, *95*, 2529-86. e) Izatt, R. M.; Pawlak, K.; Bradshaw, J. S. *Chem. Rev.* **1991**, *91*, 1721-2085. f) Merz, T.; Wirtz, H.; Vögtle, F. *Angew. Chem., Int. Ed.* **1986**, *25*, 567-568.
- [15] Isaacs, N. *Physical Organic Chemistry*, Longmans, England, 1995, pp. 56-62, 2nd Ed.
- [16] a few exception include a) Bartoli, S.; Roelens, S. *J. Am. Chem. Soc.* **2002**, *124*, 8307-8315. b) Kavallieratos, K.; Moyer, B. A. *Chem. Comm.* **2001**, *17*, 1620-1621. c) Shukla, R.; Kida, T.; Smith, B. D. *Org. Lett.* **2000**, *2*, 3099-3102. d) Monk, P. M. S.; Hodgkinson, N. M.; Patridge, R. D. *Dyes and Pigments* **1999**, *43*, 241-251. e) Hossain, M. A.; Schneider, H. -J. *Chem. Eur. J.* **1999**, *5*, 1284-1290. f) Arnaud-Neu, F.; Asfari, Z.; Souley, B.; Vicens, J. *New J. Chem.* **1996**, *20*, 453-463. g) Buschmann, H.-J.; Cleve, E.; Schollmeyer, E. *J. Solution Chem.* **1994**, *23*, 569-577. h) Kolthoff, I. M. *Can. J. Chem.* **1981**, *59*, 1548-1551.
- [17] Ashton, P. R.; Campbell, P. J.; Chrystal, E. J. T.; Glinke, P. T.; Menzer, S.; Philp, D.; Spencer, N.; Stoddart, J. F.; Tasker, P. A.; Williams, D. J. *Angew. Chem. Int. Ed.* **1995**, *34*, 1865-1869.
- [18] Debye, P.; Hückel, E. *Z. Physik* **1923**, *24*, 305-325.
- [19] Pedersen, C. J. *J. Am. Chem. Soc.* **1967**, *89*, 7017-7036.
- [20] Frensdorff, H. K. *J. Am. Chem. Soc.* **1971**, *93*, 4684-4688.
- [21] For R_4NX (R = Me, *n*-Pr, *n*-Bu, *i*-Am; X = PF₆, B(C₆H₅)₄, ClO₄, Cl, SCN) in CH₃CN $K_{ipd} = 2 - 4 \times 10^{-2}$ M [Barthel, J.; Iberl, L.; Rossmair, J. Gores, H. J.; Kaukal, B. *J. Solution Chem.* **1990**, *19*, 321-337], in acetone $K_{ipd} = 1 - 3 \times 10^{-3}$ M [Sayedoff, L. G. *J. Am. Chem. Soc.* **1966**, *88*, 664-667] and in CH₂Cl₂ $K_{ipd} = 1 \times 10^{-4}$ to 5×10^{-5} M [Romeo, R.; Arena, G.; Scolaro, L. M.; Plutino, M. R. *Inorg. Chem. Acta* **1995**, *240*, 81-92.]
- [22] exceptions include a) Mahoney, J. M.; Davis, J. P.; Beatty, A. M.; Smith, B. D. *J. Org. Chem.* **2003**, *68*, 9819-9820. b) Yamamoto, T.; Arif, A. M.; Stang, P. J. *J.*

- Am. Chem. Soc.* **2003**, *125*, 12309-12317. c) Arnaud-Neu, F.; Delgado, R.; Chaves, S. *Pure Applied Chem.* **2003**, *75*, 71-102. d) Buschmann, H. –J.; Schollmeyer, G. W. *Inorg. Chem. Comm.* **2001**, *4*, 53-56. e) D'Aprano, A.; Sesta, B.; Mauro, V.; Salomon, M. *J. J. Inclusion Phenomena Macrocyclic Chem.* **1999**, *35*, 451-465. f) Tusek-Bozic, L. *Electrochimica Acta* **1994**, *39*, 471-473. g) Chen, C.; Wallace, W.; Eyring, E. M.; Petrucci, S. *J. Phys. Chem.* **1984**, 5445-5450. h) Cambillau, C.; Bram, G.; Corset, J.; Riche, C. *Can. J. Chem.* **1982**, *60*, 2554-2565.
- [23] Jones, J. W.; Gibson, H. W. *J. Am. Chem. Soc.* **2003**, *125*, 7001-7004.
- [24] This approach does share some features with the use of ion-selective electrodes for determining osmotic and activity coefficients. See for example Barriada, J. L.; Covington, A. K.; Katakya, R. *J. Solution Chem.* **1999**, *28*, 555-565.
- [25] for related pre-equilibrium schemes, see a) Farber, H.; Petrucci, S. *J. Phys. Chem.* **1981**, *85*, 1396-1401 and b) Richman, H.; Harada, Y.; Eyring, E. M.; Petrucci, S. *J. Phys. Chem.* **1985**, *89*, 2373-2376.
- [26] any number of experimental techniques may be utilized, however calorimetric methods should not be employed to study complexations involving electrolytes, as these methods assume that corrected heats arise strictly from complex formation, thereby neglecting ion pair dissociation and ionic strength issues [D'Aprano, A.; Salomon, M.; Mauro, V. *J. Solution Chem.* **1995**, *24*, 685-702].
- [27] Bittenger, M. L.; Ellenbogen, D. J.; Johnson, B. *Elementary and Intermediate Algebra*; Addison-Wesley Publishing Co.: Reading, MA 1996; p 749.
- [28] Huang, F.; Jones, J. W.; Slebodnick, C.; Gibson, H. W. *J. Am. Chem. Soc.* **2003**, *125*, 14458-14464.
- [29] See a) Perlmutter-Hayman, B. *Acc. Chem. Res.* **1986**, *19*, 90-96. b) Freifelder, D. *Physical Biochemistry: Applications to Biochemistry and Molecular Biology*; W. H. Freeman and Co.: San Francisco, CA, 1982; 660-661.
- [30] Hill, A. V. *J. Physiol.* **1910**, *40*, iv-vii.

Chapter III
Supramolecular Interactions in Non-Aqueous Solvents:
Testing of an Equilibrium Model

III.1 Quantification of Pseudorotaxane Complexation and Error Analysis

The method of analysis for stoichiometric host/guest complexes involving a singularly charged component in non-aqueous solvents at moderate concentrations has been laid out in Chapter II. The foundation for these derivations resided in our inability to reproduce literature values of association constants for pseudorotaxane **1**•**2**-PF₆ by ¹H NMR spectroscopy. Importantly, we found that the “apparent association constant” ($K_{a,exp}$) was highly concentration dependent, displaying a significant 16-fold variation under the concentrations studied (Figure II-4 and Table II-1). Although the cause of the large variation was determined to be due to the failure of Eq. 2 to adequately account for ion pairing in such complexes, we nonetheless undertook error analyses to establish the validity of our technique.



To minimize experimental error in these studies, solutions were prepared by precisely weighing a minimum of 1.0×10^{-2} g each of the host or guest component by means of an analytical balance which read to 1.0×10^{-4} g into a 5.00 (± 0.02) or 10.00 (± 0.02) mL volumetric flask equipped with a ground glass stopper to make a moderately concentrated (nominally 16.0 mM) master solution. This solution was then sequentially diluted (no more than four sequential dilutions per master solution) by transferring specific volumes of the higher concentration solution to a clean volumetric flask via a to-

deliver volumetric pipette (± 0.006 mL) and diluting to the mark. The fresh solutions were filtered through a cotton-filled disposable pipette before 0.500 (± 0.006) mL of each solution component (both host and guest) at a specified concentration was transferred via a to-deliver pipette to a 5.0 mm NMR tube. NMR spectroscopic (NMRS) data were collected on a temperature (± 0.5 °C) controlled 400 MHz spectrometer within 1 hour of mixing the host and guest solutions. The fraction of total crown moieties occupied by guest (represented by θ) was determined by integration of the complexed and uncomplexed crown signals H_γ and/or $H_{ar,H}$; in cases where the crown signals overlapped neighboring resonances, the fraction of host occupied was determined by integration of the complexed and uncomplexed guest signals H_1 and/or $H_{ar,G}$. When feasible, all isolated resonances sets were checked against each other for consistency.

Concentration errors were calculated by accumulation of weighing and dilution errors. For example, the error in preparing $[1]_0 = 0.985$ mM was calculated as follows: 1.1104×10^{-2} g **1** (error in weighing = 5.0×10^{-5} g / 0.01104 g = 0.45%) was added to a 5.00 mL volumetric flask and diluted to the mark (dilution error = 2.0×10^{-5} L / 5.00×10^{-3} L = 0.4%). 2.000 mL of this 4.92 mM solution of **1** was then transferred by means of a volumetric pipette (pipette error = 6.0×10^{-6} mL / 2.00×10^{-3} mL = 0.3%) to a 10 mL volumetric flask and diluted to the mark (dilution error = 2.0×10^{-5} L / 10.00×10^{-3} L = 0.2%) to yield $[1]_0 = 0.985$ mM. The cumulative error is thus 1.35% . When equal volumes of host and guest are mixed, the cumulative error in both components is increased by 1.2% (6.0×10^{-6} L / 5.0×10^{-4} L = 1.2%); this is the largest source of error.

Spectrometer based errors were determined by preparing seven independent master solutions 8.00×10^{-3} M in **1** and seven independent master solutions 8.00×10^{-3} M in **2-TFA**. A total of twelve independent **1/2-TFA** mixtures at 4.00 mM in each component were then investigated by following H_γ , chosen because the pseudorotaxane resonance is well resolved from that of the free host. The average percentage of complexed crown was determined to be 23.9% , with a standard deviation of 0.3% (Table III-1). Nearly identical percent binding and standard deviations were found for the aromatic (24.2% , 0.3%) and benzylic (23.5% , 0.4%) protons of **2-TFA**. Because integration limits were manually set in these studies, and thus error introduced, a randomly chosen sample from the above twelve **1/2-TFA** mixtures was further examined.

Five independent Fourier transformations yielded a standard deviation in percent binding of 0.1%, signifying the high reproducibility of manual transformations (Table III-2). Of note, these studies were performed over the course of a full year: although relative humidity fluctuated greatly over this time frame, percent complexation did not (see Table III-1). We conclude that atmospheric water has little influence over binding properties in this system.

Table III-1. Percentage of Host occupied by Guest (θ) for twelve independently prepared solutions, initially 4.0 mM in both **1** and **2**-TFA, CDCl₃:CD₃CN (3:2), 295 K.

Sample	θ^a	θ^b	θ^c	θ^d
A	0.240	0.250	0.238	0.230
B	0.237	0.260	0.232	0.241
C	0.238	0.250	0.232	0.239
D	0.248	0.251	0.231	0.239
E	0.245	0.248	0.238	0.238
F	0.243	0.250	0.239	0.242
G	0.245	0.246	0.238	0.239
H	0.242	0.245	0.232	0.237
I	0.239	0.245	0.226	0.239
J	0.242	0.245	0.239	0.239
K	0.244	0.250	0.239	0.238
L	0.241	0.251	0.237	0.241
Ave	0.242	0.249	0.235	0.239
Std Dev	0.003	0.004	0.004	0.003

Determined by ^{a)} H_{Ar,G}, ^{b)} H_{Ar,H}, ^{c)} H₁, or ^{d)} H_γ

Table III-2. Percentage of Host occupied by guest (θ) for 5 independent Fourier transformations of a randomly chosen sample from Table III-2 ($[1]_0 = [2\text{-TFA}]_0 = 4.00$ mM, $\text{CDCl}_3:\text{CD}_3\text{CN}$ (3:2), 295 K).

Sample	θ^a	θ^b	θ^c	θ^d
L	0.241	0.251	0.237	0.241
L	0.244	0.252	0.235	0.242
L	0.242	0.253	0.236	0.243
L	0.244	0.251	0.239	0.242
L	0.243	0.252	0.236	0.242
Ave	0.243	0.252	0.237	0.242
Std Dev	0.001	0.001	0.002	0.001

Determined by ^{a)} $H_{\text{Ar,G}}$, ^{b)} $H_{\text{Ar,H}}$, ^{c)} H_1 , or ^{d)} H_γ

We factored into our calculations errors from solution preparation and NMRS integration. For integration errors, we allowed a standard deviation of $\pm 2\%$ in the calculated percentage of complexed **1**, which grossly overestimates the true errors as determined from Tables III-2 and III-3. These errors are then followed through all subsequent calculations, resulting in the maximum possible error in these studies. For analysis, data points above 90% and below 10% complexed were ignored. [1]

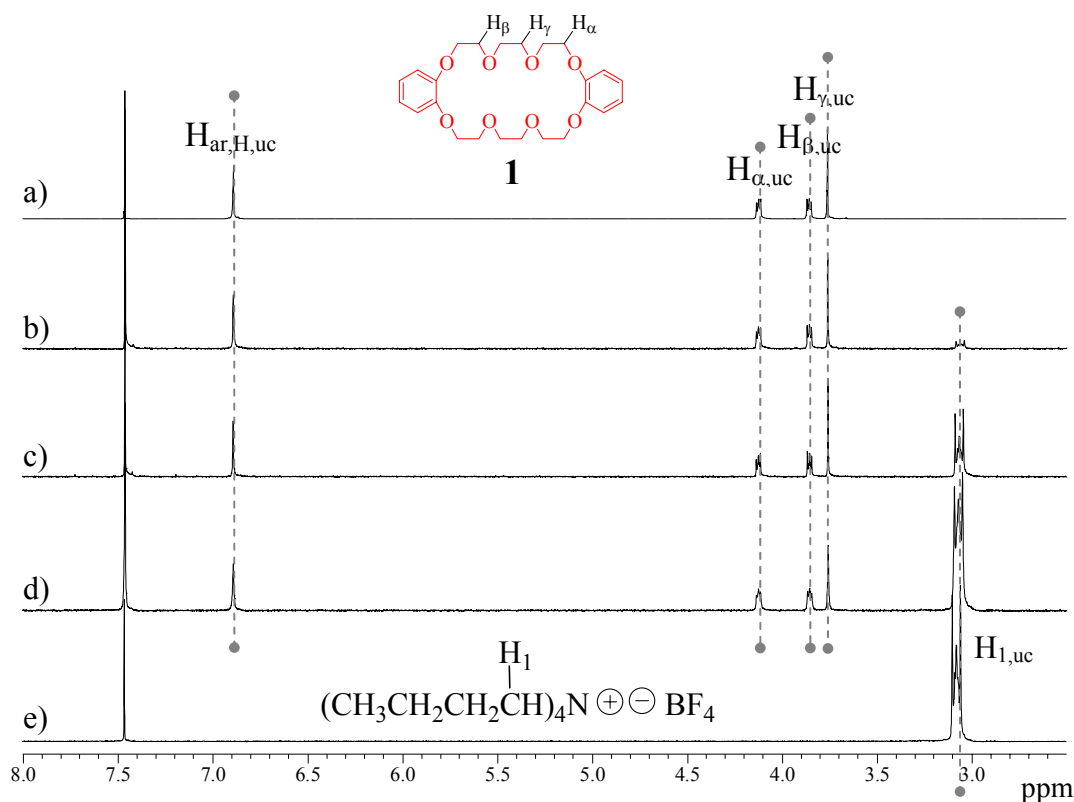
III.2 *Probing Inconsistencies From the Literature*

Given the high reproducibility displayed in Tables III-1 and III-2, we were confident that our experimental methods were valid, and that the concentration dependence displayed in Figure II-4 and Table II-1 was real, as expected in light of the work of Debye and Hückel. [2] Recognizing the failure of Eq. 2 to adequately incorporate ionic strength effects into complexations involving charged species, we developed three model experiments designed to probe the influence of ion pairing in pseudorotaxane **1•2-X**. For these studies, a series of **2-X** salts [X= chloride, hexafluorophosphate,

methanesulfonate, *p*-toluenesulfonate (OTs), tetrafluoroborate, trifluoromethanesulfonate and trifluoroacetate (TFA)] were prepared.

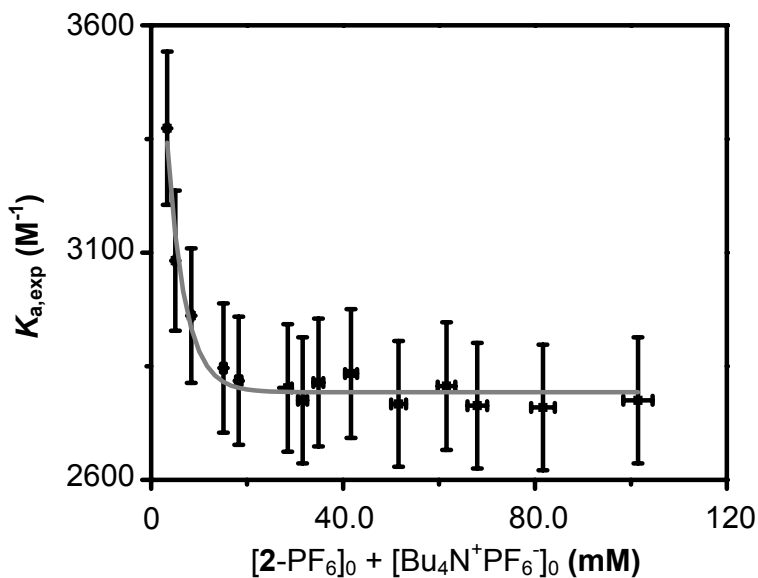
In the first model experiment, $(n\text{-Bu})_4\text{N}^+\text{BF}_4^-$ (0.313 to 6.20 mM) was titrated into a 0.657 mM solution of **1** in $\text{CDCl}_3:\text{CD}_3\text{CN}$ (3:2). Shown in Figure III-1, the addition of $(n\text{-Bu})_4\text{N}^+\text{BF}_4^-$ to **1** had no influence on the ^1H NMR chemical shifts of **1**, implying no interaction between salt and crown. Identical results were found for $(n\text{-Bu})_4\text{N}^+\text{PF}_6^-$ as well as $(n\text{-Et})_4\text{N}^+\text{TFA}^-$.

Figure III-1. ^1H NMR spectra (400 MHz) of a) **1**, b) **1** (0.657 mM initially) and $(n\text{-Bu})_4\text{N}^+\text{BF}_4^-$ (0.627 mM initially), c) **1** (0.657 mM initially) and $(n\text{-Bu})_4\text{N}^+\text{BF}_4^-$ (2.50 mM initially), d) **1** (0.657 mM initially) and $(n\text{-Bu})_4\text{N}^+\text{BF}_4^-$ (6.20 mM initially), and e) $(n\text{-Bu})_4\text{N}^+\text{BF}_4^-$ in $\text{CDCl}_3:\text{CD}_3\text{CN}$ (3:2), 295 K.



For the second model experiment, $(n\text{-Bu})_4\text{N}^+\text{BF}_4^-$ (0.313 to 6.20 mM) was titrated into a $\text{CDCl}_3:\text{CD}_3\text{CN}$ (3:2) solution 0.657 mM in **1** and 1.27 mM in **2-BF**₄. $K_{a,\text{exp}}$ (Eq. 2) reached an asymptotic limit approaching $9.3 \times 10^2 \text{ M}^{-1}$ at high salt concentrations. An asymptotic limit approaching $2.7 \times 10^3 \text{ M}^{-1}$ was found for the case where $(n\text{-Bu})_4\text{N}^+\text{PF}_6^-$ (1.68 to 100 mM) was titrated into a constant concentration of **1** and **2-PF**₆ (1.67 mM in each) as shown in Figure III-2. Furthermore, the ¹H NMR complex signals were found to merge into the baseline when 50.2 mM $(\text{CH}_3\text{CH}_2)_4\text{N}^+\text{TFA}^-$ was added to a solution 2.50 mM in **1** and **2-TFA**; the same observation was noted upon 50.0 mM addition of $(n\text{-Bu})_4\text{N}^+\text{OTs}^-$ to a $\text{CDCl}_3:\text{CD}_3\text{CN}$ (3:2) solution 2.50 mM in **1** and **2-OTs**. It is important to note that the associated error bars in Figure III-2, and all subsequent figures, are maximum values as described above.

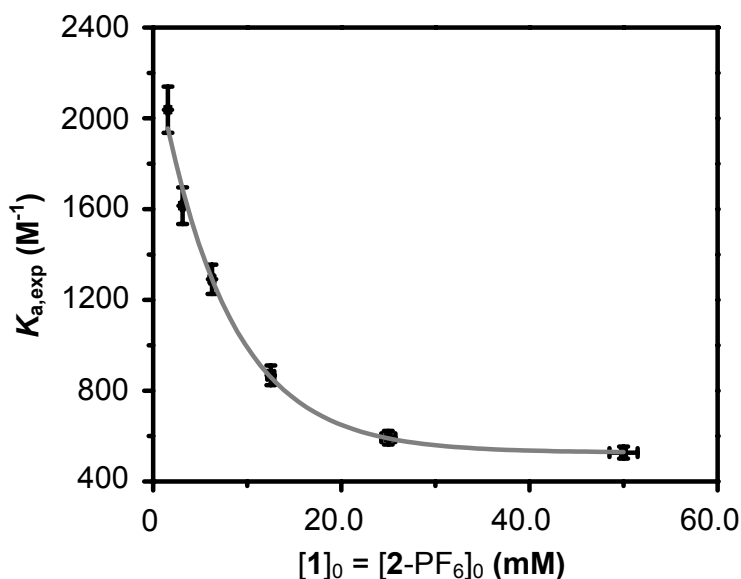
Figure III-2. Influence of $\text{Bu}_4\text{N}^+\text{PF}_6^-$ on $K_{a,\text{exp}}$ when added at various concentrations to equimolar (1.67 mM initially) solutions of **1/2-PF**₆ in $\text{CDCl}_3:\text{CD}_3\text{CN}$ (3:2), 295 K. A 1st order exponential decay has been added to guide the eye.



In the third, $\text{CDCl}_3:\text{CD}_3\text{CN}$ (3:2) solutions of **1/2-PF**₆ were investigated over a broad range of equimolar concentrations (1 to 50 mM). A plot of $K_{a,\text{exp}}$ versus $[\mathbf{2-PF}_6]$

resulted in a downward sloping, non-linear curve which again approached an asymptotic limit at high ionic strength (Figure III-3), but this limit ($4.5 \times 10^2 \text{ M}^{-1}$) was different than that of Figure III-2. The same asymptotic behavior was found when stoichiometric ratios of $1/2\text{-BF}_4$ were investigated (with a limit approaching $1.3 \times 10^3 \text{ M}^{-1}$).

Figure III-3. Influence of component concentration on $K_{a,\text{exp}}$ for equimolar solutions of **1** and **2-PF₆** in $\text{CDCl}_3:\text{CD}_3\text{CN}$ (3:2), 299 K. A 1st order exponential decay has been added to guide the eye.



From a pragmatic standpoint, the leveling off of $K_{a,\text{exp}}$ at high ionic strength is advantageous in that reproducible values of $K_{a,\text{exp}}$ are realized. From a more rigorous perspective, however, the above studies confirm the concentration dependence exhibited in Figure II-4 and unambiguously demonstrate that Eq. 2 is not a valid treatment for these systems as the variation in $K_{a,\text{exp}}$ is well outside experimental error. The observed changes in $K_{a,\text{exp}}$ with electrolyte concentration indicate that ion pairing needs to be considered, as expected given the known propensity of salts to ion pair in low-dielectric (i.e., $\epsilon < 30$) constant solvents. [3] These factors have not been accounted for in Eq. 2, which again incorrectly assumes that the ion paired salt is the active component and that the complex is also ion paired (or, alternatively, that both the guest salt and complex are

100% dissociated). [4] Further information was gleaned from observations in the ^1H NMR (Figure III-4): the chemical shifts attributed to the pseudorotaxane complex were invariant with concentration, whereas the chemical shifts attributed to free **2**-TFA moved downfield with decreasing concentration. The same observations were noted for every **2**-X (X = PF_6 , BF_4 , OTs) salt investigated. It is noteworthy that the absolute shifts of complex peaks did not change with anion (Figure III-5). This result is consistent with observations previously reported. [5]

Figure III-4. ^1H NMR spectra (400 MHz) of solutions of **1** (3.82 mM initially) and **2**-TFA [initially a) 20.0 mM, b) 15.4 mM, c) 7.71 mM, and d) 3.85 mM] in $\text{CDCl}_3:\text{CD}_3\text{CN}$ (3:2), 295 K.

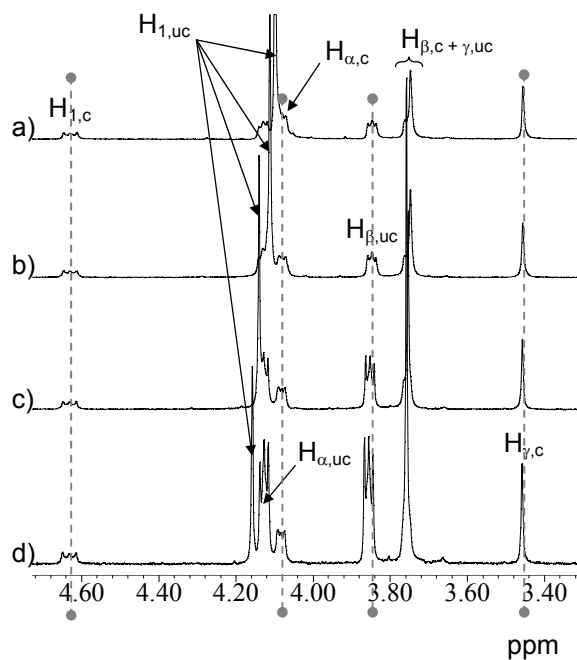
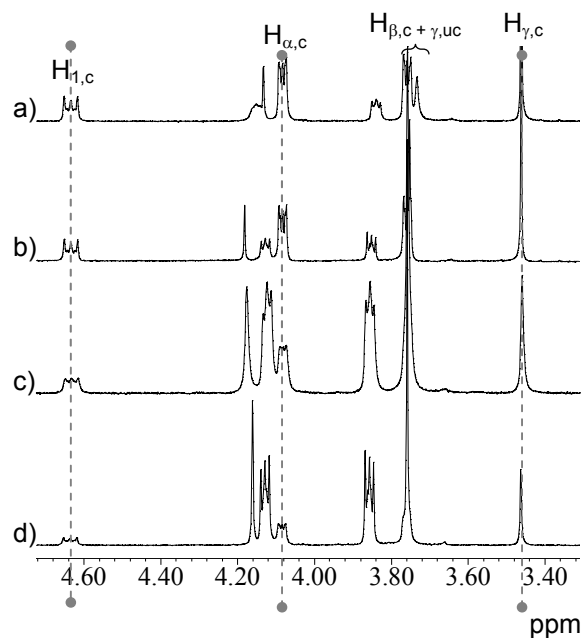


Figure III-5. ^1H NMR spectra (400 MHz) of equimolar solutions (4.00 mM initially) of **1** and a) **2-PF₆**, b) **2-BF₄**, c) **2-OTs**, and d) **2-TFA** in $\text{CDCl}_3:\text{CD}_3\text{CN}$ (3:2), 295 K.



From these studies, we conclude that 1) a distinct ion pair equilibrium exists for the secondary ammonium salts, here observed as a fast exchange process, [6] and 2) the complex is not ion paired as the chemical shifts of the complex are static with respect to concentration (i.e., the fast exchange process observed for the salt does not exist for the complex, Figure III-4) and anion (Figure III-5). In support of these observations, Montalti and Prodi earlier reported that addition of $\text{Bu}_4\text{N}^+\text{Cl}^-$ to a solution of **1** and 9-anthrylmethylmethylammonium- PF_6 in CD_2Cl_2 effectively resulted in dethreading of the known pseudorotaxane, a phenomenon attributed to the formation of a tight ammonium chloride ion pair which hinders complex formation. [7] Montalti and Prodi's results also qualitatively justify the loss of complex signal for **1/2-OTs** and **1/2-TFA** upon the addition of a large excess of $\text{R}_4\text{N}^+\text{X}^-$: because quaternary ammonium ion pairs are more readily solvated than are secondary ammonium salts, the free X^- drives ion pairing of **2-X**, resulting in less free **2⁺** available for complexation. In addition, these results also reveal why the two asymptotes of Figures III-2 and III-3 are different: addition of $[\text{X}^-]$

from a more readily ionized source dramatically shifts the equilibrium of the charged guests relative to the case when the guest ion pair is the only electrolyte in the system.

Discussed in Chapter I, [2.2.2]cryptands are known to fully envelope K^+ , Rb^+ , and Cs^+ ions, thereby forming separated ion pairs, as determined by spectroscopic studies. [8] Complexation of the same metal ions by the less sterically insulating host 18-crown-6, on the other hand, enables contact ion pairs to form. Kochi et al. have recently reinvestigated ion pairing in both complexes and confirmed the spectroscopic results on the basis on X-ray crystallography. [9] Classifying contact versus separated ion pairs according to the intercharge distance between the positive and negative centers, the researchers establish contact ion pairs as having an intimate contact of less than 3 Å, while separated ion pairs show charge center separations of 6 Å or more. Importantly, the researchers noted that the same spectral characteristics inherent in the solid-state spectra exist in a THF solution of the dissolved pure crystalline complexes, demonstrating the validity in extending lessons learned in the solid state to solution.

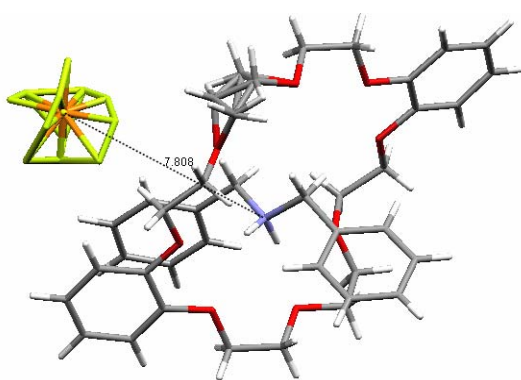
Intrigued by these investigations, we have explored available single crystal X-ray structures of pseudorotaxane **1**•**2**-PF₆. [10] The large separation between the cation and anion centers (Figure III-6a, 7.808 Å) corroborate results from Figures III-4 and III-5, further suggesting that according to Kochi's definition the complexes are not ion paired *even in the solid state*, which is void of solvent/ion interactions that would otherwise impart stability to an isolated ion in the form of charge shielding. The absolute distances given in Figure III-6 will be reduced by 2.5 Å if one considers distance from the nearest neighboring PF₆⁻ fluorine to the cationic center. Additional crystal structures of DB24C8 complexes with ammonium PF₆ (Figure III-6b), [11] bis(4-chlorobenzyl)ammonium PF₆ (Figure III-6c), [12] and bis(3-nitrobenzyl)ammonium PF₆ (Figure III-6d), [12] display similar results.

Interestingly, Stoddart et al. reached the same conclusion in 1999, [13] stating that because the PF₆ anions are disordered [14] in ammonium complexes involving host **1**, "there is no interaction with the cationic species (in the solid state)." This statement is the opposite conclusion reached in this work by solving the crystal structures of the guest salts themselves, **2**-TFA, **2**-OTs, and **2**-CF₃SO₃. Intimate association of the ions (i.e., < 2.8 Å) results in alternating linear self-assembled arrays (**2**-TFA, Figure III-7 and **2**-OTs,

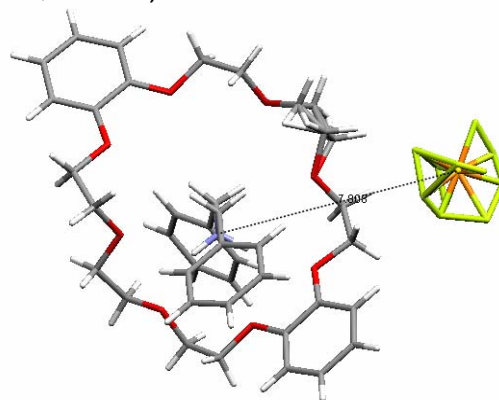
Figure III-8) or dimers ($2\text{-CF}_3\text{SO}_3$, Figure III-9) due to the di- and tritopic anions which H-bond to the acidic ammonium cation.

Figure III-6. Published crystal structures showing the charge separation between cation and anion centers for complexes with **1** and *a*) 2-PF_6 (7.808 Å), *b*) ammonium- PF_6 (7.423 Å) *c*) bis(4-chlorobenzyl)ammonium- PF_6 (7.866 Å), and *d*) bis(3-nitrobenzyl) ammonium- PF_6 (8.246 Å).

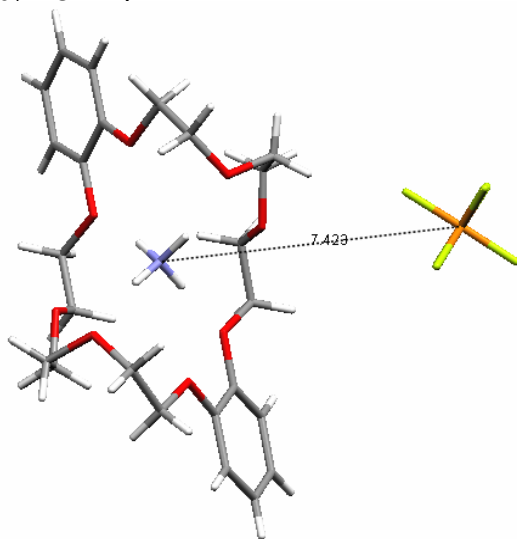
a, view 1)



a, view 2)



b, view 1)



b, view 2)

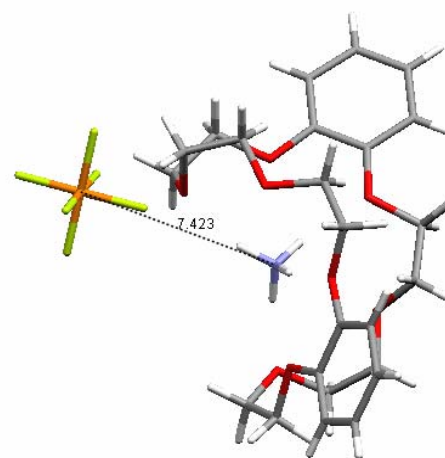
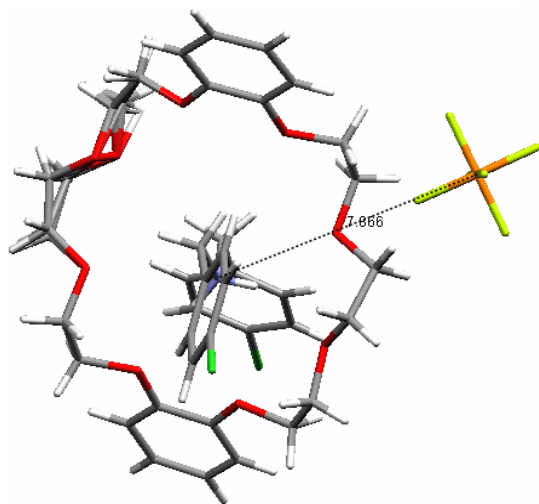
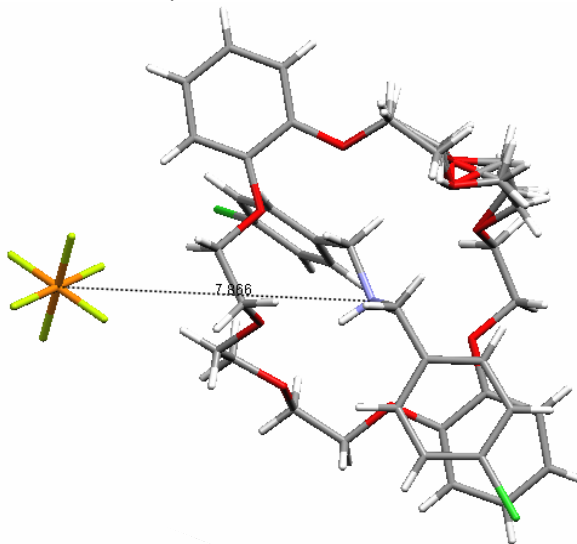


Figure III-6. Published crystal structures showing the charge separation between cation and anion centers for complexes with **1** and *a*) 2-PF₆ (7.808 Å), *b*) ammonium-PF₆ (7.423 Å), *c*) bis(4-chlorobenzyl)ammonium-PF₆ (7.866 Å), and *d*) bis(3-nitrobenzyl) ammonium-PF₆ (8.246 Å).

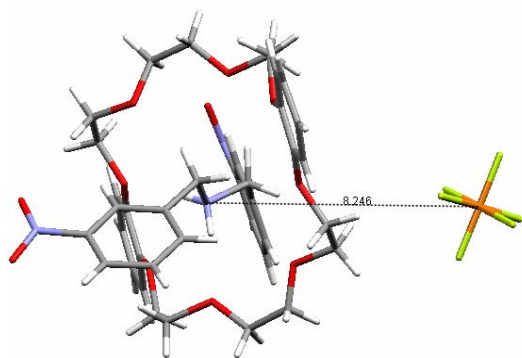
c, view 1)



c, view 2)



d, view 1)



d, view 2)

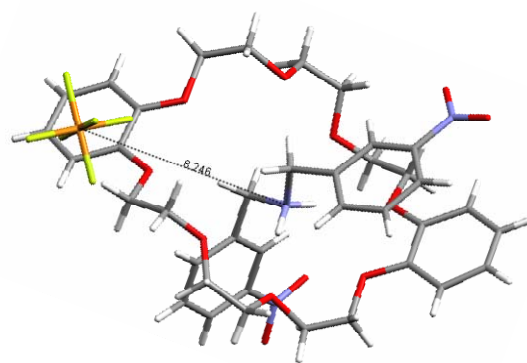


Figure III-7. Crystal packing diagrams of 2-TFA. The dashed lines show all contacts that lie within the van der Waal's radii of individual atoms.

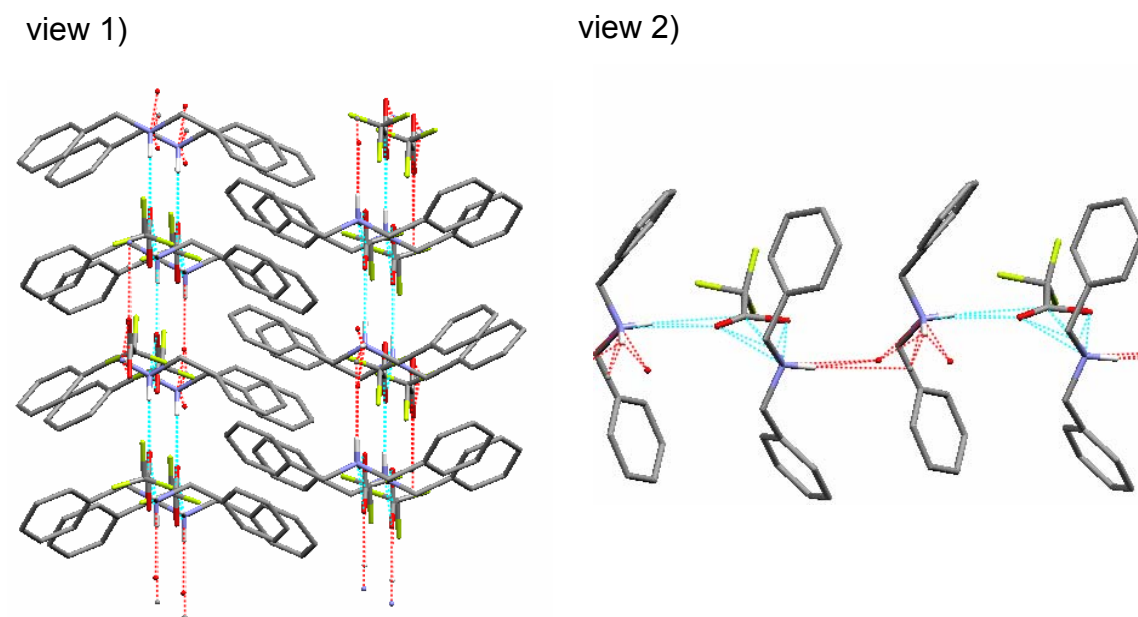


Figure III-8. Crystal packing diagrams of 2-OTs. The dashed lines show all H-bond contacts.

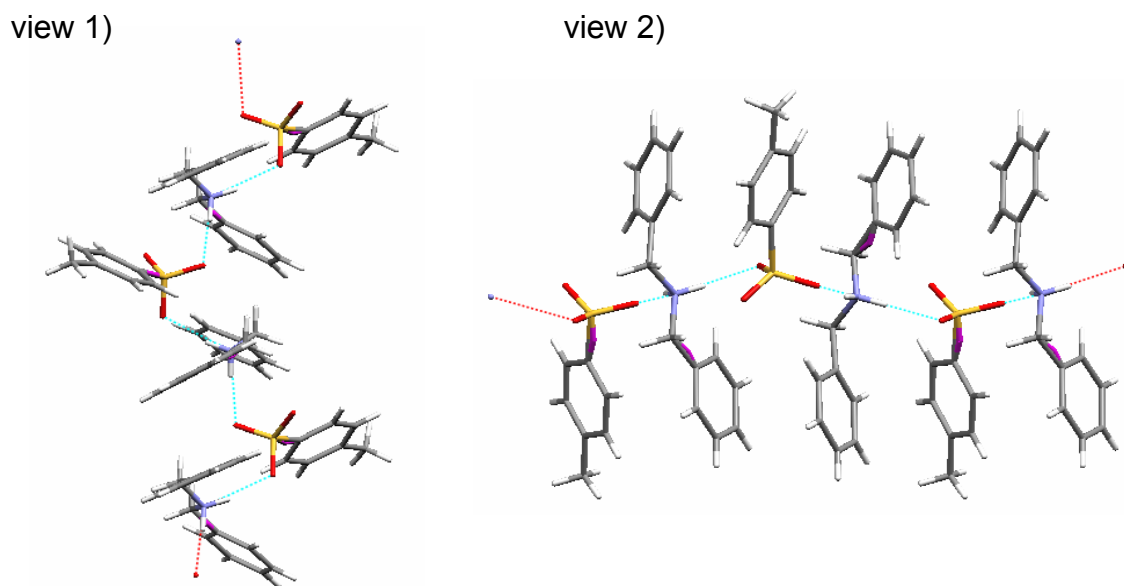
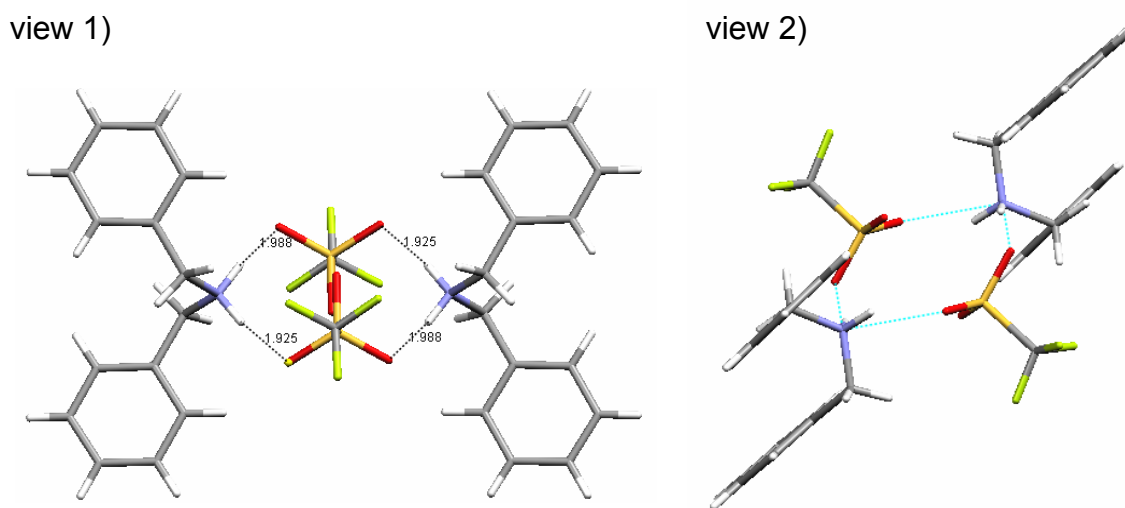


Figure III-9. Crystal packing diagrams of **2-CF₃SO₃**. The dashed lines show all H-bond contacts. Distances given in Å.



III.3 *Piecing Together the Puzzle: Application of the Pre-Equilibrium Model to Pseudorotaxane 1•2-X*

To formulate an equilibrium model which accounts for each of the observations made in Section II.4, we consider ion pair dissociation as a pre-equilibrium step in the complexation process and assume that a) the electrolyte exists in solution as a monomer in equilibrium with its component ions, b) it is the free ammonium ion that forms the complex, the latter being fully dissociated, and c) there are no other species present. [15] Accordingly, Eq. 7k may be solved using concentrations determined experimentally by spectroscopic means. Because ion pair dissociation of **2-X** is a fast exchange process (Figure III-4), one must assume that all of the free guest exists as the fully ion paired salt; thus $[G^+]_{\text{observed}} \approx [G^+X^-]$. As previously described, this assumption is only approximately valid in the specific instance that $[G^+X^-]_0 / K_{\text{ipd}}$ is large (Figure III-7), thereby leading to an overestimate of $[G^+X^-]$ in all other cases.

We thus investigated pseudorotaxane **1•2-X** formation under the $K_{\text{assoc}}[\text{H}] \gg 1$ and $K_{\text{assoc}}[\text{H}] \ll 1$ binding regimes according to Eqs. 7m and 7o and have relied

exclusively on ^1H NMR to follow complexation. [16] Under the condition $K_{\text{assoc}}[\text{H}] \gg 1$, provisionally assuming $K_{\text{assoc}} = 5.0 \times 10^2 \text{ M}^{-1}$, we studied host/guest solutions in which $[\mathbf{1}]_0 \geq 15.0 \text{ mM}$ ($K_{\text{assoc}}[\text{H}] \geq 7.5 \gg 1.0$, Figure III-10). At the other extreme, $K_{\text{assoc}}[\text{H}] \ll 1$, we studied host/guest solutions in which $[\mathbf{1}]_0 \leq 0.500 \text{ mM}$ ($K_{\text{assoc}}[\text{H}] \leq 0.25 \ll 1.0$, Figure III-11), allowing $[\text{'G'}]_{\text{observed}} \approx [\text{G}^+\text{X}^-]$. Interestingly, Figures III-10 and III-11 were found to be linear under experimental conditions, which suggests that either γ_{\pm} is constant under the conditions explored, an unlikely scenario, or that γ_{\pm} varies linearly with concentration.

Table III-3 is based upon plots of Eqs. 7m (Figure III-10) and 7o (Figure III-11) for $\mathbf{1}/\mathbf{2}\text{-X}$ [$\text{X} = \text{a) PF}_6, \text{b) BF}_4, \text{c) TFA, d) OTs}$]. Reassuringly, the values of K_{ipd} in Table III-3 are in accord with reported activity-based values for tetraalkylammonium salts [17] and concur with the observation that PF_6 salts are generally the most dissociated. [18] Moreover, the values of K_{assoc} for all salts are within experimental error, as mandated by this equilibrium treatment. Because Table III-3 includes analysis based on activity coefficients, whereas all other previously published values assume $\gamma_{\pm} = 1$, we believe these to be the most accurate K_{assoc} and K_{ipd} values reported to date.

Table III-3. K_{assoc} and K_{ipd} values for $\mathbf{2}\text{-X}$ salts with $\mathbf{1}$ in $\text{CDCl}_3:\text{CD}_3\text{CN}$ (3:2), 295 K, as calculated according to Eqs. 6l and 6n.

X^-	$K_{\text{assoc}} (\text{M}^{-1})$	$K_{\text{ipd}} (\text{M})$
PF_6	$5.1 \pm 0.8 \times 10^2$	$6.9 \pm 3.4 \times 10^{-3}$
BF_4	$5.0 \pm 1.1 \times 10^2$	$3.9 \pm 3.0 \times 10^{-3}$
OTs	$5.1 \pm 0.3 \times 10^2$	$4.6 \pm 0.8 \times 10^{-4}$
TFA	$5.0 \pm 0.3 \times 10^2$	$1.9 \pm 0.3 \times 10^{-4}$

Figure III-10. Plots of Eq. 7m ($K_{\text{assoc}}[\text{H}] \gg 1$) for solutions of **1** and a) **2**-PF₆, b) **2**-BF₄, c) **2**-OTs, and d) **2**-TFA in CDCl₃:CD₃CN (3:2), 295 K.

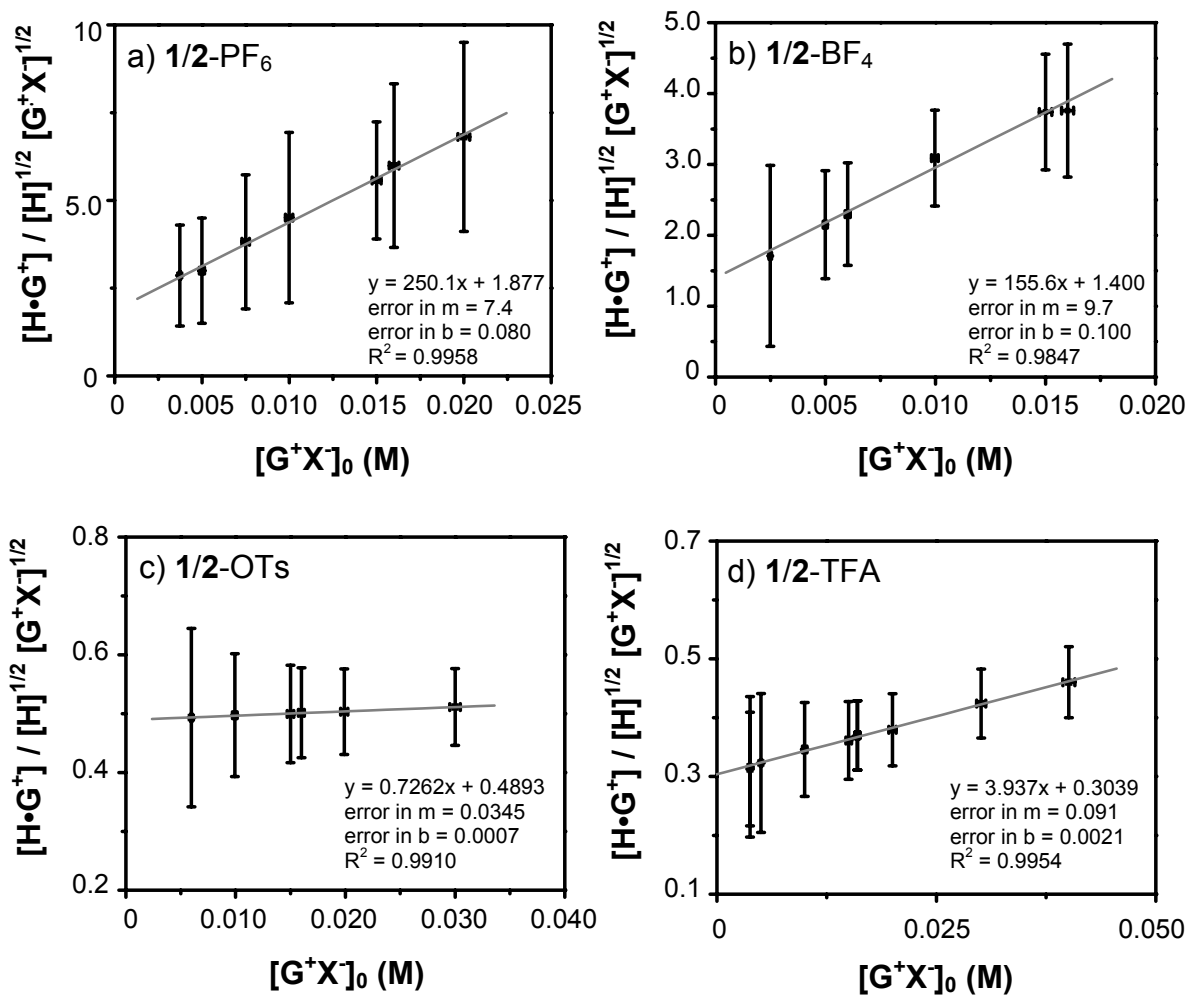
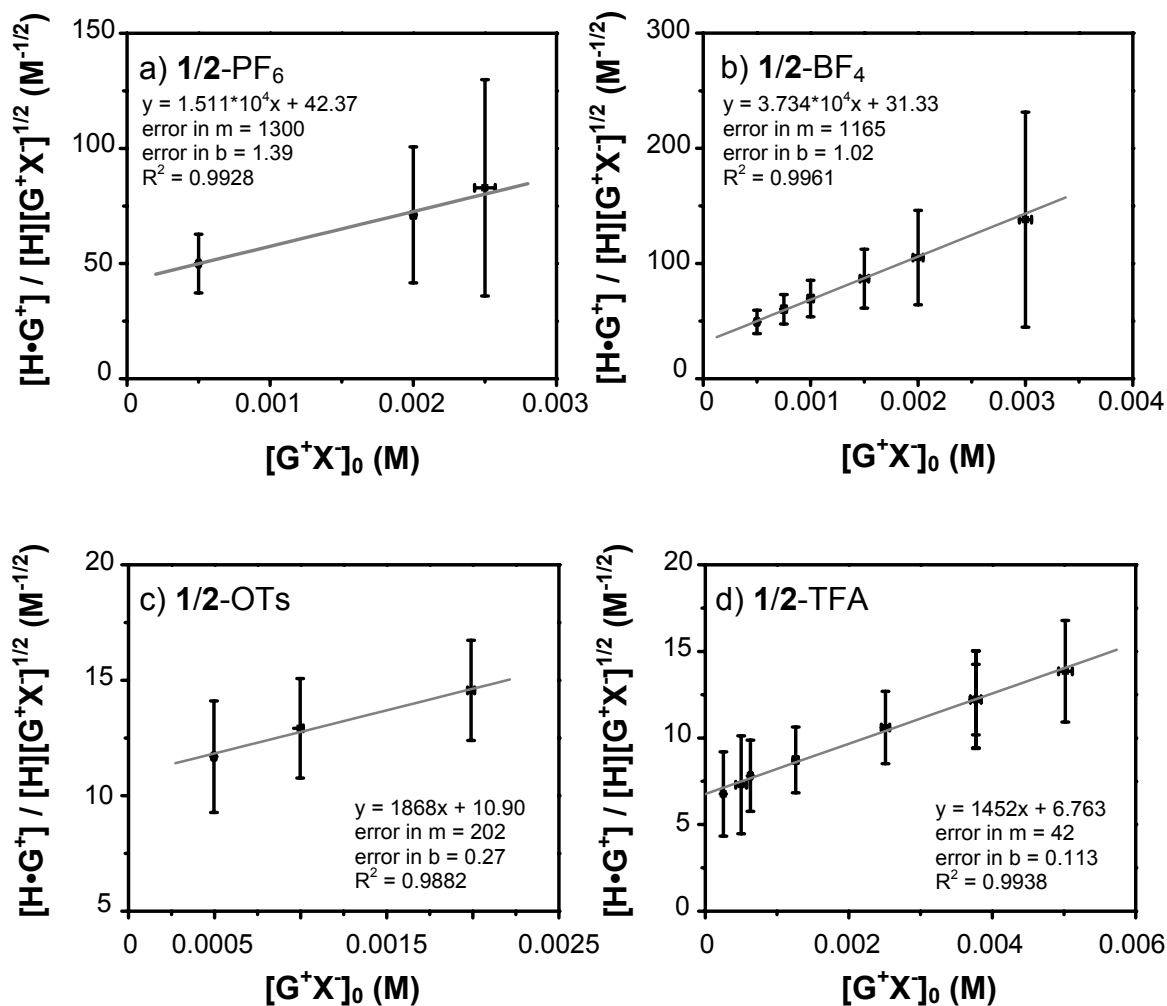


Figure III-11. Plots of Eq. 7o ($K_{\text{assoc}}[\text{H}] \ll 1$) for solutions of **1** and a) **2**-PF₆, b) **2**-BF₄, c) **2**-OTs, and d) **2**-TFA in CDCl₃:CD₃CN (3:2), 295 K.



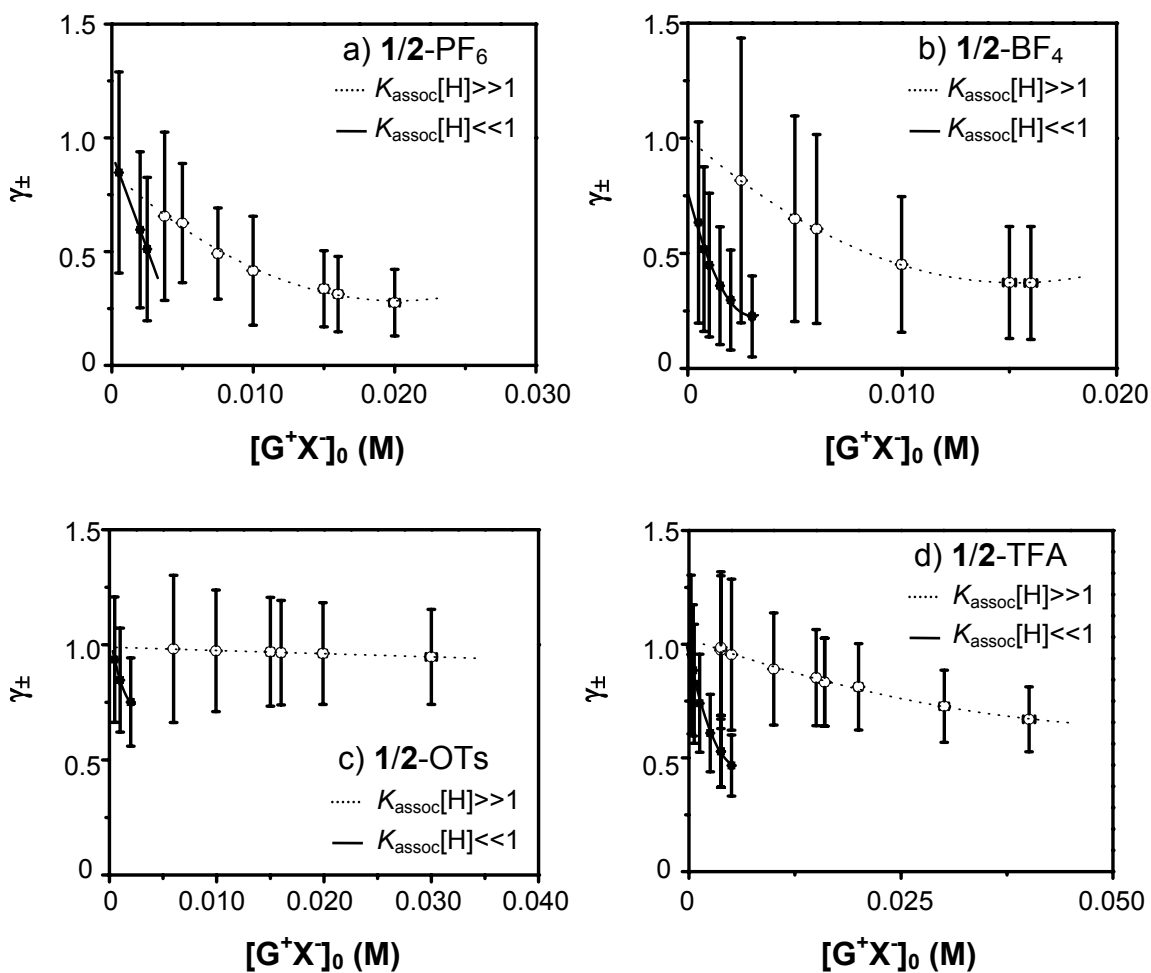
III.4 Determination of Activity Coefficients

γ_{\pm} may be calculated for every data point according to Eqs. 7m and 7o. Figure III-12 displays such results for each 1/2-X solution and demonstrates the large variation in experimental γ_{\pm} with $[\text{G}^+\text{X}]_0$, directly challenging the validity of concentration based equilibrium values for these and like systems in non-aqueous media. As discussed in

Section III.3, γ_{\pm} was indeed found to vary linearly with concentration within experimental error, as presumed to be the case from Figures III-10 and III-11.2

The existence of two families of activity curves is not unexpected: when $K_{\text{assoc}}[\text{H}] \gg 1$ (Figure III-12, top dotted curve), ionic strength is predominantly controlled by complex formation; at the other extreme (Figure III-12, $K_{\text{assoc}}[\text{H}] \ll 1$, bottom solid curve), ionic strength is dominated by **2**-X dissociation. When the ions are generated as a result of pseudorotaxane formation ($K_{\text{assoc}}[\text{H}] \gg 1$), γ_{\pm} is much less sensitive to $[\text{G}^+\text{X}^-]_0$ than is the case when the ions result from ion pair dissociation ($K_{\text{assoc}}[\text{H}] \ll 1$). This is most likely a consequence of the lower solvation energy of the larger pseudorotaxane cation $\mathbf{1}\cdot\mathbf{2}^+$ relative to $\mathbf{2}^+$, as described to a first approximation by the Born model. [19] We also speculate that this difference may be due to delocalization of charge in the pseudorotaxane cation, which would effectively impart more “ideal” character to the complex ion, $\mathbf{1}\cdot\mathbf{2}^+$, than is the case for the “naked” 2° ammonium ion, $\mathbf{2}^+$. Taking note of the region $K_{\text{assoc}}[\text{H}] \gg 1$ (Figure III-12, top, dotted curves), it is tempting to correlate the apparent activity coefficient “sensitivity” with $[\mathbf{2}\text{-X}]_0$ to K_{ipd} : it certainly appears to be the general case (**2**-OTs being unique) that the salts which more readily dissociate (larger K_{ipd}) display larger variations in γ_{\pm} with $[\mathbf{2}\text{-X}]_0$ than do the **2**-X salts with lower K_{ipd} . Of course, recalling that the activity coefficient measured for any given system is an average solution activity (Eq. 3), the variance with anion is really not surprising.

Figure III-12. γ_{\pm} as calculated according to Eq. 7m ($K_{\text{assoc}}[\text{H}] \gg 1$, top dotted curve) and Eq. 7o ($K_{\text{assoc}}[\text{H}] \ll 1$, bottom solid curve) vs. $[\text{G}^+\text{X}^-]_0$ for solutions of **1** and a) **2**-PF₆, b) **2**-BF₄, c) **2**-OTs, and d) **2**-TFA in CDCl₃:CD₃CN (3:2), 295 K. 1st order exponential decays have been added only to guide the eye.



III.5 *Non-Linear Least-Squares Fit of the Pre-Equilibrium Model*

The advantage of the non-linear least squares (NLLS) fit discussed in Chapter II.4 is that the experimenter is not limited to complexation in the limits of ion pair dissociation of the guest ($K_{\text{assoc}}[\text{H}] \ll 1$) or complex ($K_{\text{assoc}}[\text{H}] \gg 1$). Instead, data in the intermediate region, in which X^- is liberated by both pathways, may be used as well. While this is an attractive feature, one must remember that the NLLS fitting treatment has a major disadvantage: by definition, γ_{\pm} is assumed to equal unity. Thus, the individual constants will be underestimated by this treatment (Eq. 7k).

We have applied a NLLS fit to a wide range of $[2-X]$ with **1** (Table III-4 [20]) by inputting the data into a root finding algorithm to calculate the root of Eq. 8c and Eq. 8e in order to solve for K_{ipd} , again permitting $[G^-]_{\text{observed}} \approx [G^+X^-]$. As is obvious from Figure III-13, the resultant NLLS fits experience significant deviation at high $[H]$ values, and these fits were worse for salts with high K_{ipd} , which may reflect the change in γ_{\pm} across the concentration range investigated. As a result of the large scatter at high $[H]$, substantial deviations in K_{assoc} values were noted (Table III-5).

Because large deviations in K_{assoc} are not expected in accord with the pre-equilibrium model, the data from Table III-4 were amended by rejecting high concentrations of initial H for each series. For **1/2-PF₆** and **1/2-OTs**, all data points in which $[H]_0 \geq 20.0$ mM were rejected; for **1/2-BF₄**, data points in which $[H]_0 \geq 16.0$ mM were rejected. **1/2-TFA** was left unchanged. The amended and much better behaved fits are shown in Figure III-14, resulting in reasonable K_{ipd} and K_{assoc} values (Table III-5).

Table III-4. Percentage of Host occupied by Guest (θ) as a function of $[1]_0$ and $[2-X]_0$, $CDCl_3:CD_3CN$ (3:2), 295 K. Non-bold data points correspond to values which were rejected in the amended treatment (Figure III-14).

$[1]_0$ (mM)	$[2-PF_6]_0$ (mM)	θ	$[1]_0$ (mM)	$[2-BF_4]_0$ (mM)	θ	$[1]_0$ (mM)	$[2-OTs]_0$ (mM)	θ	$[1]_0$ (mM)	$[2-TFA]_0$ (mM)	θ
20.0	4.99	0.241	20.0	15.0	0.659	20.0	30.0	0.410	20.0	20.0	0.275
20.0	20.0	0.872	20.0	10.0	0.458	20.0	19.9	0.334	16.0	16.0	0.271
20.0	15.0	0.698	20.0	6.01	0.28	20.0	15.0	0.287	16.0	16.0	0.290
20.0	9.99	0.478	20.0	4.99	0.234	20.0	9.93	0.227	8.00	8.00	0.269
20.0	7.50	0.361	20.0	2.49	0.119	16.0	16.0	0.350	8.00	8.00	0.258
20.0	4.99	0.241	16.0	16.0	0.790	8.00	8.00	0.336	4.00	4.00	0.224
14.9	3.73	0.241	8.00	8.00	0.759	8.00	8.00	0.329	4.00	4.00	0.241
10.0	3.73	0.343	8.00	8.00	0.761	4.00	4.00	0.325	3.82	20.0	0.501
7.45	3.73	0.446	4.00	4.00	0.707	4.00	4.00	0.304	3.82	15.4	0.442
5.00	3.73	0.636	4.00	4.00	0.709	3.82	3.75	0.306	3.82	10.0	0.373
4.00	4.00	0.716	3.82	3.74	0.688	2.00	2.00	0.294	3.82	7.71	0.324
3.73	3.80	0.646	3.73	3.81	0.679	2.00	2.00	0.279	3.82	5.00	0.272
3.73	3.73	0.771	3.72	3.83	0.723	1.89	3.75	0.365	3.82	3.85	0.237
3.73	1.93	0.437	2.00	2.00	0.620	1.20	3.75	0.418	3.82	3.77	0.269
3.73	1.19	0.285	2.00	2.00	0.662	1.00	1.00	0.240	3.82	3.76	0.232
3.73	0.918	0.231	1.00	1.00	0.562	1.00	1.00	0.241	2.00	2.00	0.207
3.73	5.00	0.85	1.00	1.00	0.565	0.95	3.75	0.444	2.00	2.00	0.225
2.00	2.00	0.668	0.492	2.00	0.8	0.492	1.99	0.382	1.20	3.77	0.408
1.89	3.73	0.710	0.492	1.50	0.728	0.492	0.997	0.275	1.00	1.00	0.219
1.00	1.00	0.588	0.492	1.00	0.663				0.75	3.77	0.405
1.00	0.998	0.575	0.492	0.751	0.567				0.502	5.02	0.489
0.492	3.75	0.802	0.492	0.500	0.443				0.502	2.51	0.339
0.492	2.50	0.792							0.502	1.26	0.236
0.492	2.00	0.742							0.34	3.77	0.424
0.492	0.999	0.672									
0.492	0.500	0.454									

Table III-5. K_{assoc} and K_{ipd} values for **2-X** salts with **1** in $CDCl_3:CD_3CN$ (3:2), 295 K, as calculated from non-linear least-square fitting treatments.

X	Original Data Series		Amended Data^a	
	K_{ipd} (M)	K_{assoc} (M^{-1})	K_{ipd} (M)	K_{assoc} (M^{-1})
PF ₆	5.8×10^{-3}	1.9×10^3	4.4×10^{-2}	2.5×10^2
BF ₄	data did not converge		6.6×10^{-2}	3.0×10^2
OTs	1.3×10^{-4}	2.0×10^3	6.1×10^{-4}	5.5×10^2
TFA	8.3×10^{-4}	2.6×10^2	8.3×10^{-4}	2.6×10^2

^a Data from Table III-4 has been amended in rejecting $[H]_0 \geq 20.0$ mM for **2-PF₆** and **2-OTs** and $[H]_0 \geq 16.0$ mM for **2-BF₄**; data for **2-TFA** remained consistent between fits.

Figure III-13. $\{[H \cdot G^+]/[G^+X^-]^{1/2}\}^2$ versus $[H]$ for solutions of **1** and a) **2**-PF₆, b) **2**-BF₄, c) **2**-OTs, and d) **2**-TFA in CDCl₃:CD₃CN (3:2), 295 K, incorporating all results from Table III-4. The curves correspond to non-linear least square fits according to Eqs. 8c and 8e.

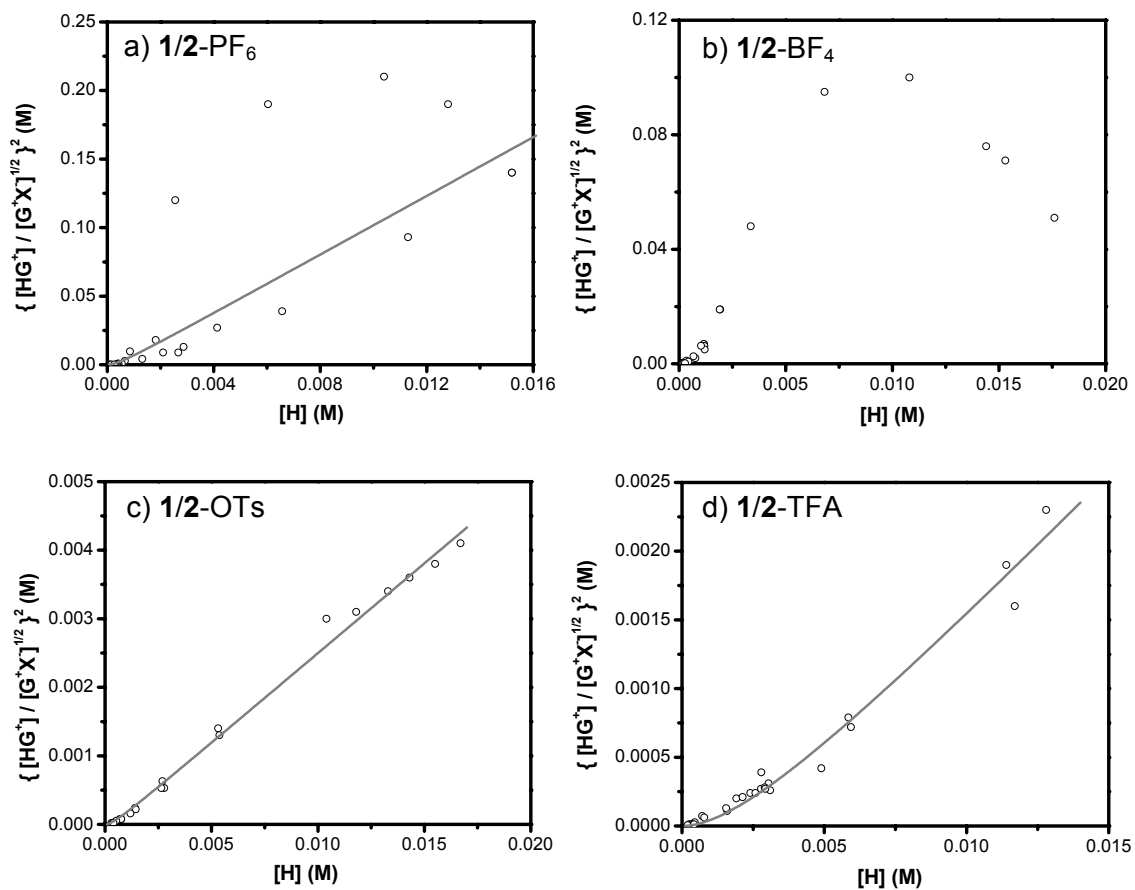
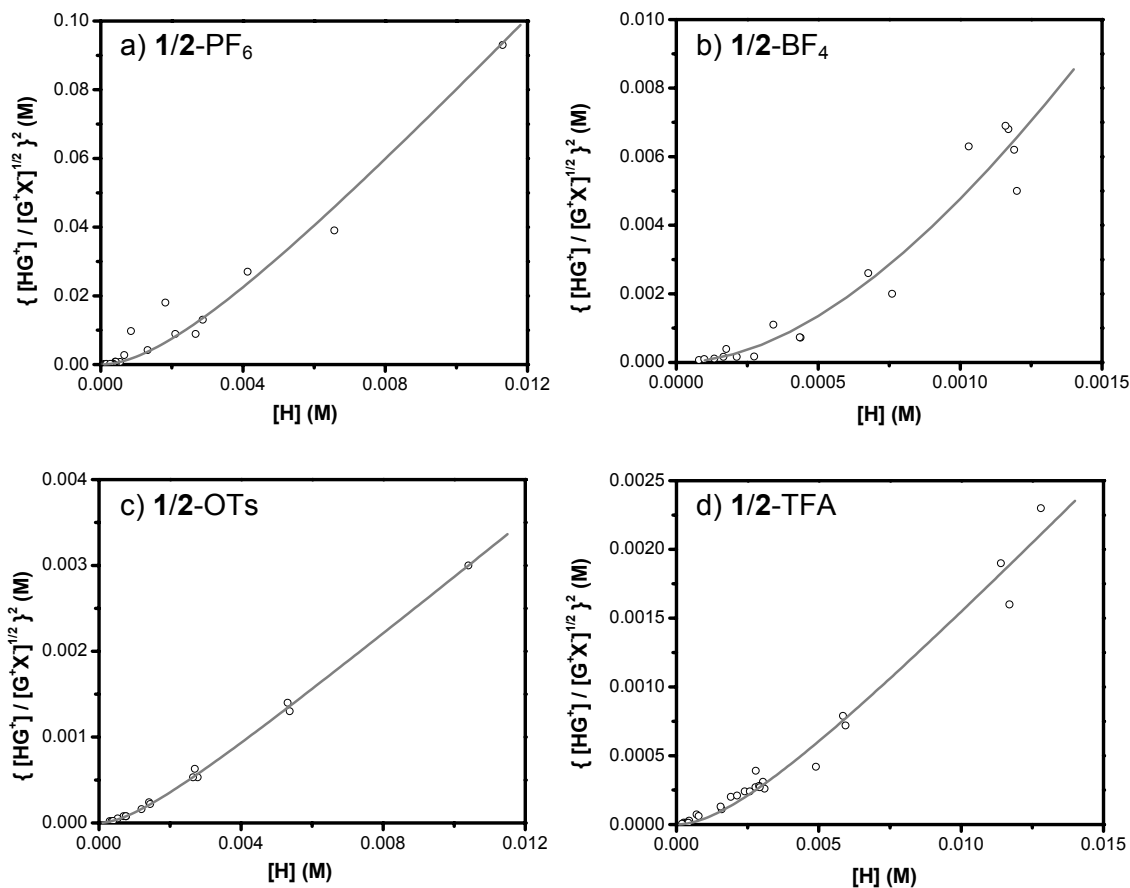


Figure III-14. $\{[H \cdot G^+]/[G^+X^-]^{1/2}\}^2$ versus $[H]$ for solutions of **1** and a) **2**-PF₆, b) **2**-BF₄, c) **2**-OTs, and d) **2**-TFA in CDCl₃:CD₃CN (3:2), 295 K, incorporating $[H]_0$ limited values from Table III-4. The curves correspond to non-linear least square fits according to Eqs. 8c and 8e.



III.6 Approximation of the Pre-Equilibrium Model

We also considered an approximation of the individual constants by applying the first two terms of the binomial expansion to Eq. 7k. For this treatment, and provisionally assuming $K_{\text{assoc}} = 5.0 \times 10^2 \text{ M}^{-1}$, we restricted analysis to the limit $[H] \leq 3.00 \text{ mM}$ (i.e., $K_{\text{assoc}}[H] \leq 1.5$), as required. While this restriction enables the researcher to minimize experimental time relative to the full pre-equilibrium method, minimizing host concentration may limit the observable percent binding, dependent upon relative K_{ipd} and

K_{assoc} values. This feature is a drawback if one wishes to explore the full 20-80% complexation range that provides acceptable experimental errors for spectroscopic determinations (Figure II-2).

Table III-6 has been compiled by imposing the limit $[H] \leq 3.00$ mM on the data from Table III-4. Figure III-15 was then constructed on the basis of Eq. 9c, allowing $[G^+]_{\text{observed}} \approx [G^+X^-]$. Although R^2 values are not excellent, Eq. 9c fit the data fairly well and allowed the tabulation of K_{ipd} and K_{assoc} for each 1/2-X system (Table III-7).

Table III-6. Percentage of Host occupied by Guest (θ) as a function of $[1]_0$ and $[2-X]_0$ in the limit $[H] \leq 3.00$ mM, $\text{CDCl}_3:\text{CD}_3\text{CN}$ (3:2), 295 K.

$[1]_0$ (mM)	$[2\text{-PF}_6]_0$ (mM)	θ	$[1]_0$ (mM)	$[2\text{-BF}_4]_0$ (mM)	θ	$[1]_0$ (mM)	$[2\text{-OTs}]_0$ (mM)	θ	$[1]_0$ (mM)	$[2\text{-TFA}]_0$ (mM)	θ
5.00	3.73	0.636	8.00	8.00	0.759	20.0	30.0	0.410	3.82	20.0	0.501
3.73	3.80	0.646	8.00	8.00	0.761	20.0	19.9	0.334	3.82	15.4	0.442
3.73	3.73	0.771	4.00	4.00	0.707	20.0	15.0	0.287	3.82	10.0	0.373
3.73	1.93	0.437	4.00	4.00	0.709	20.0	9.93	0.227	3.82	7.71	0.324
3.73	1.19	0.285	3.82	3.74	0.688	16.0	16.0	0.350	3.82	5.00	0.272
3.73	0.918	0.231	3.73	3.81	0.679	8.00	8.00	0.336	3.82	3.85	0.237
2.00	2.00	0.668	3.72	3.83	0.723	8.00	8.00	0.329	3.82	3.77	0.269
1.89	3.73	0.710	2.00	2.00	0.620	4.00	4.00	0.325	3.82	3.76	0.232
1.00	1.00	0.588	2.00	2.00	0.662	4.00	4.00	0.304	2.00	2.00	0.225
1.00	0.998	0.575	1.00	1.00	0.562	3.82	3.75	0.306	1.20	3.77	0.408
0.492	3.75	0.802	1.00	1.00	0.565	2.00	2.00	0.294	1.00	1.00	0.219
0.492	2.50	0.792	0.492	1.50	0.728	2.00	2.00	0.279	0.75	3.77	0.405
0.492	2.00	0.742	0.492	1.00	0.663	1.89	3.75	0.365	0.502	5.02	0.489
0.492	0.999	0.672	0.492	0.751	0.567	1.20	3.75	0.418	0.502	2.51	0.339
0.492	0.500	0.454	0.492	0.500	0.443	1.00	1.00	0.240	0.502	1.26	0.236
						1.00	1.00	0.241	0.34	3.77	0.424
						0.95	3.75	0.444			
						0.492	1.99	0.382			
						0.492	0.997	0.275			

Figure III-15. Plots of Eq. 9c for solutions of **1** and a) **2**-PF₆, b) **2**-BF₄, c) **2**-OTs, and d) **2**-TFA, [H] ≤ 3.00 mM in CDCl₃:CD₃CN (3:2), 295 K.

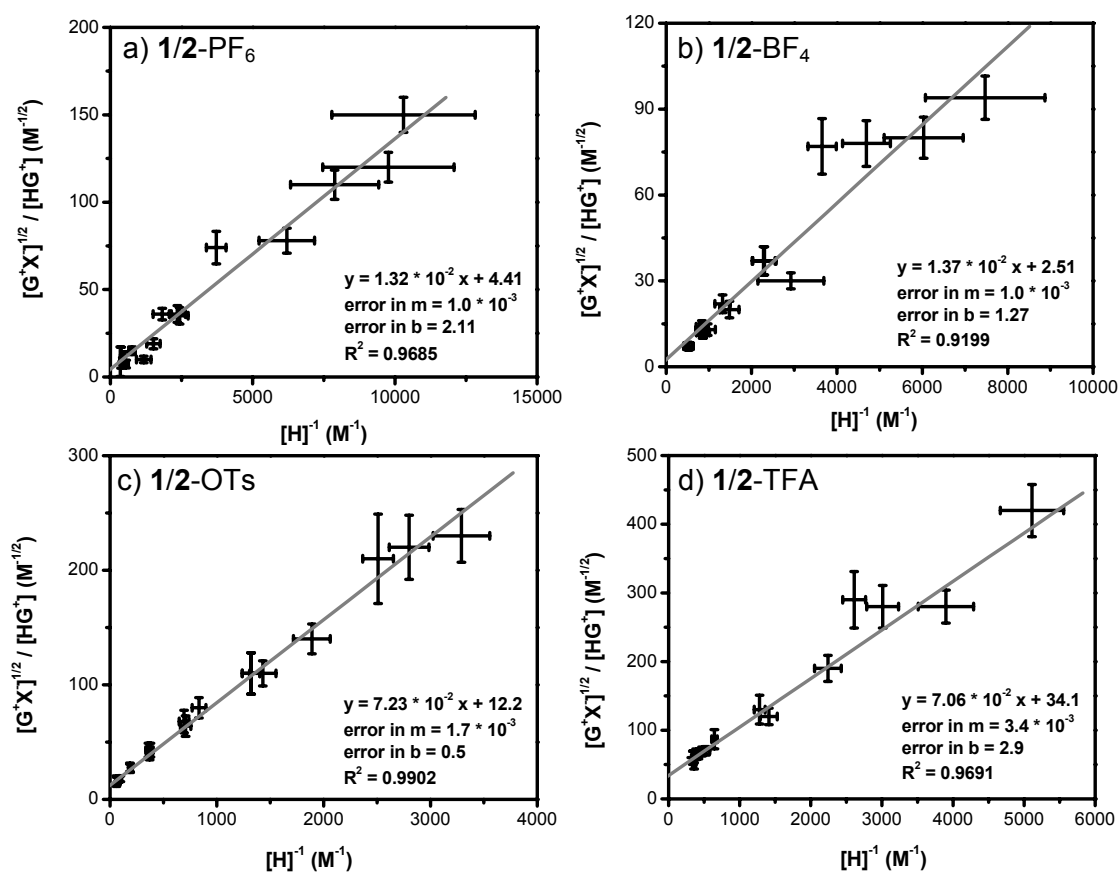


Table III-7. K_{assoc} and K_{ipd} values for **2**-X salts with **1** in CDCl₃:CD₃CN (3:2), 295 K, as calculated according to Eq. 9c.

[X ⁻]	K_{ipd} (M)	K_{assoc} (M ⁻¹)
PF ₆	$1.3 \pm 3.4 \times 10^{-2}$	$6.7 \pm 4.0 \times 10^2$
BF ₄	$4.0 \pm 12 \times 10^{-2}$	$3.7 \pm 2.3 \times 10^2$
OTs	$1.3 \pm 0.2 \times 10^{-3}$	$3.4 \pm 0.2 \times 10^2$
TFA	$2.2 \pm 0.4 \times 10^{-4}$	$9.6 \pm 1.3 \times 10^2$

III.7 Comparison of Three Pre-Equilibrium Treatments

K_{ipd} and K_{assoc} values as calculated in Sections III.3-6 according to the full pre-equilibrium model, the NLLS fitting treatment, and the approximation by the binomial expansion have been compiled in Table III-8. In all cases, the treatments have been solved allowing $[\text{'G'}]_{\text{observed}} \approx [\text{G}^+\text{X}^-]$. Because no other assumptions were made to solve for the pre-equilibrium model, we consider results from this treatment to be the most accurate values reported to date, and provide the basis by which the other data sets are judged. The only other assumption made in the binomial expansion was that the $\{1+K_{\text{assoc}}[\text{H}]\}^{1/2}$ term of Eq. 7k was well approximated by the first two terms of the binomial expansion. To ensure the validity of this assumption, only data sets of $[\text{H}] \leq 3.00$ mM (i.e., $K_{\text{assoc}}[\text{H}] \leq 1.5$, allowing $K_{\text{assoc}}=500 \text{ M}^{-1}$) were utilized. Finally, the NLLS treatment was solved assuming $\gamma_{\pm} = 1$. Furthermore, due to wide scatter in the data according to Eq. 7k at high $[\text{H}]$, the data sets were generally limited to $[\text{H}]_0 < 16.0$ mM in the NLLS method.

Table III-8. K_{assoc} and K_{ipd} values for 2-X salts with 1 in $\text{CDCl}_3:\text{CD}_3\text{CN}$ (3:2), 295 K, as calculated according to three independent pre-equilibrium treatments.

X^-	Pre-Equilibrium Model (Eqs. 7m and 7o)		Binomial Expansion (Eq. 9c)		NLLS Fit ^a (Eq. 7k)	
	$K_{\text{ipd}} \times 10^3$ (M)	$K_{\text{assoc}} \times 10^{-2}$ (M^{-1})	$K_{\text{ipd}} \times 10^3$ (M)	$K_{\text{assoc}} \times 10^{-2}$ (M^{-1})	$K_{\text{ipd}} \times 10^3$ (M)	$K_{\text{assoc}} \times 10^{-2}$ (M^{-1})
PF ₆	6.9 ± 3.4	5.1 ± 0.8	13 ± 34	6.7 ± 4.0	44	2.5
BF ₄	3.9 ± 3.0	5.0 ± 1.1	40 ± 120	3.7 ± 2.3	66	3
OTs	0.46 ± 0.08	5.1 ± 0.3	1.3 ± 0.2	3.4 ± 0.2	0.61	5.5
TFA	0.19 ± 0.03	5.0 ± 0.3	0.22 ± 0.04	9.6 ± 1.3	0.83	2.6
Average (±Std. Dev.)		5.1 ± 0.1		5.9 ± 2.9		3.4 ± 1.4

^a Taken from the amended taken set of Table III-5

K_{assoc} values are fairly consistent among the treatments. K_{assoc} determined according to the NLLS method were found on average to be diminished relative to the pre-equilibrium set, as anticipated under the assumption $\gamma_{\pm} = 1$ (Eq. 7k), while the binomial expansion K_{assoc} are to a rough approximation within experimental error of the pre-equilibrium model. The agreement of K_{assoc} in all cases gives us confidence that the true value has been calculated by the pre-equilibrium method.

K_{ipd} values, on the other hand, vary significantly between treatments often by an order of magnitude or more, while the absolute relative order of $\text{PF}_6 > \text{BF}_4 > \text{OTs} > \text{TFA}$ of the pre-equilibrium model changes to $\text{BF}_4 > \text{PF}_6 > \text{TFA} > \text{OTs}$ in the binomial expansion and NLLS method. The lack of agreement between treatments gives us little confidence in the absolute values of K_{ipd} . Furthermore, from Table III-8 alone, it is impossible to judge relative values, particularly in light of the large errors introduced for the $1/2\text{-PF}_6$ and $1/2\text{-BF}_4$ data sets. It is informative, however to deliberate on the source of the large errors for these two data sets, especially in relation to $1/2\text{-OTs}$ and $1/2\text{-TFA}$.

Returning to our initial assumption that the dissociated cation 2^+ is the active participant in complex formation, the large errors for $1/2\text{-PF}_6$ and $1/2\text{-BF}_4$ may be rationalized by considering ionic strength effects. Due to the relative K_{ipd} values, at any given concentration of 2-X , more free cation is available for complexation when 2-PF_6 is utilized versus 2-TFA , for example, resulting in the leveling off phenomenon described above as an asymptotic limit in Figures III-2 and III-3. Moreover, because $K_{\text{assoc}} \gg K_{\text{ipd}}$, all of the free 2^+ is immediately tied up in host/guest complexation. Thus, at any given concentration and again comparing 2-PF_6 with 2-TFA , because K_{assoc} is independent of anion one expects that the percentage of host **1** occupied by guest will be greater when 2-PF_6 is utilized than is the case for 2-TFA . Indeed, experimental evidence (see Table III-4) verifies this assertion and gives credence to our pre-equilibrium model.

Continuing this rationalization permits us to gauge each of the three models with respect to relative K_{ipd} ordering. Focusing on the $[\mathbf{1}]_0 = [2\text{-X}]_0 = 1.00 \text{ mM}$ data sets from Table III-4, because relative K_{ipd} is positively correlated to percent complexation, we anticipate an order of 2-PF_6 ($\theta = 59\%$) $>$ 2-BF_4 ($\theta = 56\%$) $>$ 2-OTs ($\theta = 24\%$) $>$ 2-TFA ($\theta = 22\%$) in K_{ipd} .

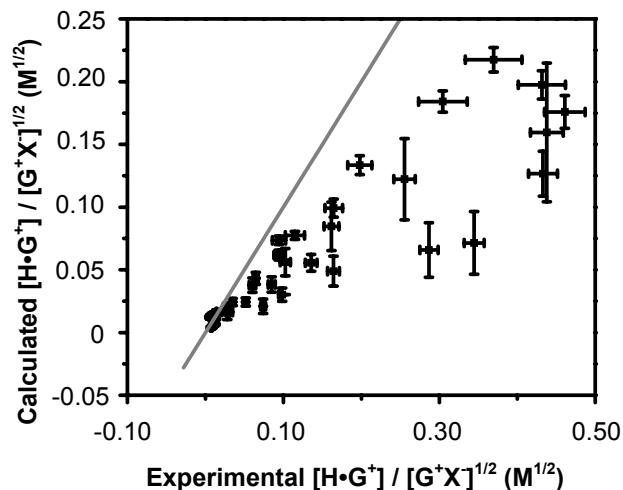
In light of this argument, and because few assumptions were made when host concentrations were not limited to low values only, we believe the K_{ipd} values calculated according to the pre-equilibrium model to be the most accurate. Nonetheless, Table III-8 highlights the value of independently calculating K_{ipd} in the absence of host. Towards this end, electrical conductance, [21] vapor phase osmometry, [22] and vibrational spectroscopy [9,23] have been applied in the literature. In addition, a few reports have reported K_{ipd} on the basis of chemical shift data and found results which compared favorably to other methods listed above,[24] although there is some controversy about the comparisons. [25]

While this remains an area of future work for us, Appendix A describes preliminary studies for the independent determination of K_{ipd} for **2**-TFA.

III.8 Utilization of the Model as a Predictive Tool

Due to the fact that the activity coefficients vary significantly depending upon concentration (Figure III-12), prediction of extents of complexation using the derived K_{ipd} and K_{assoc} values becomes a daunting task. This is readily apparent upon inspection of Eq. 7j, in which an estimation of γ_{\pm} is necessary to solve $K_{\text{a,exp}}$ or $[\text{H}\cdot\text{G}^+]/[\text{G}^+\text{X}^-]^{1/2}$. To clarify this observation, $[\text{H}\cdot\text{G}^+]/[\text{G}^+\text{X}^-]^{1/2}$ (determined experimentally) has been plotted versus $[\text{H}\cdot\text{G}^+]/[\text{G}^+\text{X}^-]^{1/2}$ calculated according to Eq. 7k (Figure III-16) and assuming $\gamma_{\pm} = 1$, $K_{\text{assoc}} = 5.1 \times 10^2 \text{ M}^{-1}$ and $K_{\text{ipd}} = 6.9 \times 10^{-3} \text{ M}$; the grey line corresponds to a perfect relationship. There is a clear lack of agreement between predicted and experimental values: at any given calculated value (ordinate), a wide range of experimental values (abscissa) are feasible. These results reflect the fact that the activity coefficient is lower at higher ionic strength, leading to relatively greater extents of complexation on a molar basis relative to the low ionic strength situation, as can be seen from Eq. 7j. These results also reflect the dependence of the activity coefficient on the nature of the cation, whether existing as a free guest or complex (Figure III-12). Disregard of γ_{\pm} , an extremely important parameter, mirrors the widespread use of untested and invalid Eq. 2 in the literature.

Figure III-16. Plots of $[\text{H}\cdot\text{G}^+]/[\text{G}^+\text{X}^-]^{1/2}$ calculated according to Eq. 7k (solid line, $\gamma_{\pm}=1$) versus $[\text{H}\cdot\text{G}^+]/[\text{G}^+\text{X}^-]^{1/2}$ as determined by experiment for solutions of **1/2**-PF₆, in CDCl₃:CD₃CN (3:2), 295 K.



To utilize the binding constants for their intended purpose as predictive tools, activity coefficients must therefore be known (or be capable of being estimated) *a priori*. While the activity coefficients are well-behaved under each binding regime (Figure III-17, $K_{\text{assoc}}[\text{H}] \gg 1$, and Figure III-18, $K_{\text{assoc}}[\text{H}] \ll 1$), they are dependent on the nature of the cation and the host concentration. Based on these arguments, we conclude that it is difficult, if not impossible, to use the two equilibrium constants involved in these processes to predict extents of complexation.

Figure III-17. Plots of $-\log \gamma_{\pm}$ versus $[1 \cdot 2^+]$ for solutions of **1** and a) **2**-PF₆, b) **2**-BF₄, c) **2**-OTs, and d) **2**-TFA in CDCl₃:CD₃CN (3:2), 295 K, $K_{\text{assoc}}[\text{H}] \gg 1$.

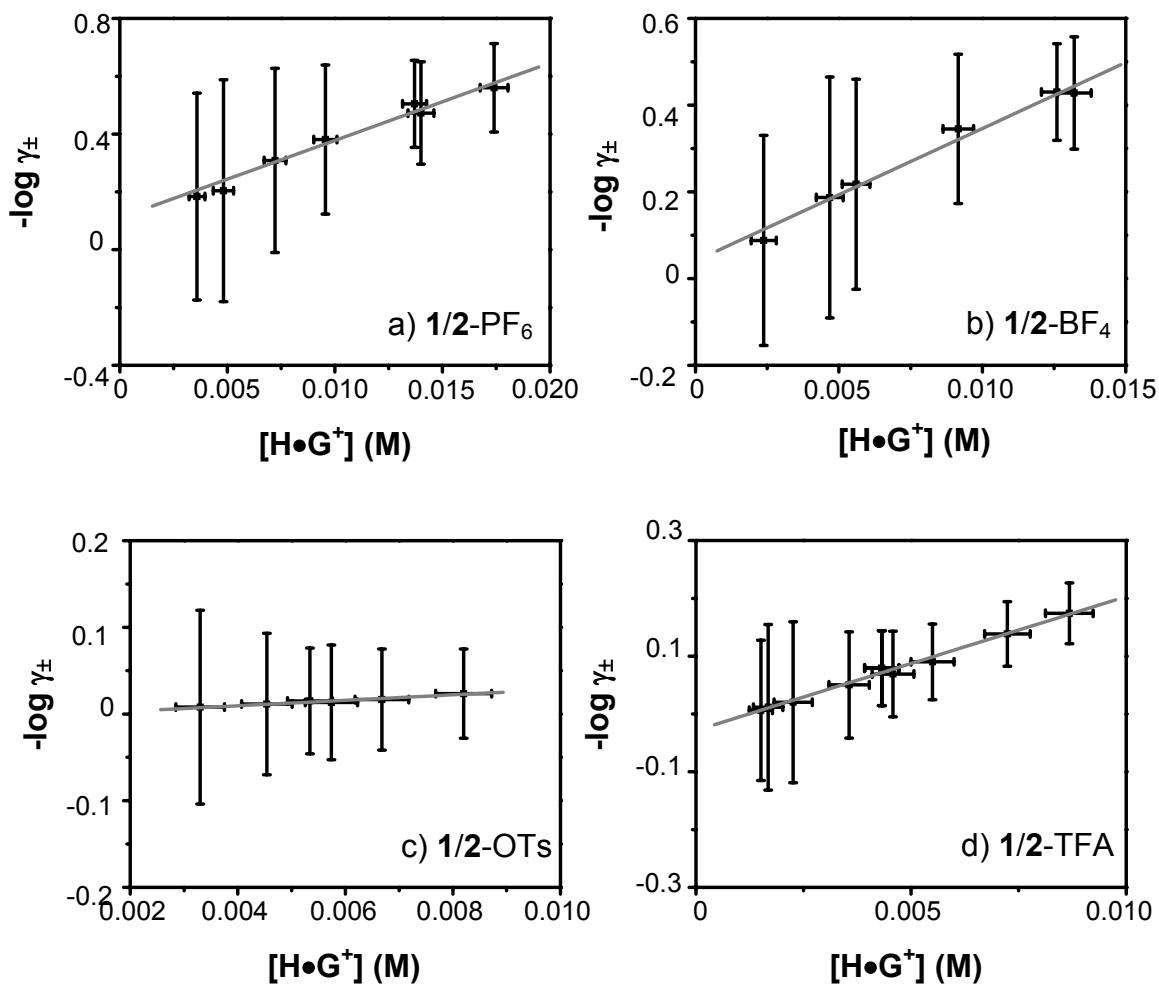
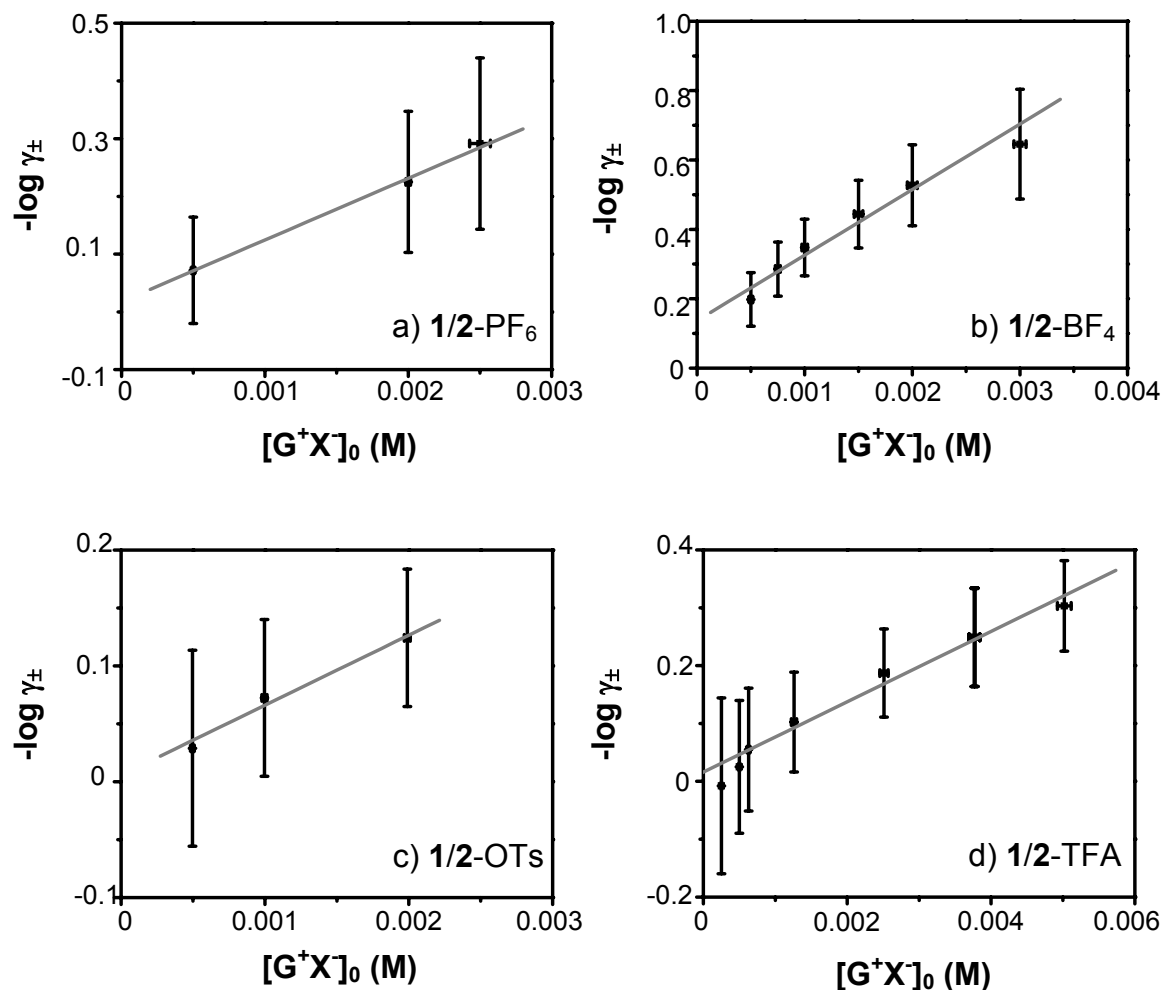


Figure III-18. Plots of $-\log \gamma_{\pm}$ versus $[2-X]_0$ for solutions of **1** and a) **2**-PF₆, b) **2**-BF₄, c) **2**-OTs, and d) **2**-TFA in CDCl₃:CD₃CN (3:2), 295 K, $K_{\text{assoc}}[\text{H}] \ll 1$.



Despite the inherent difficulty in estimating extents of complexation, the model does allow one to predict other behavior in this and similar systems. From the overall equilibrium expression (K_{total} , Eq. 7a) we immediately recognized the detrimental affect free X^- has on complexes which are not fully ion paired: according to Eq. 7h, the apparent association constant, $K_{\text{a,exp}}$, is inversely related to $[X^-]$. In accord with Le Chatellier's principle, removal of $[X^-]$ from the system should therefore result in increased extents of complexation. Indeed, introduction of a well known chloride anion host, [26] 1,3-bis(4-nitrophenyl)urea (**3**), to a solution of **1**/2-Cl, confirms this prediction. Despite the poor

solubility of both **2-Cl** and **3** in our solvent system, [27] nearly a 1.5x increase in the percentage of **1** occupied results upon addition of only 0.15 equivalents of **3** (relative to **2-X**, Table III-8) corresponding to a near doubling of $K_{a,exp}$. This concept has been validated by several independent research groups, who report increased extents of complexation as a result of binding both the cation and anion via ditopic [28] or molecularly separate hosts. [29]

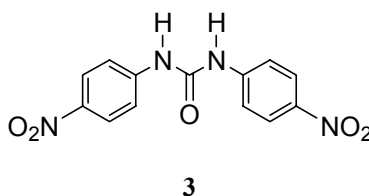


Table III-9. Percentage of Host occupied by Guest (θ) and $K_{a,exp}$ of **1/2-Cl** as a function of added anion host **3** [$CDCl_3:CD_3CN$ (3:2), 22 °C].

$[1]_0$ (mM)	$[2-Cl]_0^a$ (mM)	$[3]_0^a$ (mM)	θ	$K_{a,exp}$ (M^{-1})
2.0	4.2	0.00	26	1.3×10^2
2.0	4.3	0.30	34	1.9×10^2
2.0	4.2	0.57	38	2.3×10^2

^a Concentrations determined by integration of each species relative to **1**.

Equally important, this extension to anion complexation provides an efficient means of screening host/guest systems involving charged species for ion pairing of the complex: if $K_{a,exp}$ increases upon addition of an anion trap, one may conclude that the complex is not fully ion paired. In this case, one should expect $K_{a,exp}$ to vary with host and guest concentration. On the other hand, if introduction of an anion host does not influence $K_{a,exp}$, one may conclude that the complex is ion paired; $K_{a,exp}$ should not vary with $[host]_0$ and $[guest]_0$. Consequently, these implications suggest that each of the

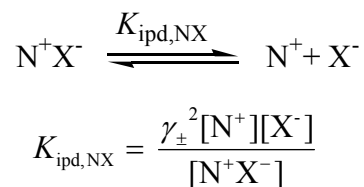
above referenced ditopic or molecularly separate host/guest systems should be treatable by our above equilibrium model.

In light of this discussion, the use of tightly ion paired guests may afford better opportunity for efficient binding than their weakly paired counterparts, since well solvated, charge delocalized anions are much more difficult to bind than are small, charge localized anions. The literature contains similar viewpoints with respect to other systems. [28,29]

III.9 Comparisons Between Hosts for Any Given Guest

While the prediction of K_{assoc} was shown to be a daunting task, results from early studies do suggest the design of a new experimental method to directly compare the binding efficiencies of two or more hosts for any given guest. Such a comparison is of high practical interest: the ultimate goal in many host/guest studies is the development of a host moiety that selectively and strongly binds a specific guest species. [30] We therefore propose the adoption of a method suggested by Figure III-2, in which $K_{\text{a,exp}}$ was shown to reach an asymptotic limit at high ionic strength upon addition of a salt whose cation does not interact with the host and whose anion is identical to that of the guest.

The addition of a large excess of salt such that essentially all of the free anion results from ion pair dissociation of this salt alone ($K_{\text{ipd,NX}}$) affords a quantitative means of evaluating relative “constants”, as follows:



Solving for $[\text{X}^-]$:

$$[\text{X}^-] = \left(\frac{K_{\text{ipd,NX}} [\text{N}^+\text{X}^-]}{\gamma_{\pm}^2} \right)^{1/2} \quad \text{Eq. 10a}$$

Substitution of Eq. 10a into Eq. 7h leads to

$$K_{a,\text{exp}} = \frac{K_{\text{ipd}} K_{\text{assoc}}}{\gamma_{\pm} (K_{\text{ipd,NX}} [\text{N}^+ \text{X}^-])^{1/2}} \quad \text{Eq. 10b}$$

Eq. 10b provides a means of evaluating the relative values of K_{assoc} for two or more hosts and any given guest in the presence of excess spectator salt. K_{assoc} values are not sensitive to ionic strength in this particular case (Eq. 6c), and no further assumptions regarding ion pairing need be made. The ionic strength will be equivalent for each system employing the same excess salt, provided enough salt has been added to reach the plateau region. Thus, from Eq. 10b the ratio $K_{a,\text{exp},1} / K_{a,\text{exp},2}$ is equivalent to $K_{\text{assoc},1} / K_{\text{assoc},2}$, providing a rigorous quantitative comparison of binding efficiencies. To put such measurements in perspective we recommend that the fraction of binding that takes place in 1 mM solutions of host and guest species also be reported.

Eq. 10b was tested with 1/2-PF₆/(*n*-Bu)₄N-PF₆. At 100 mM total salt, well within the plateau region (Figure III-2), and assuming $K_{\text{ipd,NX}}$ of (*n*-Bu)₄N-PF₆ to be 5.0×10^{-4} M, [31] the concentration of free PF₆⁻ is estimated to be 6.8 mM. From Figure III-2 and ignoring the influence of γ_{\pm} , the asymptotic limit of $K_{a,\text{exp}} = 2.7 \times 10^3 \text{ M}^{-1}$ corresponds to $K_{\text{ipd}}K_{\text{assoc}} / 6.8 \times 10^{-3} \text{ M}$ (Eq. 10b), from which $K_{\text{ipd}}K_{\text{assoc}}$ is estimated to be 18. If we allow $K_{\text{assoc}} = 2.5 \times 10^2 \text{ M}^{-1}$, as previously determined (Table III-5, $\gamma_{\pm} = 1$), we calculate $K_{\text{ipd}} = 7.2 \times 10^{-2} \text{ M}$, in reasonable agreement with that determined earlier when activity coefficients were also ignored ($K_{\text{ipd}} = (4.4 \pm 2.5) \times 10^{-2} \text{ M}$, Table III-5).

III.10 Acknowledgement of Assumptions Used to Derive K_{ipd} and K_{assoc}

Unless otherwise noted, it needs to be restated that the above host/guest model studies rely on the assumption that all of the free guest exists as the fully ion paired salt; thus $[\text{G}']_{\text{observed}} \approx [\text{G}^+ \text{X}^-]$. This requirement falls from our inability to calculate $[\text{X}^-]$, resulting in the derivation of Eqs. 6l-p, and 7j-o. Although such an assumption is valid under the condition $K_{\text{assoc}}[\text{H}] \gg 1$ (Eq. 7m), this is not the case when $K_{\text{assoc}}[\text{H}] \ll 1$ (Eq. 7o) and the majority of free $[\text{X}^-]$ is generated by ion pair dissociation.

In order to account for the error introduced under this assumption, we utilize the relationship that activity coefficients are proportional to the extent of ion pairing (Figure II-5) and return to the simplest case where $[X^-]$ may be calculated directly, that of ion pair dissociation in the absence of host. According to Eq. 5, $[X^-]$ may be calculated in the absence of γ_{\pm} for any given $[G^+X^-]_0$ and K_{ipd} . Because $[X^-]$ will be equivalent to the ionic strength in the absence of other added species, one may then utilize Eq. 3 to solve for γ_{\pm} at each $[X^-]$. Once an activity coefficient has been estimated for each $[G^+X^-]_0$, given K_{ipd} , Eq. 11 may then be applied to determine $[X^-]$ utilizing γ_{\pm} under the same conditions, yielding a “corrected” value. This process may be repeated with the “corrected” value until a constant $[X^-]$ and γ_{\pm} are reached; for present purposes, only the first iteration will be considered. Table III-10 was thus constructed from Tables III-3 and III-4, allowing the dielectric constant of $CDCl_3:CD_3CN$ (3:2) to be approximated by $\epsilon_{mixture} = (3/5)*\epsilon_{CDCl_3} + (2/5)*\epsilon_{CD_3CN} = 17.5$.

$$[X^-] = \frac{-\frac{K_{ipd}}{\gamma_{\pm}^2} \pm \left(\frac{K_{ipd}^2}{\gamma_{\pm}^4} + 4 \frac{K_{ipd}}{\gamma_{\pm}^2} [G^+X^-]_0 \right)^{1/2}}{2} \quad \text{Eq. 11}$$

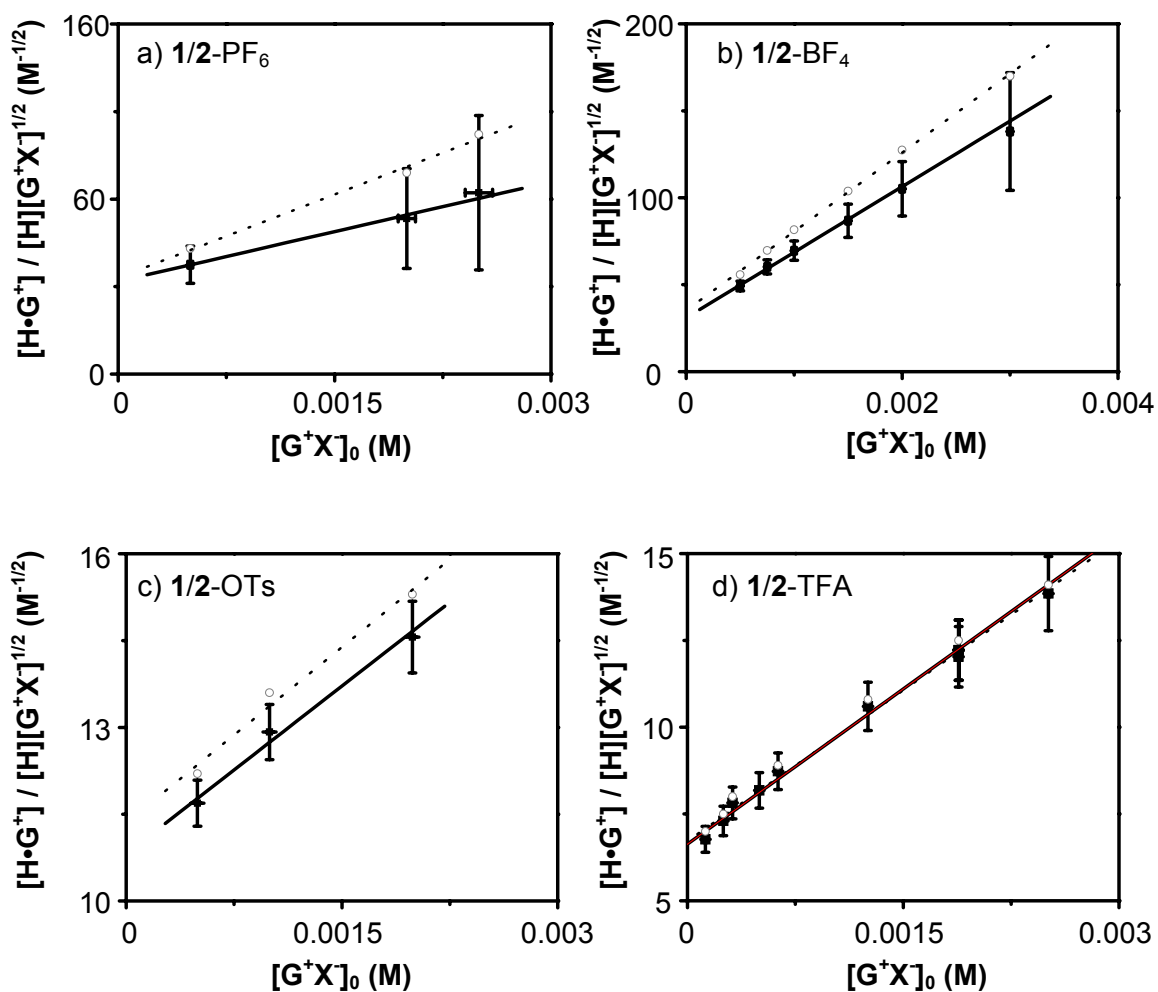
Table III-10. Uncorrected $[X^-]$ and $[G^+X^-]$ values, calculated as a function of K_{ipd} as well as “corrected” values, calculated as a function of K_{ipd} and γ_{\pm} at 298 K with $\varepsilon = 17.5$.

PF₆ $K_{ipd} = 6.9 \times 10^{-3}$	$[G^+X^-]_0$	$[X^-]^a$	$[G^+X^-]^a$	γ_{\pm}^b	$[X^-]_{corrected}^c$	% error in $[X^-]$	$[G^+X^-]_{corrected}^c$	% error in $[G^+X^-]$	% error in $[G^+X^-]^{1/2}$
	(M)	(M)	(M)		(M)		(M)		
	5.00x10 ⁻⁴	4.68x10 ⁻⁴	3.18x10 ⁻⁵	0.786	4.79x10 ⁻⁴	0.02	2.06x10 ⁻⁵	0.54	0.24
	2.00x10 ⁻³	1.62x10 ⁻³	3.80x10 ⁻⁴	0.639	1.81x10 ⁻³	0.10	1.93x10 ⁻⁴	0.97	0.40
	2.50x10 ⁻³	1.95x10 ⁻³	5.51x10 ⁻⁴	0.612	2.23x10 ⁻³	0.13	2.70x10 ⁻⁴	1.04	0.43
BF₄ $K_{ipd} = 3.9 \times 10^{-3}$	$[G^+X^-]_0$	$[X^-]^a$	$[G^+X^-]^a$	g_{\pm}^b	$[X^-]_{corrected}^c$	% error in $[X^-]$	$[G^+X^-]_{corrected}^c$	% error in $[G^+X^-]$	% error in $[G^+X^-]^{1/2}$
	(M)	(M)	(M)		(M)		(M)		
	5.00x10 ⁻⁴	4.48x10 ⁻⁴	5.16x10 ⁻⁵	0.790	4.65x10 ⁻⁴	0.04	3.47x10 ⁻⁵	0.49	0.22
	7.51x10 ⁻⁴	6.44x10 ⁻⁴	1.07x10 ⁻⁴	0.754	6.83x10 ⁻⁴	0.06	6.80x10 ⁻⁵	0.57	0.25
	1.00x10 ⁻³	8.25x10 ⁻⁴	1.75x10 ⁻⁴	0.727	8.92x10 ⁻⁴	0.07	1.08x10 ⁻⁴	0.62	0.27
	1.50x10 ⁻³	1.16x10 ⁻³	3.43x10 ⁻⁴	0.685	1.30x10 ⁻³	0.11	2.03x10 ⁻⁴	0.69	0.30
	2.00x10 ⁻³	1.46x10 ⁻³	5.44x10 ⁻⁴	0.654	1.69x10 ⁻³	0.14	3.12x10 ⁻⁴	0.74	0.32
	3.00x10 ⁻³	1.99x10 ⁻³	1.01x10 ⁻³	0.609	2.44x10 ⁻³	0.18	5.64x10 ⁻⁴	0.79	0.34
OTs $K_{ipd} = 4.6 \times 10^{-4}$	$[G^+X^-]_0$	$[X^-]^a$	$[G^+X^-]^a$	g_{\pm}^b	$[X^-]_{corrected}^c$	% error in $[X^-]$	$[G^+X^-]_{corrected}^c$	% error in $[G^+X^-]$	% error in $[G^+X^-]^{1/2}$
	(M)	(M)	(M)		(M)		(M)		
	4.96x10 ⁻⁴	3.00x10 ⁻⁴	1.96x10 ⁻⁴	0.825	3.33x10 ⁻⁴	0.10	1.63x10 ⁻⁴	0.20	0.09
	9.97x10 ⁻⁴	4.85x10 ⁻⁴	5.12x10 ⁻⁴	0.783	5.68x10 ⁻⁴	0.15	4.29x10 ⁻⁴	0.19	0.09
	1.99x10 ⁻³	7.54x10 ⁻⁴	1.24x10 ⁻³	0.737	9.42x10 ⁻⁴	0.20	1.05x10 ⁻³	0.18	0.09
TFA $K_{ipd} = 1.9 \times 10^{-4}$	$[G^+X^-]_0$	$[X^-]^a$	$[G^+X^-]^a$	g_{\pm}^b	$[X^-]_{corrected}^c$	% error in $[X^-]$	$[G^+X^-]_{corrected}^c$	% error in $[G^+X^-]$	% error in $[G^+X^-]^{1/2}$
	(M)	(M)	(M)		(M)		(M)		
	2.50x10 ⁻⁴	1.43x10 ⁻⁴	1.07x10 ⁻⁴	0.876	1.54x10 ⁻⁴	0.07	9.59x10 ⁻⁵	0.12	0.06
	5.00x10 ⁻⁴	2.28x10 ⁻⁴	2.72x10 ⁻⁴	0.846	2.55x10 ⁻⁴	0.11	2.45x10 ⁻⁴	0.11	0.05
	6.28x10 ⁻⁴	2.63x10 ⁻⁴	3.65x10 ⁻⁴	0.835	2.99x10 ⁻⁴	0.12	3.29x10 ⁻⁴	0.11	0.05
	1.26x10 ⁻³	4.03x10 ⁻⁴	8.57x10 ⁻⁴	0.800	4.81x10 ⁻⁴	0.16	7.79x10 ⁻⁴	0.10	0.05
	2.51x10 ⁻³	6.02x10 ⁻⁴	1.91x10 ⁻³	0.761	7.58x10 ⁻⁴	0.21	1.75x10 ⁻³	0.09	0.04
	3.77x10 ⁻³	7.57x10 ⁻⁴	3.01x10 ⁻³	0.736	9.87x10 ⁻⁴	0.23	2.78x10 ⁻³	0.08	0.04
	5.02x10 ⁻³	8.86x10 ⁻⁴	4.13x10 ⁻³	0.718	1.19x10 ⁻³	0.25	3.83x10 ⁻³	0.08	0.04

Calculated according to ^a)Eq. 5, ^b)Eq. 3, or ^c)Eq. 9.

Acknowledging that the same treatment may not be utilized to calculate $[X^-]$ for complex formation (Eq. 7i), we have nonetheless directly transferred the relative percent error in $[G^+X^-]^{1/2}$ as calculated in Table III-10 for the individual salts to Figure III-11. This process enabled the construction of Figure III-19, which shows to a rough approximation the errors resulting from the assumption $[G']_{\text{observed}} \approx [G^+X^-]$. [32] Because the extent of ion pairing at any given concentration increases with decreasing K_{ipd} , the errors resulting from the assumption $[G']_{\text{observed}} \approx [G^+X^-]$ are directly related to the errors in the extrapolated value of $K_{\text{ipd}}^{1/2}K_{\text{assoc}}$. Consequently, the relative error in $K_{\text{ipd}}^{1/2}K_{\text{assoc}}$ increases in the order **1/2-TFA** < **1/2-OTs** < **1/2-BF₄** < **1/2-PF₆**, as seen in Figure III-21. More importantly, the relative percent errors are shown to decrease with concentration, ultimately resulting in an intercept (Figure III-19, dotted linear fit) that does not vary much from the case where $[G']_{\text{observed}} \approx [G^+X^-]$ (Figure III-19, solid linear trend). We conclude from this information that estimating $[G^+X^-]$ by $[G']_{\text{observed}}$, as routinely performed above, is approximately valid.

Figure III-19. Plots of Eq. 7o ($K_{\text{assoc}}[\text{H}] \ll 1$, crosshairs and solid linear fit, assuming $[\text{G}^+]_{\text{observed}} \approx [\text{G}^+\text{X}^-]$) for solutions of **1** and a) **2**-PF₆, b) **2**-BF₄, c) **2**-OTs, and d) **2**-TFA in CDCl₃:CD₃CN (3:2), 295 K. The open circles and dotted linear fits correspond to “corrected” plots, utilizing $[\text{G}^+\text{X}^-]$ values as determined in Table III-9.



III.11 *Experimental*

Unless otherwise noted, all reagents were purchased from commercial suppliers and used without further purification. For all complexation studies, precisely weighed amounts of each component were added into a 5.00 mL volumetric flask (± 0.02 mL) equipped with a ground glass stopper to make a moderately concentrated (nominally 16 mM) master solution. This solution was then sequentially diluted (no more than four sequential dilutions were performed per master solution) as needed by transferring exactly half of the higher concentration solution to a clean volumetric flask by means of to-deliver volumetric pipettes (± 0.006 mL) and diluting to the 5.00 mL mark. The fresh solutions were passed through a filter before 0.500 mL of each solution component (both host and guest) at a specified concentration was transferred via a to-deliver pipette to a 5 mm NMR tube. ^1H NMR data were collected on a temperature controlled spectrometer (400 MHz).

A $\text{CDCl}_3:\text{CD}_3\text{CN}$ (3:2, by volume) solvent mixture was chosen because the **2-X** salts investigated displayed a wide range of solubility behaviors in the lower dielectric constant solvent, whereas they were all well-solvated by CH_3CN .

Errors bars were calculated by assuming a $\pm 2\%$ deviation in percent complexation (as determined by integration of the corresponding ^1H NMR spectra) and following the error through each respective equation, as needed. For analysis, data points above 90% and below 10% complexation were ignored. [1] Linear regressions were performed using the entire error range (abscissa and ordinate) at each data point; standard errors in both the intercept and slope coefficients based on regression were used to determine errors in K_{assoc} , K_{ipd} , and/or K_{ipc} .

Preparation of Dibenzylammonium Chloride (2-Cl)

As described by Stoddart et al. [10] 42 mL of a 122 M stock HCl solution were transferred to a 250 mL round bottom flask and diluted with dionized water to yield a 2.05 M HCl solution. To the acid solution, dibenzylamine (4.9416 g, 25.05 mmol) was slowly added, whereupon the white precipitate of dibenzylammonium chloride was immediately observed. The reaction mixture was allowed to stir at room temperature over a period of

six hours before the chloride salt was collected via vacuum filtration, recrystallized in H₂O (3 times) and dried, 4.60 g (80%), mp = 275-277 °C (mp not reported in literature). ¹H-NMR (DMSO, 400 MHz) δ 9.89 (br s, 2H), 7.57 (d, *J* = 7 Hz, 4H), 7.43-7.37 (m, 6H), 4.10 (s, 4H). Elemental analysis calculated (%) for C₁₄H₁₆NCl: C 71.9, H 6.9, N 6.0; found: C 71.91, H 6.83, N 5.96.

Preparation of Dibenzylammonium Hexafluorophosphate (2-PF₆)

Also described by Stoddart et al., [10] 100 mL warm, deionized water were added to dibenzylammonium chloride. Further heating resulted in complete solvation of the chloride salt, whereupon slow addition of saturated aqueous ammonium hexafluorophosphate yielded a thick, white, precipitate. The precipitate was collected via vacuum filtration, washed excessively with warm water and dried, 4.30 g (50%), mp = 208-210 °C (mp lit = 192-193 °C [10] and 207-209 °C [33]). ¹H-NMR (CD₃CN, 400 MHz) δ 7.49 (s, 10H), 4.25 (s, 4H).

Preparation of Dibenzylammonium Methanesulfonate (2-CH₃SO₃)

Methanesulfonic acid (1.00019 g, 10.41 mmol) was added to 100 mL diethyl ether at room temperature and 2 mL of dibenzylamine (10.40 mmol, as delivered via a 2 mL TD volumetric pipette) were added dropwise to the stirred acid solution, resulting in an immediate white precipitate. The precipitate was collected via vacuum filtration, washed with copious amounts of diethyl ether, and dried, 3.05 g (95%), mp = 135-137 °C (no literature available). ¹H-NMR (CDCl₃, 400 MHz) δ 9.24 (br s, 2H), 7.45 (d, *J* = 8 Hz, 4H), 7.39-7.30 (m, 6H), 3.94 (t, *J* = 5 Hz, 4H), 2.60 (s, 3H). Elemental analysis calculated (%) for C₁₅H₁₉NO₃S: C 61.41, H 6.53, N 4.77; found: C 61.21, H 6.49, N 4.70.

Preparation of Dibenzylammonium *p*-Toluenesulfonate (2-OTs)

p-Toluenesulfonic (2.8533 g, 15.13 mmol) was added to 25 mL methanol at room temperature. Dibenzylamine (2.9660 g, 15.03 mmol) was added dropwise to the stirred acid solution, resulting in a white precipitate. The precipitate was collected via vacuum filtration, washed with cold methanol, and dried, 5.35 g (92%), mp = 166-168 °C (no literature available). ¹H-NMR (CDCl₃, 400 MHz) δ 9.27 (br s, 2H), 7.59 (d, *J* = 8 Hz,

2H), 7.38 (m, 4H), 7.27 (m, 6H), 7.13 (d, $J = 8$ Hz, 2H), 3.91 (t, $J = 5$ Hz, 4H), 2.38 (s, 3H). Elemental analysis calculated (%) for $C_{21}H_{23}NO_3S$: C 68.27, H 6.27, N 3.79; found: C 68.09, H 6.23, N 3.80.

Preparation of Dibenzylammonium Tetrafluoroborate (2-BF₄)

Tetrafluoroboric acid, 54% by weight in diethyl ether, (1.5500 g, 17.65 mmol) was added to 100 mL diethyl ether at room temperature. Dibenzylamine (10.40 mmol, as delivered via a 2 mL TD volumetric pipette) was added dropwise to the stirred acid solution. A white precipitate was observed immediately, collected via vacuum filtration, washed with ether and dried, 2.00 g (68%), mp = 196-198 °C (mp lit = 186 °C [34]). ¹H-NMR (CDCl₃, 400 MHz) δ 7.37 (s, 10H), 4.03 (s, 4H). Elemental analysis calculated (%) for $C_{14}H_{16}NBF_4$: C 58.98, H 5.66, N 4.91; found: C 59.10; H 5.61; N 4.97.

Preparation of Dibenzylammonium Trifluoromethanesulfonate (2-CF₃SO₃)

Trifluoromethanesulfonic acid (1.64494 g, 10.96 mmol) was added to ~100 mL diethyl ether at room temperature. Dibenzylamine (10.40 mmol, as delivered via a 2 mL TD volumetric pipette) was added dropwise to the stirred acid solution. A white precipitate was observed and collected via vacuum filtration, washed with ether and dried, 2.60 g (72%), mp = 115-117 °C (no literature available). ¹H-NMR (CDCl₃, 400 MHz) δ 8.18 (br s, 2H), 7.39 (m, 10H), 3.97 (t, $J = 5$ Hz, 4H). Elemental analysis calculated (%) for $C_{15}H_{16}NF_3SO_3$: C 51.87, H 4.84, N 4.03; found: C 51.90, H 4.64, N 3.99

Preparation of Dibenzylammonium Trifluoroacetate (2-TFA)

15.40 mL trifluoroacetic acid (200 mmol) were added to a 100 mL volumetric flask and diluted with dionized water, to yield a 2.00 M solution of acid. Dibenzylamine (1.98254 g, 10.24 mmol) was added to a round bottom flask, to which the TFA solution was slowly added. A white precipitate was immediately observed and was collected via vacuum filtration, washed with water, and dried, 2.23 g (71%), mp = 147-149 °C (literature not available). ¹H-NMR (CDCl₃, 400 MHz) δ 9.90 (br s, 2H), 7.21-7.31 (m, 10H), 3.81 (t, $J = 5$ Hz, 4H). Elemental analysis calculated (%) for $C_{16}H_{16}NO_2F_3$: C 61.73, H 5.18, N 4.50; found: C 61.63, H 5.28, N 4.42.

Crystallography

Long thin needles ($\sim 1.0 \times 0.2 \times 0.01 \text{ mm}^3$) of **2-OTs**, **2-TFA**, and **2-CF₃SO₃** were crystallized by vapor diffusion of pentane into chloroform solution at room temperature. A needle was cut ($\sim 0.2 \times 0.1 \times 0.02 \text{ mm}^3$), mounted on a nylon CryoLoop™ (Hampton Research) with Krytox® Oil (DuPont) and centered on the goniometer of a Oxford Diffraction XCalibur2™ diffractometer equipped with a Sapphire 2™ CCD detector. The data collection routine, unit cell refinement, and data processing were all carried out with the program CrysAlis. [35] The Laue symmetry and systematic absences were consistent with the monoclinic space groups $P2_1/n$. The structure was solved by direct methods and refined using the SHELXTL NT program package. [36] The final refinement involved an anisotropic model for all non-hydrogen atoms. Hydrogen atom positions and isotropic thermal parameters were refined independently.

III.12 References

- [1] Weber, G. *Molecular Biophysics*. Pullman, B.; Weissbluth, M., Ed. Academic Press: New York, NY, 1965, pp. 369-397.
- [2] Debye, P.; Hückel, E. *Z. Physik* **1923**, *24*, 305-325.
- [3] Isaacs, N. *Physical Organic Chemistry*, Longmans, England, 1995, pp. 56-62, 2nd Ed.
- [4] For a brief discussion on ion-pairing of complexes, see: Vögtle, F.; Weber, E. in *Chemistry of Ethers, Crown Ethers, Hydroxyl Groups and Their Sulphur Analogues*. Patai, S. ed. Wiley, Chichester, 1980, vol. 1, pp. 120-121.
- [5] a) Gibson, H. W.; Yamaguchi, N.; Hamilton, L.; Jones, J. W. *J. Am. Chem. Soc.* **2002**, *124*, 4653-4665. b) Ashton, P. R.; Ballardini, R.; Balzani, V.; Gómez – López, M.; Lawrence, S. E.; Martínez-Díaz, M. V.; Montalti, M.; Piersanti, A.; Prodi, L.; Stoddart, J. F.; Williams, D. J. *J. Am. Chem. Soc.* **1997**, *119*, 10641-10651.

- [6] For a recent report describing chemical shift changes of an electrolyte with concentration see Naidoo, K. J.; Lopis, A. S.; Westra, A. N.; Robinson, D. J.; Kock, K. R. *J. Am. Chem. Soc.* **2003**, *125*, 13330-13331.
- [7] Montalti, M.; Prodi L. *Chem. Comm.* **1998**, 1461-1462.
- [8] Dietrich, B.; Lehn, J. M.; Sauvage, J. P.; Blanzat, J. *Tetrahedron* **1973**, *29*, 1629-1645.
- [9] Davlieva, M. G.; Lü, J. -M.; Lindeman, S. V.; Kochi, J. *J. Am. Chem. Soc.* **2004**, *126*, 4557-4565.
- [10] earlier ref: Ashton, P. R.; Campbell, P. J.; Chrystal, E. J. T.; Glinke, P. T.; Menzer, S.; Philp, D.; Spencer, N.; Stoddart, J. F.; Tasker, P. A.; Williams, D. J. *Angew. Chem. Int. Ed.* **1995**, *34*, 1865-1869.
- [11] Fallon, G. D.; Lau, V. L.; Langford, S. J. *Acta Cryst. E* **2002**, *E58*, 321-323.
- [12] Ashton, P. R.; Fyfe, M. C. T.; Hickingbottom, S. K.; Stoddart, F. J.; White, A. J. P.; Williams, D. J. *J. Chem. Soc., Perkin Trans. 2* **1998**, *10*, 2117-2128.
- [13] Fyfe, M. C. T.; Stoddart, J. F.; Williams, D. J. *J. Struct. Chem.* **1999**, *10*, 243-259.
- [14] The reader will note that all images save for Figure III-6a display ordered PF₆ anions. In each case, the respective CIF file was pulled directly from the referenced publication. Save for rotations and length calculations, no other manipulations of the data were performed. The origin of the discrepancy between what is discussed in text versus what has been published in the data tables is unknown.
- [15] Jones, J. W.; Gibson, H. W. *J. Am. Chem. Soc.* **2003**, *125*, 7001-7004.
- [16] We recognized the advantage to be gained in studying complexation under the low concentration regime by fluorescence spectroscopy [see, for example Ashton, P. R.; Ballardini, R.; Balzani, V.; Gómez-López, M.; Lawrence, S. E.; Martínez-Díaz, M. V.; Montalti, M.; Piersanti, A.; Prodi, L.; Stoddart, J. F.; Williams, D. J. *J. Am. Chem. Soc.* **1997**, *119*, 10641-10651.], but found that the emission spectra for **1** and **2-X** overlap, **1** yielding $\lambda_{\max}(\text{fluorescence}) = 410$ nm, and **2-PF₆** yielding a broad emission band from 370 to > 500 nm, with $\lambda_{\max} = 425$ nm. The excitation spectra also overlap, **1** displaying $\lambda_{\max}(\text{excitation}) = 277$ nm, and **2-PF₆** yielding a

- broad excitation band from 260 to 400 nM. Incidentally, it is interesting to note that utilizing fluorescence spectroscopy to quantify a related complex (**1**•(9-anthracenyl)methylbenzylammonium-PF₆), Stoddart et al. report $K_{a,exp} = 1.0 \times 10^6$ M in CH₂Cl₂ at 298 K. In the same manuscript, the authors further report a $K_{a,exp}$ of 1.3×10^4 according to the single point method in CDCl₃:CD₃CN (6:1) at 298 K for the same complex. While the solvent system does change between $K_{a,exp}$ values, the variance in dielectric constant does not warrant a difference of two orders in magnitude. The change in $K_{a,exp}$ between methods can only be attributed to ion pairing, which is proportional to overall host/guest concentrations. This example provides further support for the failure of Eq. 2 to adequately describe association constants in charged systems solvated in non-aqueous media.
- [17] For R₄NX (R = Me, *n*-Pr, *n*-Bu, *i*-Am; X = PF₆, B(C₆H₅)₄, ClO₄, Cl, SCN) in CH₃CN $K_{ipd} = 2 - 4 \times 10^{-2}$ M [Barthel, J.; Iberl, L.; Rossmair, J. Gores, H. J.; Kaukal, B. *J. Solution Chem.* **1990**, *19*, 321-337], in acetone $K_{ipd} = 1 - 3 \times 10^{-3}$ M [Savedoff, L. G. *J. Am. Chem. Soc.* **1966**, *88*, 664-667] and in CH₂Cl₂ $K_{ipd} = 1 \times 10^{-4}$ to 5×10^{-5} M [Romeo, R.; Arena, G.; Scolaro, L. M.; Plutino, M. R. *Inorg. Chem. Acta* **1995**, *240*, 81-92].
- [18] (a) Nelson, S. F.; Ismagilov, R. F. *J. Phys. Chem. A* **1999**, *103*, 5373-5378. (b) Schmid, R.; Kirchner, K.; Dickert, F. L. *Inorg. Chem.* **1988**, *27*, 1530-1536.
- [19] Born, M. *Z. Phys.* **1920**, *1*, 45-48.
- [20] Percent crown occupied was calculated from the most fully resolved set of complexed and uncomplexed resonance pairs for each individual sample; in cases where multiple pairs are resolved, the average is given.
- [21] a) Goldfarb, D. L.; Corti, H. R. *J. Phys. Chem. B* **2004**, *108*, 3358-3367. b) Das, Debasish; Das, Bijan; Hazra, Dilip K. *J. Solution Chem.* **2003**, *32*, 77-83. c) Das, Debasish; Das, Bijan; Hazra, Dilip K. *J. Solution Chem.* **2002**, *31*, 425-431. d) Chen, Zhidong; Hojo, Masashi. *J. Phys. Chem. B* **1997**, *101*, 10896-10902.
- [22] a) Paligoric, I.; Gal, I. J. *J. Inor. Nucl. Chem.* **1976**, *38*, 1487-91. b) Paligoric, I.; Gal, I. J. *J. Chem. Soc., Faraday Trans. 1* **1972**, *68*, 1093-100.
- [23] a) Chandrani G.; Jayanti, M. C.; Sandip, K.; Bijan, D. *J. Phys. Chem. B* **2003**, *107*, 12814-12819. b) Gill, J. B. *Chem. Nonaqueous Solutions* **1994**, 149-178.

- [24] a) Haake, P.; Prigodich, R. *Inorg. Chem.* **1984**, *23*, 457-462. b) Lim, Y. -Y.; Drago, R. *J. Am. Chem. Soc.* **1972**, *94*, 84-90. c) Neuman, R. C., Jr.; Jonas, V. *J. Phys. Chem.* **1971**, *75*, 3550-3554. d) Haque, R.; Coshow, W. R.; Johnson, L. F. *J. Am. Chem. Soc.* **1969**, *91*, 3822-3827.
- [25] Khazaell, S.; Popov, A. I.; Dye, J. L. *J. Phys. Chem.* **1982**, *86*, 4238-4244.
- [26] a) Pratt, M. D.; Beer, P. D. *Polyhedron* **2003**, *22*, 649-653. b) Al-Sayah, M. H.; Branda, N. R. *Org. Lett.* **2002**, *4*, 881-884. c) Werner, F.; Schneider, H. -J. *Helvetica Chim. Acta* **2000**, *83*, 465-478. d) Nishizawa, S.; Shigemori, K.; Teramae, N. *Chem. Lett.* **1999**, *11*, 1185-1186.
- [27] The poor solubility of **2**-Cl renders us unable to observe complexation over a broad enough range of concentrations to implement the equilibrium treatment of Chapter II.
- [28] for example, see a) Levitskaia, T. G.; Bonnesen, P. V.; Chambliss, C. K.; Moyer, B. A. *Anal. Chem.* **2003**, *75*, 405-412. b) Bartoli, S.; Roelens, S. *J. Am. Chem. Soc.* **2002**, *124*, 8307-8315. c) Arduini, A.; Brindani, E.; Giorgi, G.; Pochini, A.; Secchi, A. *J. Org. Chem.* **2002**, *67*, 6188-6194. d) Casnati, A.; Massera, C.; Pelizzi, N.; Stibor, I.; Pinkassik, E.; Ugozzoli, F.; Ungaro, R. *Tetrahedron Lett.* **2002**, *43*, 7311-7314. e) Berry, N. G.; Sambrook, M. R. *J. Am. Chem. Soc.* **2002**, *124*, 12469-12476. f) Tongraung, P.; Chantarasiri, N.; Tuntulani, T. *Tetrahedron Lett.* **2002**, *44*, 29-32. g) Mahoney, J. M.; Beatty, A. M.; Smith, B. D. *J. Am. Chem. Soc.* **2001**, *123*, 5847-5848. h) Wisner, J. A.; Beer, P. D.; Drew, M. G. B. *Angew. Chem., Int. Ed.* **2001**, *40*, 3606-3609. i) Kavallieratos, K.; Moyer, B. A. *Chem. Comm.* **2001**, *17*, 1620-1621.
- [29] A few examples include: a) Cafeo, G.; Gattuso, G.; Kohnke, F. H.; Notti, A.; Occhipinti, S.; Pappalardo, S.; Parisi, M. *Angew. Chem., Int. Ed.* **2002**, *41*, 2122-2126. b) Arduini, A.; Giorgi, G.; Pochini, A.; Secchi, A.; Ugozzoli, F. *J. Org. Chem.* **2001**, *66*, 8302-8308.
- [30] see for example a) Huang, F.; Fronczek, F. R.; Gibson, H. W. *J. Am. Chem. Soc.* **2003**, *125*, 9272-9273. b) Huang, F.; Gibson, H. W.; Bryant, W. S.; Nagvekar, D. S.; Fronczek, F. R. *J. Am. Chem. Soc.* **2003**, *125*, 9367-9371. c) Jones J. W.; Zakharov L. N; Rheingold A. L; Gibson H. W. *J. Am. Chem. Soc.* **2002**, *124*,

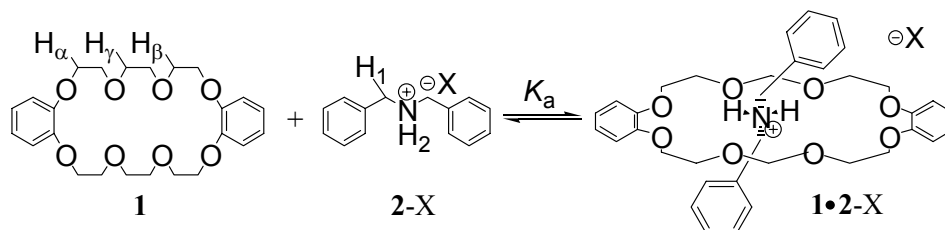
- 13378-13379. d) Bryant, W. S.; Jones, J. W.; Mason, P. E.; Guzei, I.; Rheingold, A. L.; Fronczek, F. R.; Nagvekar, D. S.; Gibson, H. W. *Org. Lett.* **1999**, *1*, 1001-1004.
- [31] as estimated from known values in MeCN and CH₂Cl₂, Reference [17]
- [32] Because $[G^+X^-]$ in the presence of host is always less than $[G^+X^-]$ in the absence of host due to complexation phenomena and release of X⁻ ions, the errors in Figure III-19 are underestimated, but this error is minimized due to the square root dependence.
- [33] Bryant, W.S. Ph.D. Dissertation, VPI&SU, 1999.
- [34] An alternative approach has been used by Mohamed, K. S.; Padma, D. K. *Indian J. Chem. Sect. A: Inorg., Phys., Theor. Anal.* **1988**, *27*, 759-763
- [35] CrysAlis v1.170, Oxford Diffraction: Wroclaw, Poland, 2002.
- [36] Sheldrick, G. M. SHELXTL NT ver. 6.12; Bruker Analytical X-ray Systems, Inc.: Madison, WI, 2001.

Chapter IV

A Cautionary Note Regarding the Investigation of Supramolecular Complexes Involving Secondary Ammonium Salts in Acetone

IV.1 *Exploring the Influence of Dielectric Constant on K_{ipd} and K_{assoc}*

Recognizing the importance that solvent dielectric constant plays in each of our host/guest modeling studies from Chapter III, we explored pseudorotaxane **1**•**2**-X formation in acetone- d_6 for comparison with the well-studied $CDCl_3:CD_3CN$ (3:2) solvent system, a logical choice given the widespread use of acetone in similar reports. [1] Our immediate goal was to compare ion pair dissociation constants (K_{ipd}) of **2**-X as well as pseudorotaxane formation constants (K_{assoc}) of **1**•**2**⁺ between solvent systems, and to correlate these results with solvent dielectric constants. Our studies revealed surprising, although not unexpected, results which constitute the focus of this chapter.

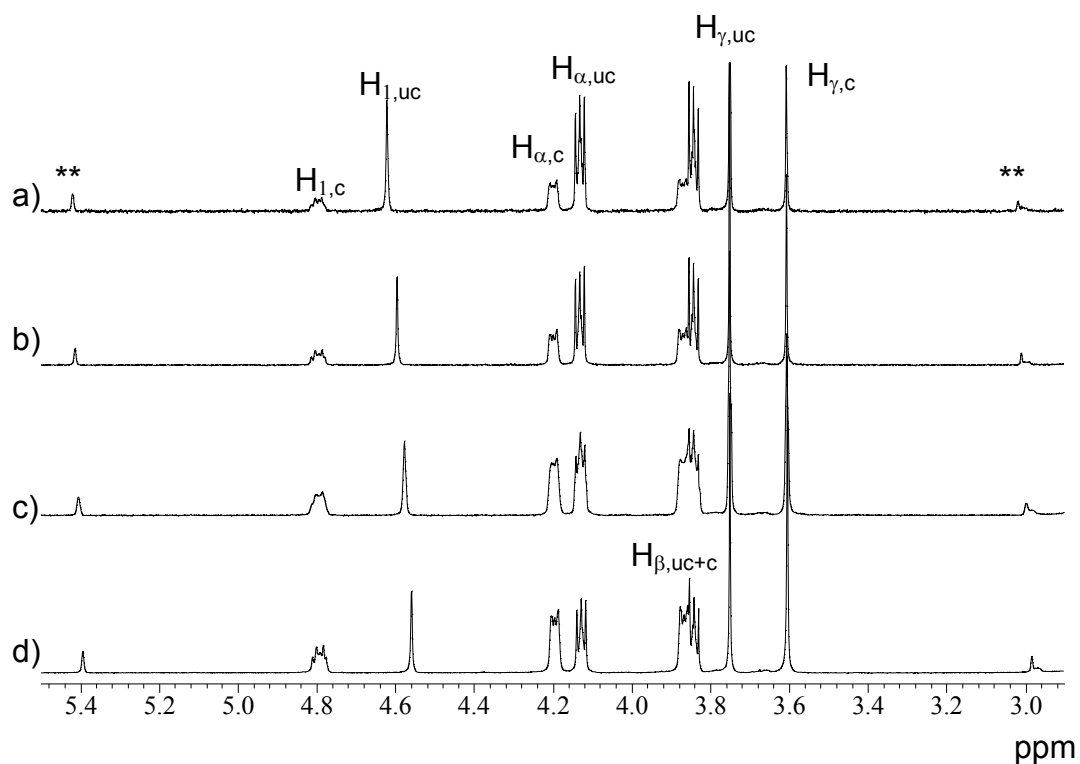


IV.2 *2° Ammonium Salts in Acetone*

Having previously reported association constants for pseudorotaxane formation between **1** and various **2**-X salts in a mixed solvent system consisting of $CDCl_3:CD_3CN$ (3:2, by volume), we undertook similar complexation studies in acetone- d_6 . Four equimolar solutions of **1** and **2**- BF_4 (16.0, 8.00, 4.00, and 2.00 mM) in acetone- d_6 were thus studied by 1H NMR spectroscopy at 295 K. In all cases, spectra were recorded within 10 minutes of mixing the host and guest components, and no longer than one hour after preparation of the individual solutions. As can be seen from Figure IV-1, evolution

of complex signals (labeled with a subscripted “c”; uncomplexed resonances are labeled with a subscripted “uc”) signify host/guest association under the slow exchange regime on the NMR time scale, as anticipated. However, two new uncharacterized resonances at 3.0 and 5.4 ppm were noted (Figure IV-1, denoted by the symbol “**”); a solvent background check confirmed the purities of solvent and starting materials. Identical complexation experiments were performed with **2**-PF₆ and **2**-TFA: once again, the same unanticipated peaks were observed with nearly identical chemical shifts.

Figure IV-1. ¹H NMR spectra (400 MHz, 295K, acetone-*d*₆) of a) 2.00 b) 4.00 c) 8.00 and d) 16.0 mM equimolar solutions of **1** and **2**-BF₄, initially.



To probe the identity of the uncharacterized signals, time dependent studies were run on the pristine salt solutions. Figure IV-2 displays results from a 16.0 mM solution of **2**-PF₆, run a) 5 minutes and b) 24 hours after solvation. Note the increase in intensity of the 5.4 and 3.0 ppm peaks; an emerging aromatic signal is also distinguishable. This time dependency was seen at all concentrations of **2**-X investigated, regardless of counteranion. Furthermore, the evolution of byproduct was not limited solely to **2**-X: the secondary ammonium salts **3**-PF₆ (Figure IV-3), **4**-2PF₆ (Figure IV-4), and **5**-BF₄ (Figure IV-5) also displayed time dependent byproduct evolution.

Figure IV-2. ¹H NMR spectra (400 MHz, 295K, acetone-*d*₆) of **2**-PF₆, 16.0 mM, collected after a) 5 minutes and b) 24 hours of solvation.

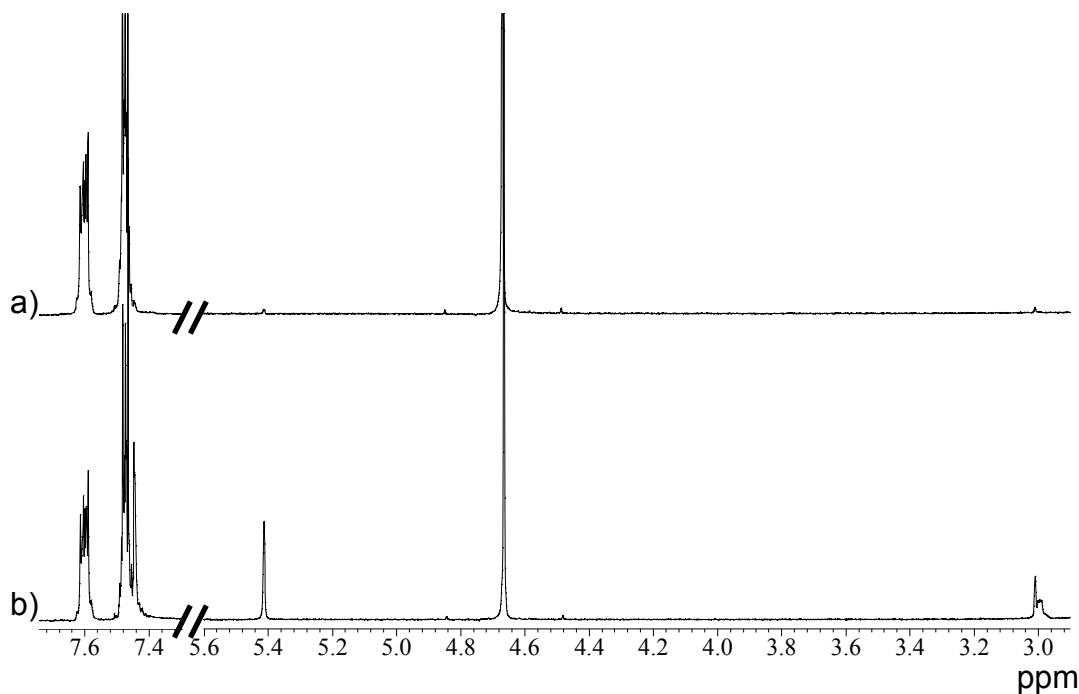


Figure IV-3. ^1H NMR spectra (400 MHz, 295K, acetone- d_6) of **3**-PF $_6$ collected after a) 5 minutes and b) 24 hours of solvation.

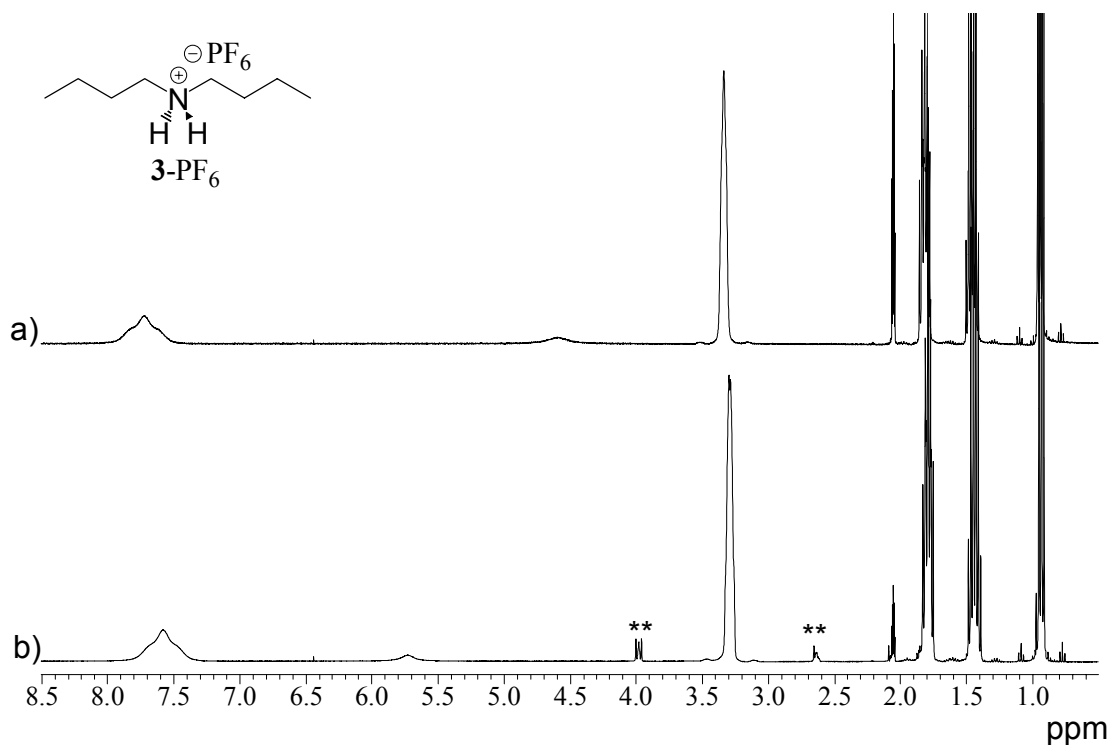


Figure IV-4. ^1H NMR spectra (400 MHz, 295K, acetone- d_6) of **4**-2PF $_6$ collected after a) 5 minutes and b) 24 hours of solvation.

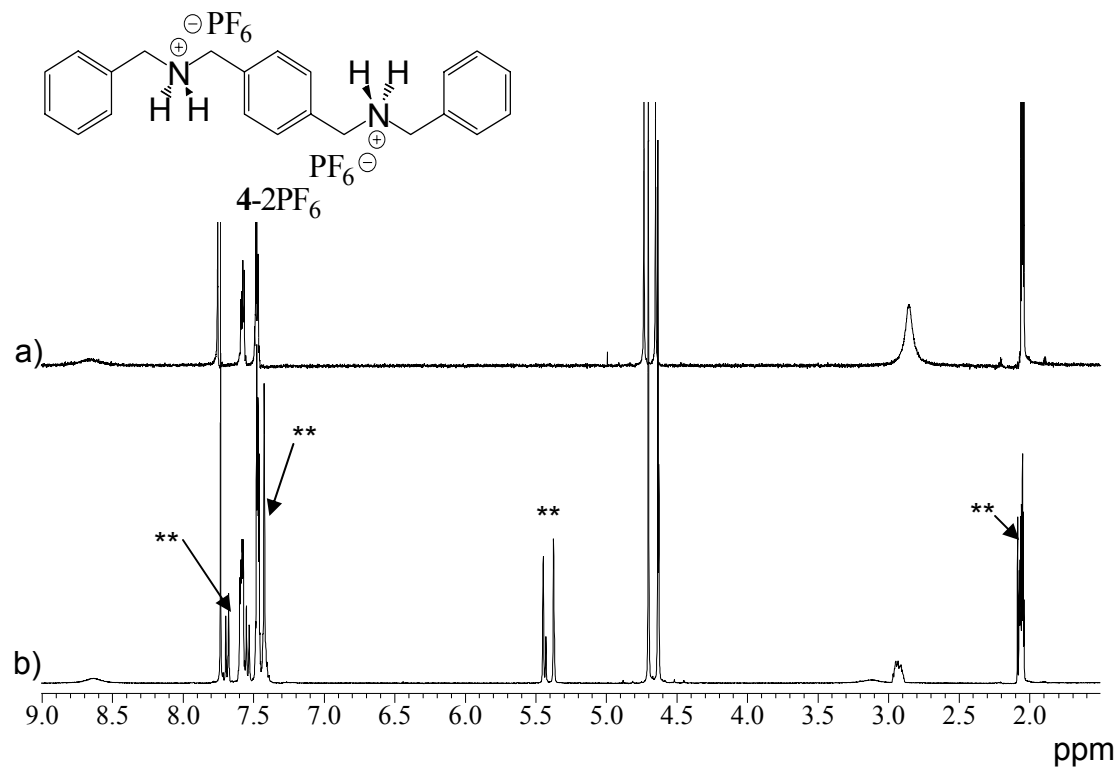
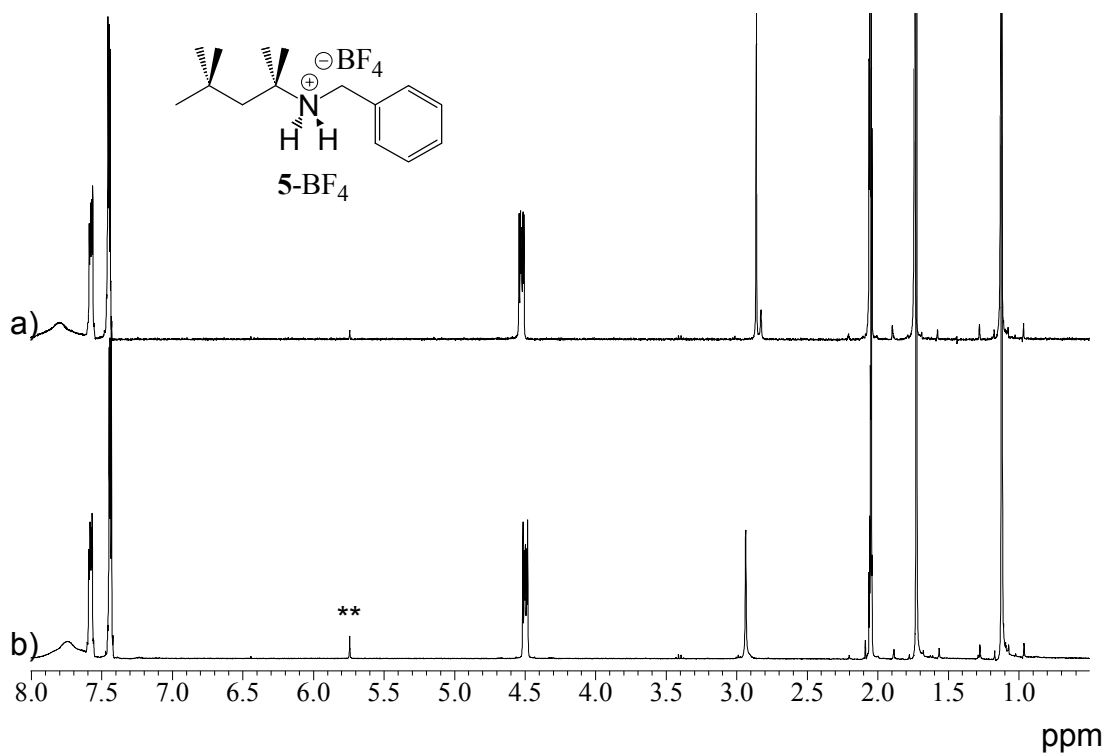


Figure IV-5. ^1H NMR spectra (400 MHz, 295K, acetone- d_6) of **5**- BF_4 collected after a) 5 minutes and b) 24 hours of solvation.



IV.3 Refocusing Our Efforts: Byproduct Identification

Because of the importance of clearly defining equilibrium concentrations based upon integration values for the determination of K_{ipd} and K_{assoc} , the emergence of a competing reaction was of immediate concern. As a result of not precisely knowing equilibrium concentrations, our focus shifted away from that of the complexation event towards the underlying chemistry of byproduct evolution.

Recalling the tendency of amines to undergo nucleophilic addition to aldehydes and ketones, [2] we believed the impurity to be an acetone condensation product, as shown in Scheme IV-1. Indeed, saturating **2**- PF_6 with freshly distilled acetone- d_6 , and allowing the solution to stir over molecular sieves for 24 hours under N_2 resulted in

nearly 95% conversion of the 2° ammonium to the byproduct, confirming the role of water evolution in this reaction (Figure IV-6a); the chemical shifts of Figure IV-6a agreed well with the formation of iminium **6**-PF₆. Addition of a drop of water to the same NMR tube resulted in complete recovery of **2**-PF₆ (Figure IV-6b). Furthermore, examination of Figure IV-1 provides corroboration of salt formation: the evolved peaks (labeled “**”) experience an upfield shift with concentration in a manner analogous to H_{1,uc}, indicative of a rapidly exchanged ion pairing event on the NMR time scale.

Scheme IV-1. Proposed mechanism for formation of observed byproduct.

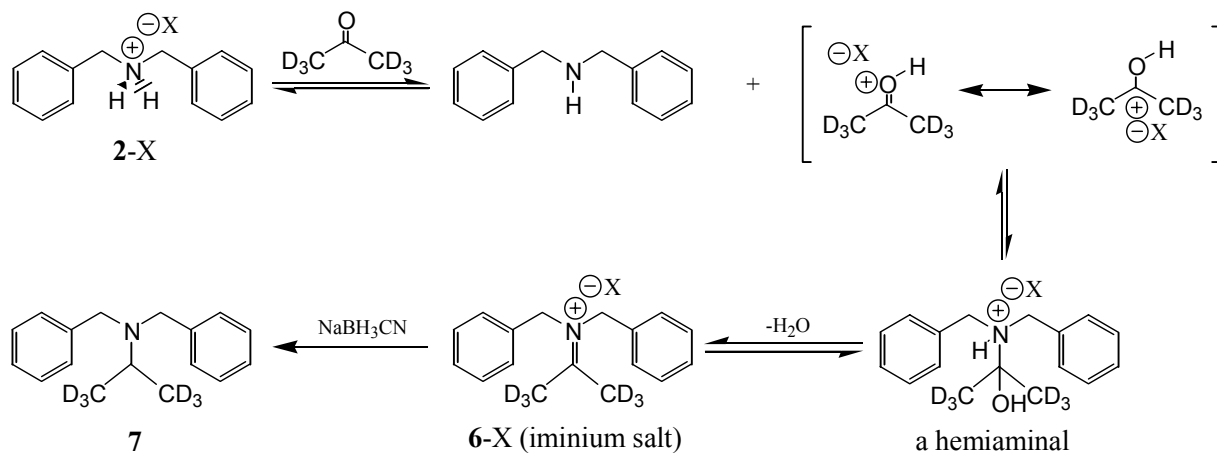
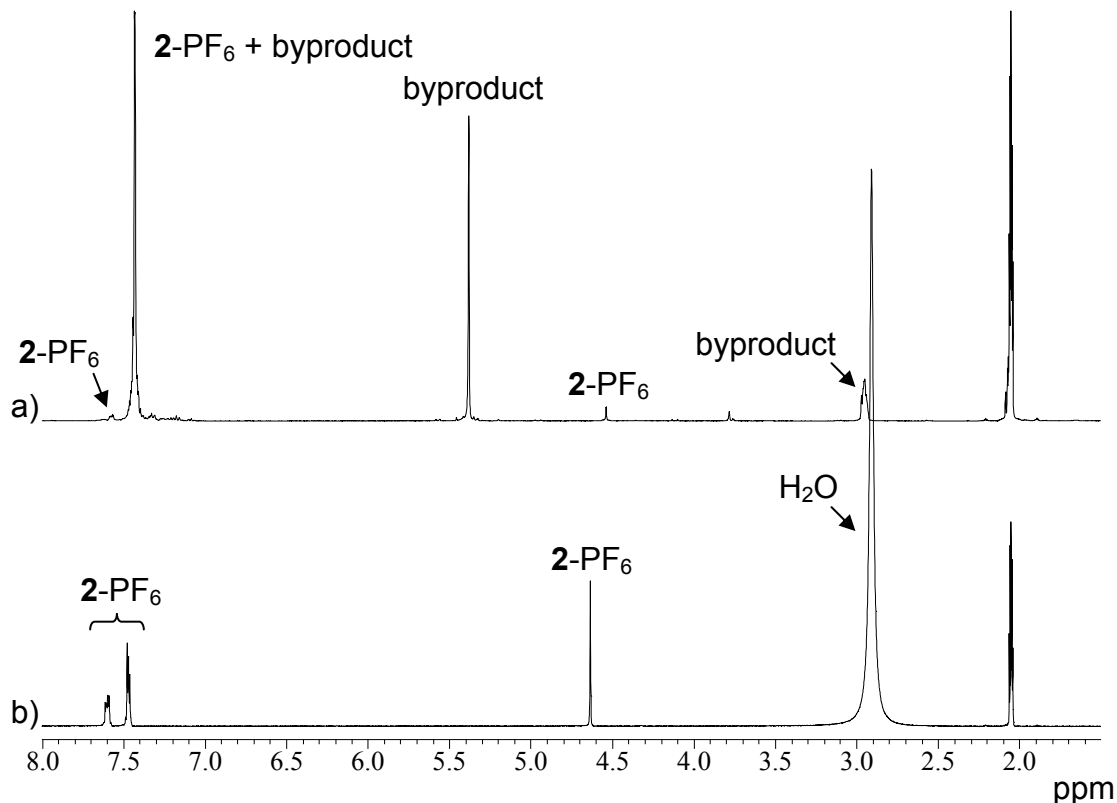


Figure IV-6. ^1H NMR spectra (400 MHz, 295K, acetone- d_6) of **2**-PF₆ a) 24 hours after solvation in dry acetone stirring over molecular sieves and b) sample from a) to which a drop of H₂O has been added.



Despite such high conversion, all attempts to isolate the byproduct were fruitless: solvent extraction, thin layer chromatography (TLC), flash column chromatography, high pressure liquid chromatography (HPLC), and selective crystallization all failed. Direct detection of the byproduct by mass spectroscopy also proved futile. Our failure to isolate and identify the predicted imine is not without precedent: salts of the type $\text{R}_2\text{C}=\text{NR}_2^+\text{X}^-$ are notoriously difficult to isolate due to the reversible nature of the condensation. [3] Nevertheless, the existence of iminium ions has been proven by isolation from such condensation reactions. [3b,4]

IV.4 *Indirect Proof of Iminium Ion Formation*

Unable to isolate the iminium base and directly prove its structure, we theorized that if **6-X** was indeed involved in the reaction sequence, we should be able to indirectly prove its existence by irreversible formation of *N,N*-dibenzylisopropylamine (**7**) through the process of reductive amination. We thus chose sodium cyanoborohydride as the reducing agent due to its solubility and selectivity: it is well known that at moderate pH ($5 < \text{pH} < 9$), the cyanohydridoborate anion preferentially reduces imines over the ketones. [5] The reduction was allowed to proceed at room temperature in dry acetone over molecular sieves utilizing a 2:1 stoichiometric ratio of reducing agent to **2-PF₆**. After 72 hours the reduction was determined by ¹H NMR analysis to be complete, resulting in the isolation of amine **7**, as anticipated, in moderate yield. Because amine **7** can only result from the intermediate iminium salt under these conditions, and because of the spectroscopic results of Figures IV-1-6, we are confident in our identification of the iminium salts as products of the condensation reactions between 2° ammonium salts and acetone.

IV.5 *Lessons From Acetone Studies*

These results call into question K_a values calculated for the complexation of 2° ammonium salts in acetone. They do not outright reject such values, however, as evolution of the intermediate Schiff base was shown to be a slow event: at 5 minutes after solvation, the concentration of **6-PF₆** was negligible (Figure IV-2a); this is not the case after 24 hours (Figure IV-2b).

Importantly, this body of work confirms quite clearly the need to characterize new individual resonances fully in what would otherwise be considered a known system. This requirement is particularly true when spectroscopic studies are being utilized for the quantification of sample concentrations. It further reminds us that solvents by definition are not inert species, and that careful consideration of the molecules to be studied in solution should be made before the solvent is chosen.

IV.6 *Experimental*

Dibenzylammonium salts (**2-X**; X = PF₆⁻, BF₄⁻, OTf⁻, TFA⁻) were prepared as described in the literature, using the appropriate corresponding acid when available. [1b] Di-*n*-butylammonium hexafluorophosphate (**3-PF₆**) [1a] and *N,N'*-dibenzyl-*p*-xylylenediammonium bis(hexafluorophosphate) (**4-PF₆**) [6] were also prepared as described in the literature. All other reagents were purchased from commercial suppliers and used without further purification. ¹H NMR spectra were recorded on a 400 MHz NMR spectrometer with the solvent proton signal as the reference.

Benzyl-1,1,3,3-tetramethylbutylammonium Tetrafluoroborate (5-BF₄): 1,1,3,3-Tetramethylbutylamine (2.5850 g, 20.0 mmol), benzaldehyde (2.1224 g, 20 mmol), and toluene (350 mL) in a 500 mL round bottom flask equipped with a Dean Stark trap were stirred under reflux for 16 hours. The toluene was removed and 5.0 grams of the dried, crude Schiff base were solvated in a mixture of THF (150 mL) and MeOH (100 mL). An excess of sodium borohydride (7.05 g, 186 mmol) was carefully added and the mixture stirred for 12 hours at reflux, at which point the product was suspended in H₂O and extracted with CH₂Cl₂ (4 x 250 mL). 2.00 g of the dried, crude product were then taken up in diethyl ether and added dropwise to a stirred solution of tetrafluoroboric acid, 54% by weight in diethyl ether, (1.5500 g, 17.65 mmol), resulting in a white precipitate which was collected via vacuum filtration, washed with water, and dried (2.10 g, 75%), mp = 121-123 °C. ¹H NMR (400 MHz, CDCl₃) δ 7.38-7.45 (5H, aromatic), 6.59 (br s, 2H, NH₂), 4.05 (m, 2H, benzylic group), 1.70 (s, 2H, CH₂), 1.40 (s, 6H, C(CH₃)₂), 1.03 (s, 9H, C(CH₃)₃). Elemental analysis calculated (%) for C₁₅H₂₆NBF₄: C 58.65, H 8.53, N 4.56; found: C 58.43, H 8.64, N 4.56.

***N,N*-Dibenzylisopropylamine (7)**: **2-TFA** (1.02 g, 3.28 mmol) was dissolved in 10 mL freshly dried acetone (distilled over molecular sieves, middle fraction retained) and stirred over molecular sieves for 24 hours, at which point sodium cyanoborohydride (0.25 g, 4.00 mmol) was added. The solution was stirred for 48 hours before additional sodium cyanoborohydride (0.200 g, 3.18 mmol) was added. After 72 total hours, the solution

was taken to dryness and the residue redissolved in warm H₂O (10 mL) and extracted with diethyl ether (5 x 10 mL). The aqueous layer was then taken to pH ~10 by addition of KOH, saturated with NaCl, and extracted with diethyl ether (3 x 10 mL). The organic extracts were combined, dried with K₂CO₃, and recrystallized in ethanol (0.50 g, 65%), mp = 30.8-31.3 °C (reported mp = 33-34 °C [7]). ¹H NMR (400 MHz, acetone-*d*₆) δ 7.39 (d, *J* = 7 Hz, 4H), 7.29 (t, *J* = 7 Hz, 4H), 7.19 (t, *J* = 7 Hz, 2H), 3.60 (s, 4H, benzylic group), 2.90 (septuplet, *J* = 6.5 Hz, 1H, CH(CH₃)₂), 1.09 (d, *J* = 6.5 Hz, 6H, CH(CH₃)₂). HRMS (FAB⁺) calculated for C₁₇H₂₂N: 240.1752, found: 240.1744. **7** was also isolated under similar conditions using **2**-PF₆ in place of **2**-TFA.

IV.7 References

- [1] For a review on 2° ammonium salts as guest ligands in an acetone medium, see Clifford, T.; Abushamleh, A.; Busch, D. H. *Proc. Natl. Acad. Sci. USA* **2002**, *99*, 4830-4836. also see a) Ashton, P. R.; Campbell, P. J.; Chrystal, E. J. T.; Glink, P. T.; Menzer, S.; Philip, D.; Spencer, N.; Stoddart, J. F.; Tasker, P. A., Williams, D. J. *Angew. Chem. Int. Ed, Engl.* **1995**, *34*, 1865-1869 and b) Ashton, P. R.; Chrystal, E. J. T.; Glink, P. T.; Menzer, S.; Schiaro, S.; Spencer, N.; Stoddart, J. F.; Tasker, P. A., White, A. J. P.; Williams, D. J. *Chem. Eur. J.* **1996**, *2*, 709-729. c) Gibson, H. W.; Yamaguchi, N.; Hamilton, L.; Yamaguchi, L. *J. Am. Chem. Soc.* **2002**, *124*, 4653-4665. d) Gibson, H. W.; Yamaguchi, N.; Jones, J. W. *J. Am. Chem. Soc.* **2003**, *125*, 3522-3533.
- [2] see for example Vollhardt, K. P. C.; Schore, N. E. *Organic Chemistry*, W. H. Freeman and Company, New York, 1994, 2nd Ed, pp. 649-654.
- [3] a) Gomez, S.; Peters, J. A.; Maschmeyer, T. *Adv. Synth. Catal.* **2002**, *344*, 1037-1057. b) Lamchen, M.; Pugh, W.; Stephen, A. M. *J. Chem. Soc.* **1954**, 4418-4425.
- [4] see Hine, J.; Evangelista, R. *J. Am. Chem. Soc.* **1980**, *102*, 1649-1655.
- [5] Borch, R. F.; Bernstein, M. D.; Durst, H. D. *J. Am. Chem. Soc.* **1971**, *93*, 2897-2904.

- [6] Ashton, P. R.; Glink, P. T.; Menzer, S.; Martínez-Díaz, M. –V.; Stoddart, J. F.; White, A. J. P.; Williams, D. J. *Angew. Chem. Int. Ed. Engl.* **1995**, *34*, 1930-1933.
- [7] Riddell, F. G.; Rogerson, M. *J. Chem. Soc., Perkin Trans. 2* **1996**, 493-504.

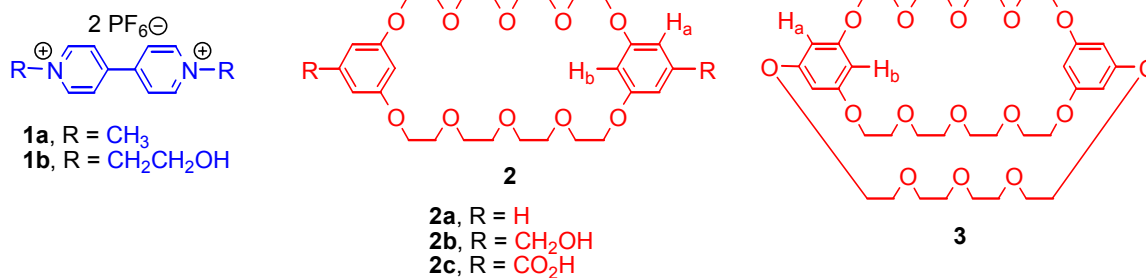
Chapter V

Cooperative Host/Guest Interactions via Counterion Assisted Chelation: Pseudorotaxanes and Pseudocryptands

V.1 *Inclusion Efficiency and General Trends*

Moving away from quantification methods and towards application driven systems, this chapter will focus on a consistent and pervasive theme throughout the four decades of rotaxane research: that of the enhancement of host/guest recognition. As discussed in Chapter I, this area is of particular relevance in the field of supramolecular polymers. [1] Because true supramolecular polymers are generally constructed of small, self-complimentary ditopic repeat units which spontaneously organize in solution, the degree of polymerization is dependent upon the strength of host/guest recognition, as verified by Meijer et al. who showed that the degree of chain extension varies inversely with the square root of K_a (Figure I-7). [2] Consequently, maximized K_a values enable enhanced control over the polymeric architecture and, ultimately, properties.

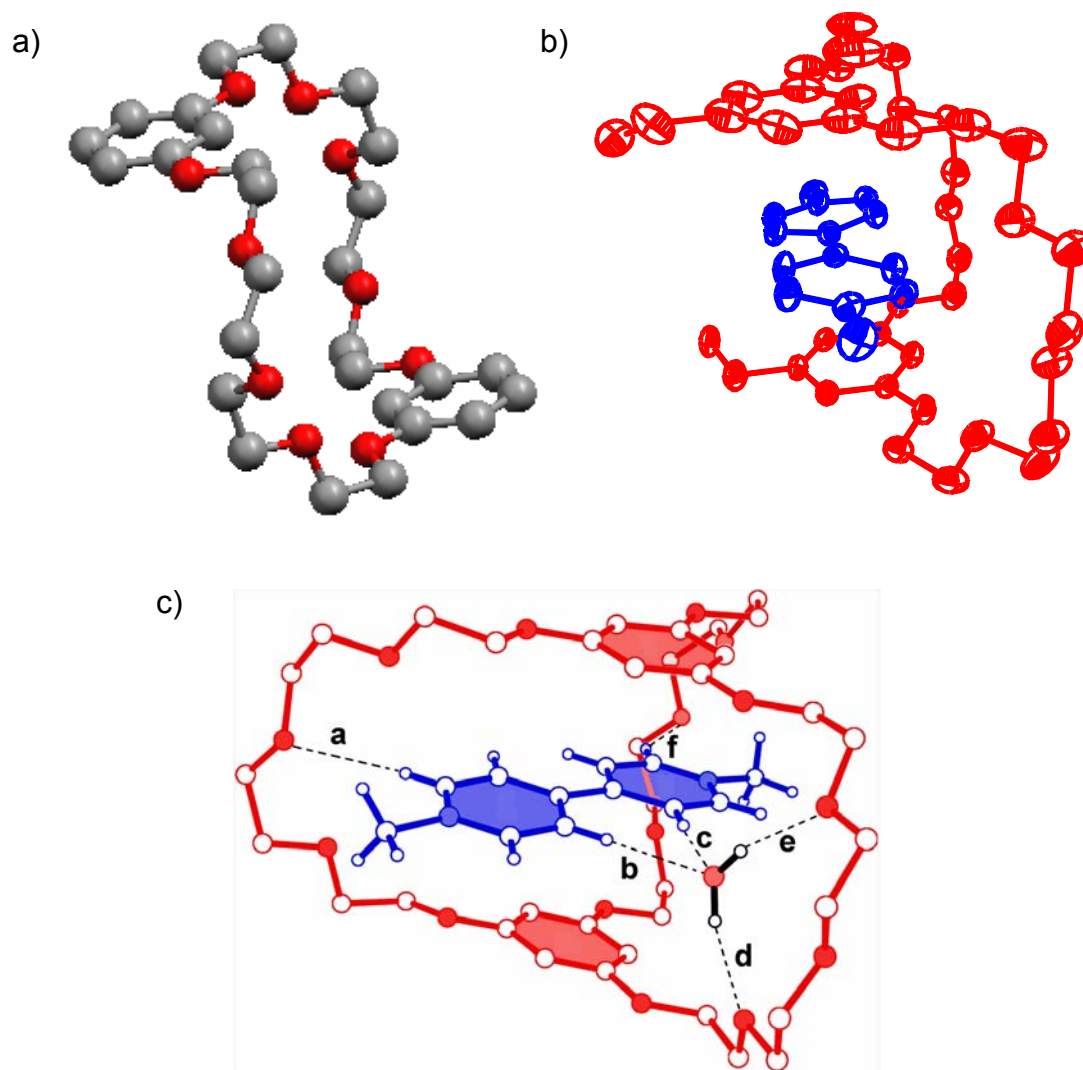
As chemists have begun to understand the importance of inclusion efficiency in self-assembled systems, quite a few reports have surfaced detailing very specific structure/property relationships involving host/guest systems. Complexes incorporating paraquat salts (i.e., dimethyl viologen, **1a**-2PF₆[⊖]) provide an excellent example of this evolution, resulting in host/guest formation constants that have steadily increased over the past decade.



Returning to Stoddart's seminal report on crown ether/paraquat complexation, it was shown in 1987 that two large crown ethers, bis(*p*-phenylene)-34-crown-10 (BPP34C10) and bis(*m*-phenylene)-32-crown-10 (BMP32C10, **2a**), complex **1a**-2PF₆ with 1:1 stoichiometry. [3] Unlike the previous dibenzo[24]-crown-8 complexes from Chapters III and IV, these systems were found to exhibit fast exchange on the NMR time scale. The time averaged resonances may be utilized to quantify host/guest interaction, as described in Appendix A according to the Benesi-Hildebrand treatment. [4] Also unlike the dibenzo[24]-crown-8 complexes, the complexes formed between viologens and the larger crown ethers were found to be ion paired, i.e., $K_{a,exp}$ is not concentration dependent; thus, the systems may be readily analyzed according to Eq. 2 from Chapter II. [5]

Based on X-ray crystal structural analysis, the research team led by Stoddart suggested that paraquat binding would be optimized by properly designed receptors which took advantage of intermolecular interactions such as [C—H•••O] hydrogen bonding, [N⁺•••O] electrostatic interactions, and charge transfer between the π -electron-rich aromatic rings of the host and the π -electron-deficient viologen. Gibson et al. showed in 1999 that in the solid-state, one of the complexes formed between bis(5-hydroxymethyl-1,3-phenylene)-32-crown-10 (**2b**) and **1a**-2PF₆ was not a pseudorotaxane, but an exo- or taco-complex (see Figure V-1b). [6] The required folding of the host (see Figure V-1a for **2a** in the absence of guest) to adopt the taco-complex suggested a favorable effect of constraining [7] the flexible host molecule to the requisite folded shape, thereby minimizing the entropic penalty of reorganization. Indeed, when a covalent linker was used to do so in forming bicyclic host **3**, a 100-fold improvement in apparent association constant ($K_{a,exp}$) resulted, increasing from $(5.5 \pm 0.5) \times 10^2 \text{ M}^{-1}$ in **2b**•**1a**-2PF₆ to $(6.0 \pm 1.0) \times 10^4 \text{ M}^{-1}$ in **3a**•**1a**-2PF₆! [6] Dynamic temperature studies indicated the increase in $K_{a,exp}$ resulted entirely from preorganization of **3a**, results which were supported by X-ray structural analyses as nearly identical geometries and interactions were noted for **2b**•**1a**-2PF₆ (Figure V-1b) and **3a**•**1a**-2PF₆ (Figure V-1c).

Figure V-1. Published ORTEP diagrams of a) **2a** [3] b) the taco-complex **2b/1a-2PF₆** [6] and c) the cryptand complex **3/1a-2PF₆** [6].



V.2 Contributions to Improved Binding Efficiencies: Model Studies

Encouraged by these exciting results, we explored other methods to drive pseudorotaxane formation. In studying the influence of counteranions on complexation, [8] we serendipitously discovered a ready and facile method of increasing K_a in the complexation of paraquats by hosts **2b** and bis(5-carboxy-1,3-phenylene)-32-crown-10 (**2c**).[9] As a control experiment, an acetone- d_6 solution of **2b** with two equivalents of (*n*-Bu) $_4$ N-PF $_6$ was studied. Neither ^1H (Figure V-2) nor ^{19}F NMR resonances shifted for either of the two components, indicating that (*n*-Bu) $_4$ N-PF $_6$ does not form a complex with **2b**. Under similar conditions, ^1H (Figure V-3) and ^{19}F NMR indicated that no interaction occurs between paraquat diol **1b**-2PF $_6$ and (*n*-Bu) $_4$ N-PF $_6$.

Figure V-2. ^1H NMR spectra (400 MHz, 295K, acetone- d_6) of a) **2b**; b) 3.00 mM **2b** + 6.95 mM (*n*-Bu) $_4$ N-PF $_6$; c) (*n*-Bu) $_4$ N-PF $_6$.

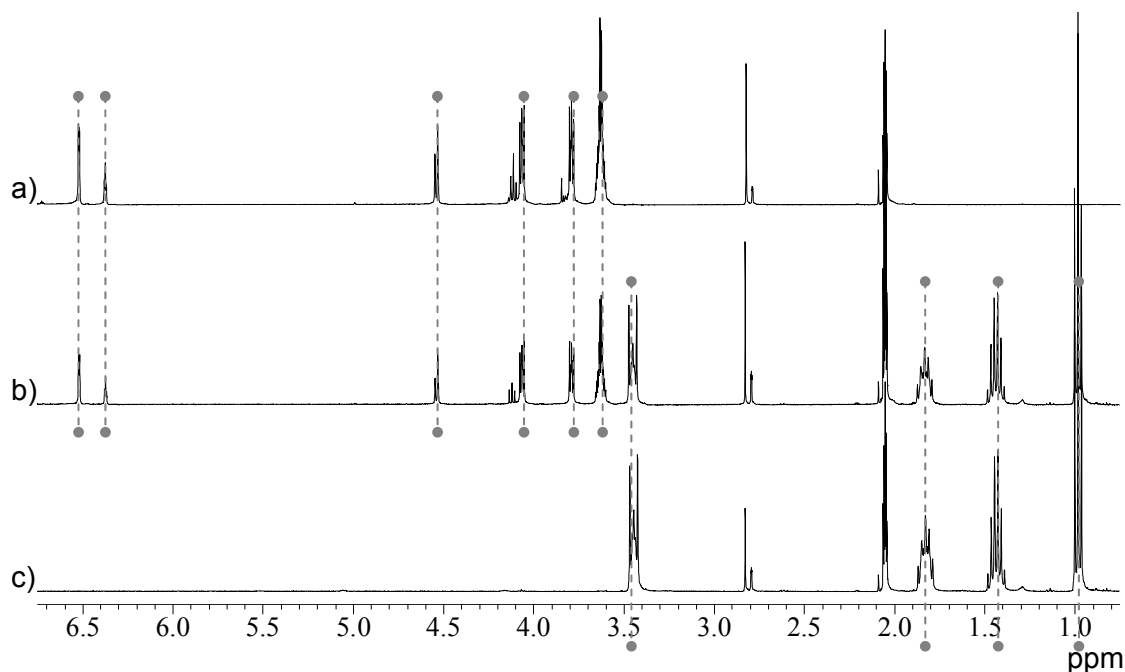
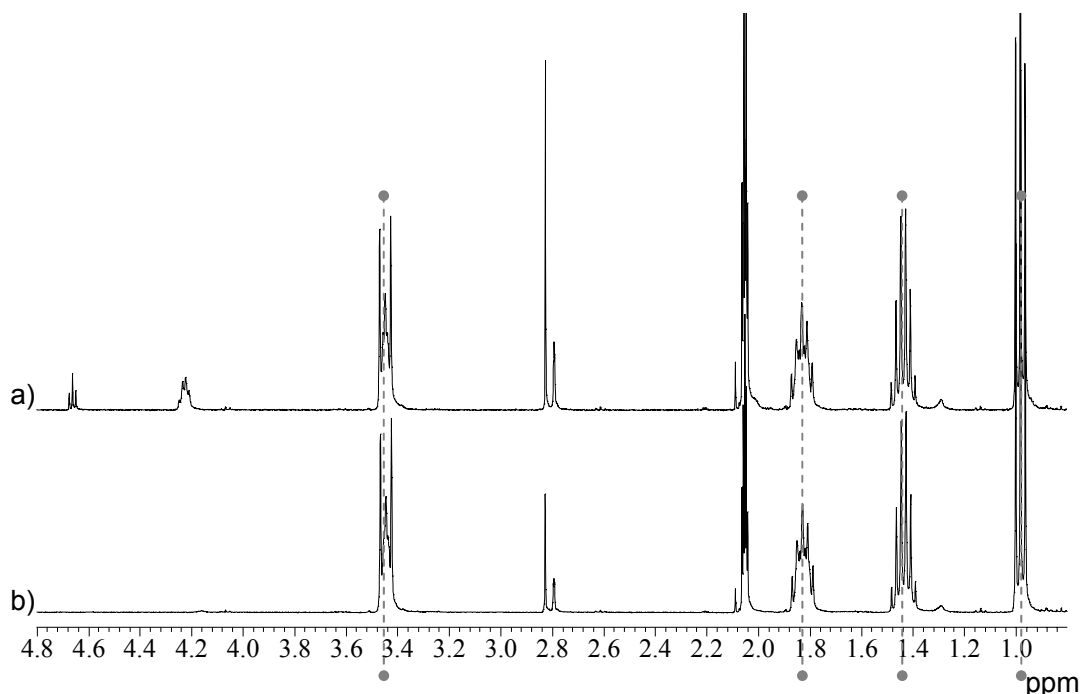
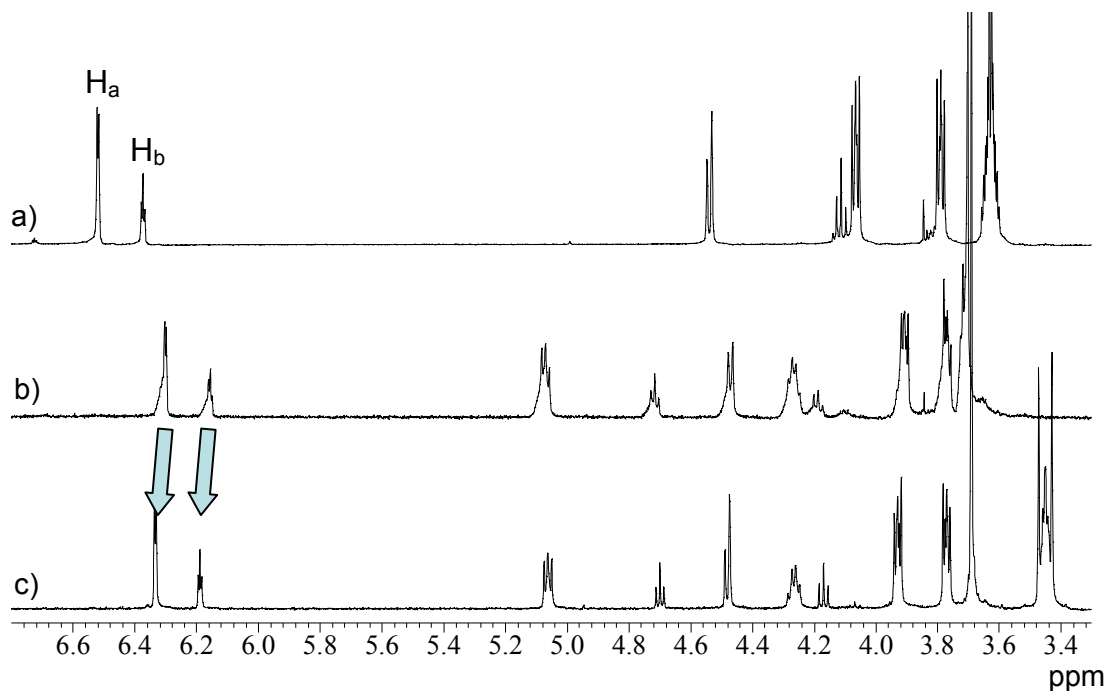


Figure V-3. ^1H NMR spectra (400 MHz, 295K, acetone- d_6) of a) 3.00 mM **1b**- 2PF_6 + 6.95 mM $(n\text{-Bu})_4\text{N-PF}_6$ and b) $(n\text{-Bu})_4\text{N-PF}_6$.



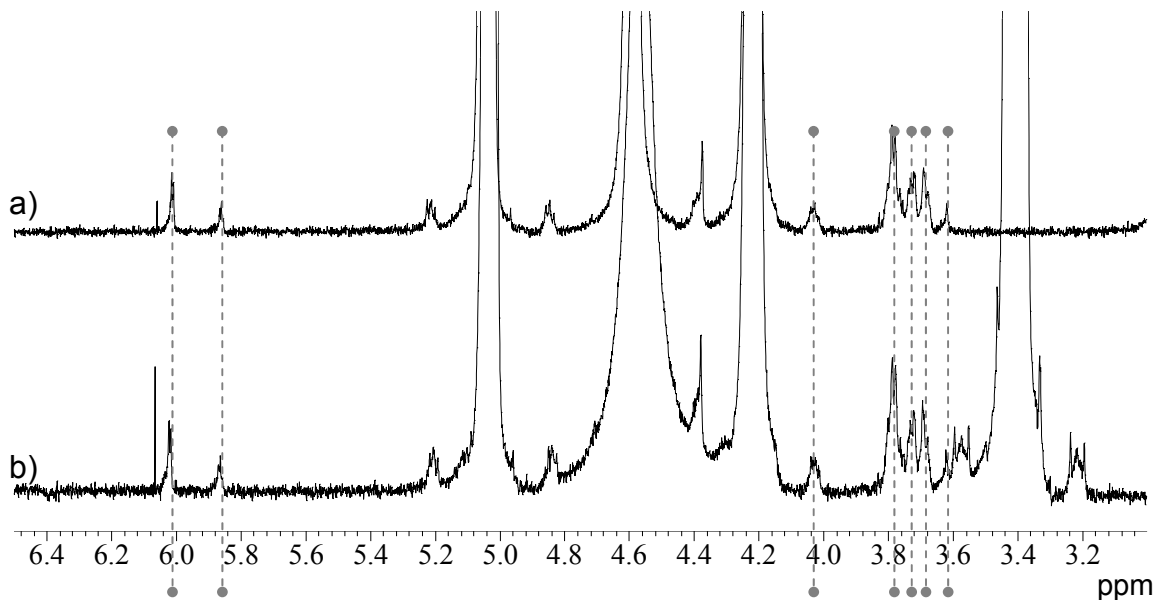
In a second control experiment designed to study the effect of added salt on complexation, we observed complexation of **1b**- 2PF_6 by **2b** in acetone- d_6 . As discussed elsewhere, [3,10] a bright orange solution resulted upon mixing the host and guest components, indicative of a charge transfer event from the electron rich host to the electron deficient viologen. We then titrated $(n\text{-Bu})_4\text{N-PF}_6$ into the solution and noted that the time averaged ^1H NMR resonances of the crown shift towards their uncomplexed positions, qualitatively signaling a decrease in association (see Figure V-4). In light of a recent report that suggests the complex **2b**•**1a**- 2PF_6 to be *fully* ion paired in acetone- d_6 , [5] this finding was unexpected: if the complex truly were 100% ion paired, one would not predict $K_{a,\text{exp}}$ to vary with ionic strength (Eq. 2). This is not the case, as clearly observed in Figure V-4. To explain this anomaly, we consider two possibilities.

Figure V-4. ^1H NMR spectra (400 MHz, 295 K, acetone- d_6) of a) **2b**; b) 2.00 mM **2b** + 2.00 mM **1b-2PF₆**; c) 2.00 mM **2b** + 2.00 mM **1b-2PF₆** + 4.63 mM (*n*-Bu)₄N-PF₆.



First, it may be the case that Δ_0 changes for the system upon addition of (*n*-Bu)₄N-PF₆. As a result, the observed chemical shift change of Figure V-4 would carry no qualitative meaning. We have tested this possibility by studying a solution 0.9 mM in **2b** and 1.0×10^2 mM in **1b-2PF₆** both before and after addition of 1.0×10^2 mM (*n*-Bu)₄N-PF₆. The 100-fold excess of guest relative to host ensured near quantitative complexation of **2b**, enabling one to approximate δ_{bound} , and thus Δ_0 , by simple observation of the host resonances. As can be seen in Figure V-5, the δ_{bound} signals do not change upon addition of (*n*-Bu)₄N-PF₆. We conclude that Δ_0 is therefore unaffected by addition of (*n*-Bu)₄N-PF₆.

Figure V-5. ^1H NMR spectra (400 MHz, 295 K, acetone- d_6) of a) 0.9 mM **2b** + 1.0×10^2 mM **1b**- 2PF_6 and b) 0.9 mM **2b** + 1.0×10^2 mM **1b**- 2PF_6 + 1.0×10^2 mM (*n*-Bu) $_4\text{N}$ - PF_6 .



Because the result of Figure V-4 is reminiscent of a similar experiment from Chapter II in which an increase in salt concentration precipitated a reduction in $K_{a,\text{exp}}$ for another pseudorotaxane system (Figure III-2), we considered the only remaining possibility to explain Figure V-4: pseudorotaxane **2b/1b**- 2PF_6 may not be fully ion paired as previously reported. If this were the case, as a result of a near order of magnitude difference in K_{ipd} between (*n*-Bu) $_4\text{N}^+\text{X}^-$ salts and **1a**- 2PF_6 [$K_{\text{ipd}}((n\text{-Bu})_4\text{N}^+\text{OTs}^-) \approx 2 \times 10^{-3}$ M [11] versus $K_{\text{ipd}}(\mathbf{1a}\text{-}2\text{PF}_6) \approx 4 \times 10^{-4}$ M 2], [5] the paraquat under the influence of a large excess of PF_6^- would become more ion paired thereby driving the complexation equilibrium towards starting materials, as observed in Figure V-4. We believe this to be the reality, and speculate that because of the small K_{ipd} of **1a**- 2PF_6 under the conditions observed in the earlier report ($10.0 \text{ mM} > [\mathbf{1a}\text{-}2\text{PF}_6] > 0.750 \text{ mM}$), minor changes in the extent of complex ion pairing would be difficult to observe. Thus, it would be challenging to distinguish between a complex that is mostly ion paired and a complex that is fully ion paired in the absence of added $[\text{X}^-]$ (Eq. 6n).

Under the assumption that the apparent reduction in binding was due to ion pairing, the spectra were analyzed to estimate $K_{a,\text{exp}}$. Because addition of $(n\text{-Bu})_4\text{N}^+\text{PF}_6^-$ was shown not to influence δ_{bound} , Δ_0 was taken from earlier studies [12] to be 0.472 ppm for H_b . Based on this value, we calculated $K_{a,\text{exp}} = (8.3 \pm 1.3) \times 10^2 \text{ M}^{-1}$ for **2b/1b-2PF₆** alone and $K_{a,\text{exp}} = (5.2 \pm 0.8) \times 10^2 \text{ M}^{-1}$ for **2b/1b-2PF₆** in the presence of $(n\text{-Bu})_4\text{N-PF}_6$, representing a significant 40% reduction in $K_{a,\text{exp}}$. [13]

V.3 Contributions to Improved Binding Efficiencies: Discovery of a Pseudocryptand

In an attempt to preorganize the host via hydrogen bonding to the diol functionalities, we then observed the influence of adding a ditopic H-bond accepting counteranion. When mixed with **2b**, $(\text{CH}_3\text{CH}_2)_4\text{N-TFA}$ demonstrated no strong interaction with the host as prescribed by ^1H (Figure V-6) and ^{19}F NMRS. Similarly, ^1H (Figure V-7) and ^{19}F NMR indicated that no interaction occurs between **1b-2PF₆** and $(\text{CH}_3\text{CH}_2)_4\text{N-TFA}$. However, in opposition to the studies described above for addition of $(n\text{-Bu})_4\text{N-PF}_6$ to a solution of **2b/1b-2PF₆**, the ^1H NMR resonances of the crown signals all shifted towards their fully complexed positions upon addition of 1.18 equivalents of $(\text{CH}_3\text{CH}_2)_4\text{N-TFA}$, signaling an increase in association (see Figure V-8c). Indeed, using Δ_0 from above, we determine a 6.8 fold improvement in $K_{a,\text{exp}}$ [$(8.3 \pm 1.3) \times 10^2 \text{ M}^{-1}$ to $(5.6 \pm 1.5) \times 10^3 \text{ M}^{-1}$]. Doubling [$(\text{CH}_3\text{CH}_2)_4\text{N-TFA}$] to 4.70 mM results in a further doubling of $K_{a,\text{exp}}$ to $(1.2 \pm 0.5) \times 10^4 \text{ M}^{-1}$ (Figure V-8d), an impressive 14-fold increase overall.

Figure V-6. ^1H NMR spectra (400 MHz, 295 K, acetone- d_6) of a) **2b**; b) 3.01 mM **2b** + 3.52 mM $(\text{CH}_3\text{CH}_2)_4\text{N-TFA}$; c) $(\text{CH}_3\text{CH}_2)_4\text{N-TFA}$.

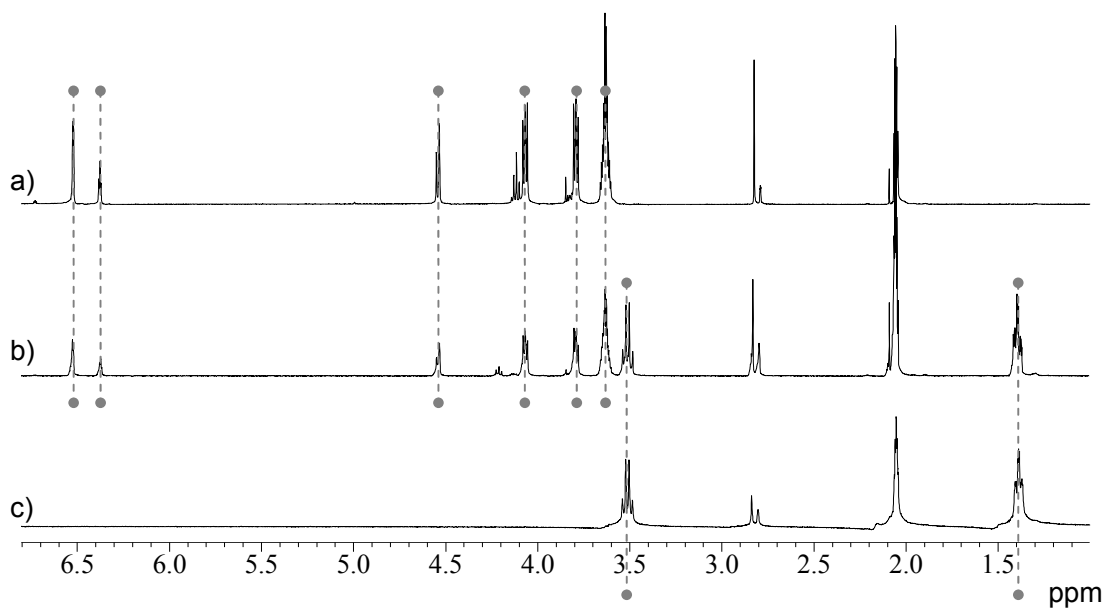


Figure V-7. ^1H NMR spectra (400 MHz, 295K, acetone- d_6) of a) 2.95 mM **1b**- 2PF_6 + 3.52 mM $(\text{CH}_3\text{CH}_2)_4\text{N-TFA}$ and b) $(\text{CH}_3\text{CH}_2)_4\text{N-TFA}$.

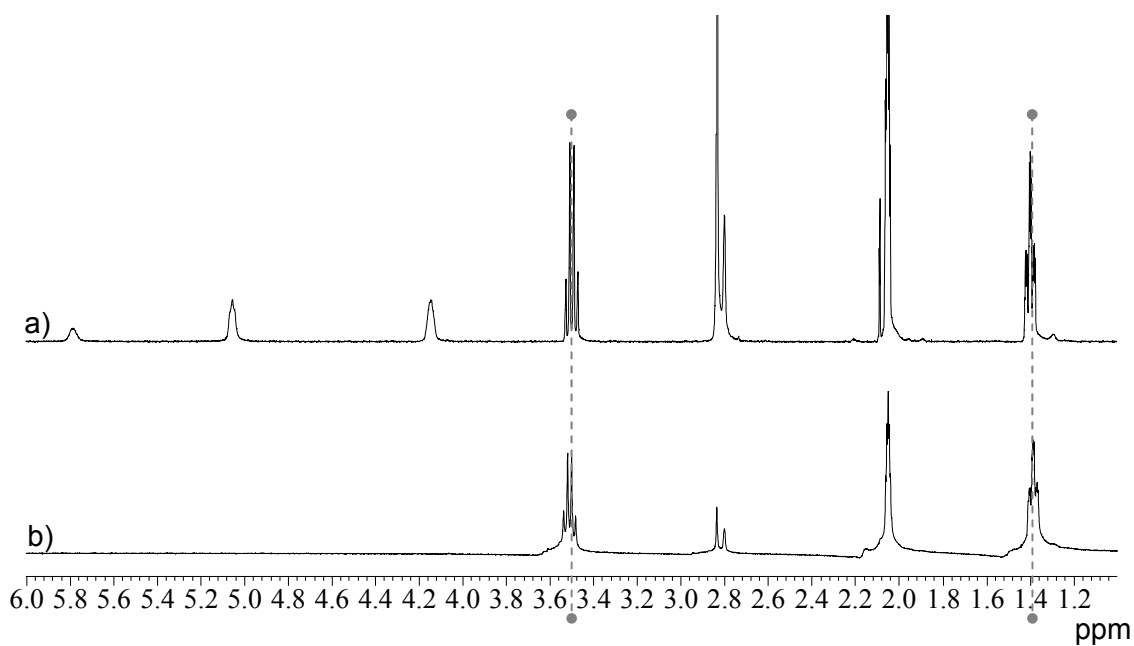
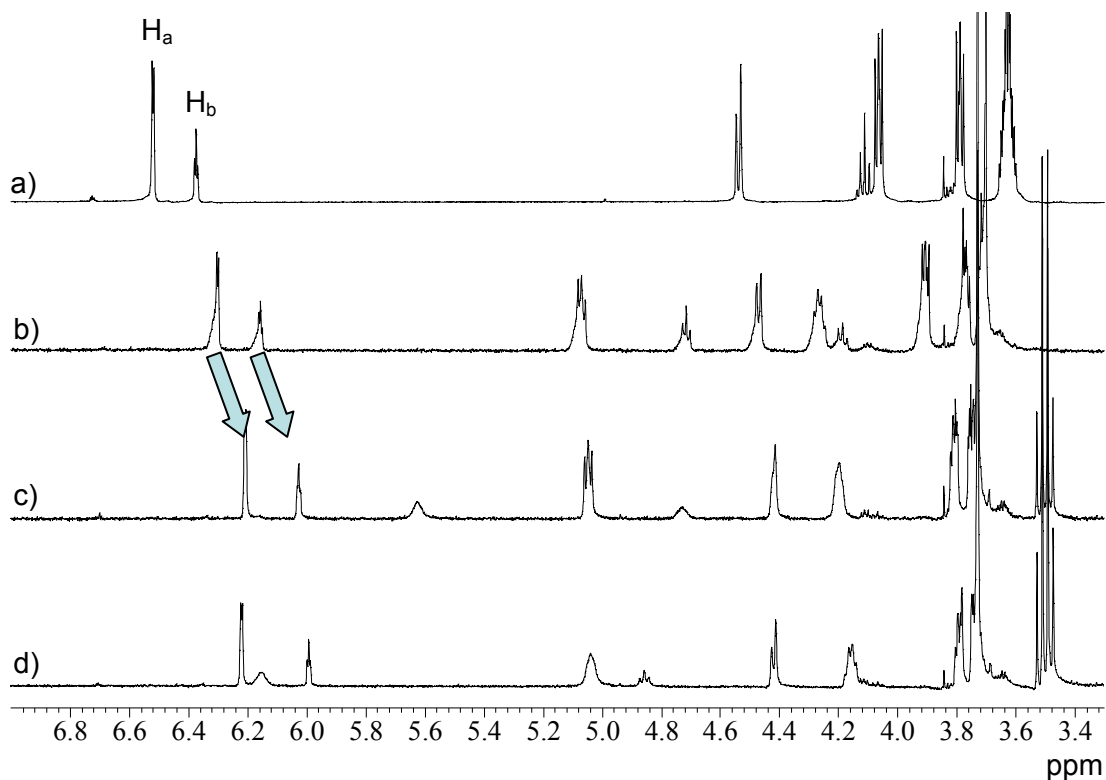
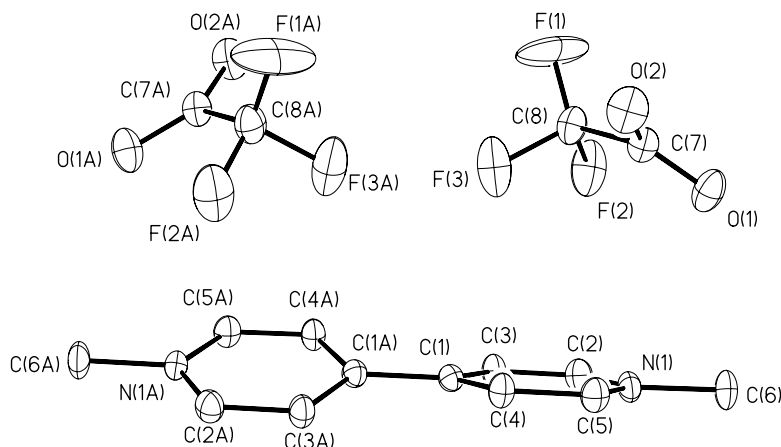


Figure V-8. ^1H NMR spectra (400 MHz, 295 K, acetone- d_6) of a) **2b**; b) 2.00 mM **2b** + 2.00 mM **1b-2PF₆**; c) 2.00 mM **2b** + 2.00 mM **1b-2PF₆** + 2.35 mM $(\text{CH}_3\text{CH}_2)_4\text{N-TFA}$; d) 2.00 mM **2b** + 2.00 mM **1b-2PF₆** + 4.70 mM $(\text{CH}_3\text{CH}_2)_4\text{N-TFA}$.



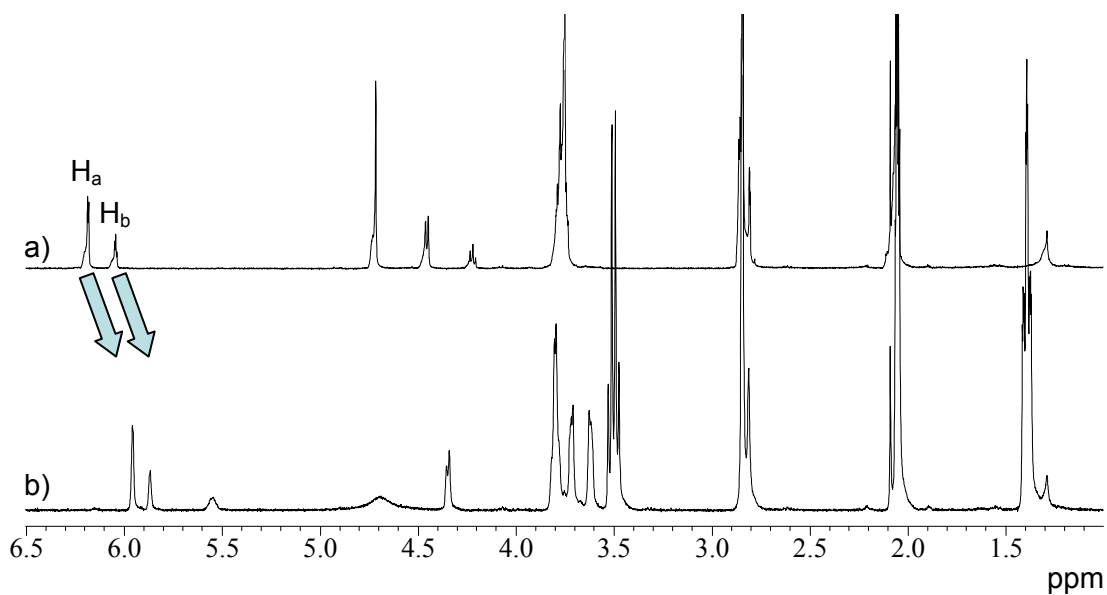
The observed upfield chemical shift upon addition of $(\text{CH}_3\text{CH}_2)_4\text{N-TFA}$ is especially noteworthy given tendency of TFA^- to form a much tighter ion pair than PF_6^- , which, as demonstrated by Figure V-4, would otherwise result in a downfield chemical shift of the complex. Indeed, in the absence of host **2**, counterion exchange under experimental conditions between **1a-** or **1b-2PF₆** and $(\text{CH}_3\text{CH}_2)_4\text{N-TFA}$ results in the precipitation of **1a-** or **1b-2TFA**, as characterized by X-ray analyses (see Figure V-9).

Figure V-9. ORTEP diagram of **1a**-2TFA with 50% probability ellipsoids. Hydrogens have been omitted for clarity.



To be certain that the hydroxyl functionality of guest **1b**-2PF₆ was not influencing association, a solution of **1a**-2PF₆ and **2b** was subjected to similar treatment. H_a and H_b shifted upfield in the presence of (CH₃CH₂)₄N-TFA (Figure V-10), indicating that the OH groups of guest **1b**-2PF₆ are not essential for the cooperative effect of (CH₃CH₂)₄N-TFA.

Figure V-10. ¹H NMR spectra (400 MHz, 295 K, acetone-*d*₆) of a) 3.00 mM **2b** + 3.00 mM **1a**-2PF₆ and b) 2.00 mM **2b** + 2.00 mM **1a**-2PF₆ + 6.60 mM (CH₃CH₂)₄N-TFA.



Further confirmation of the key role of host **2b**'s OH moieties was obtained by use of unsubstituted crown **2a**. Addition of $(\text{CH}_3\text{CH}_2)_4\text{N-TFA}$ to solutions of **1a-2PF₆/2a** (Figure V-11) and **1b-2PF₆/2a** (Figure V-12) resulted in reduced $K_{a,\text{exp}}$ values (i.e., the crown signals all shift towards their uncomplexed positions).

Figure V-11. ^1H NMR spectra (400 MHz, 295 K, acetone- d_6) of a) 3.00 mM **2a** + 3.00 mM **1a-2PF₆** and b) 2.00 mM **2a** + 2.00 mM **1a-2PF₆** + 2.50 mM $(\text{CH}_3\text{CH}_2)_4\text{N-TFA}$.

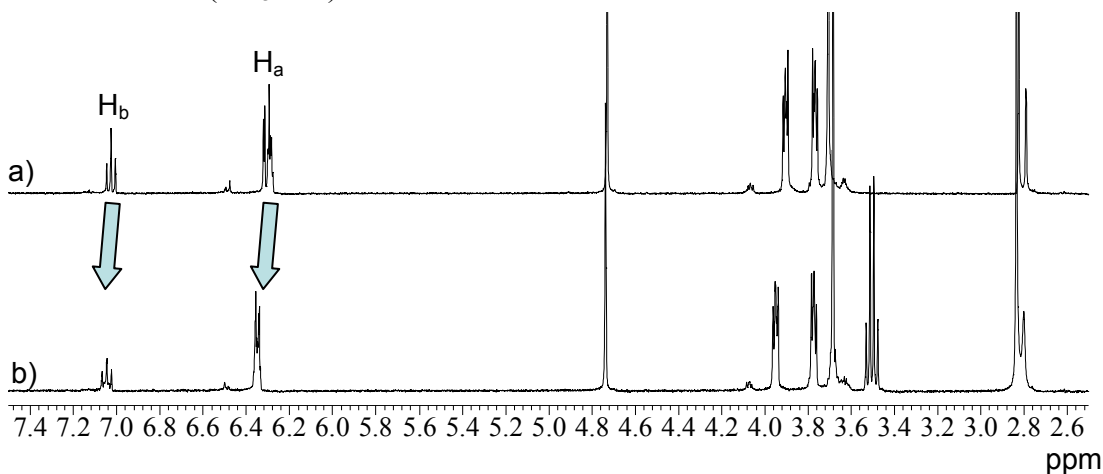
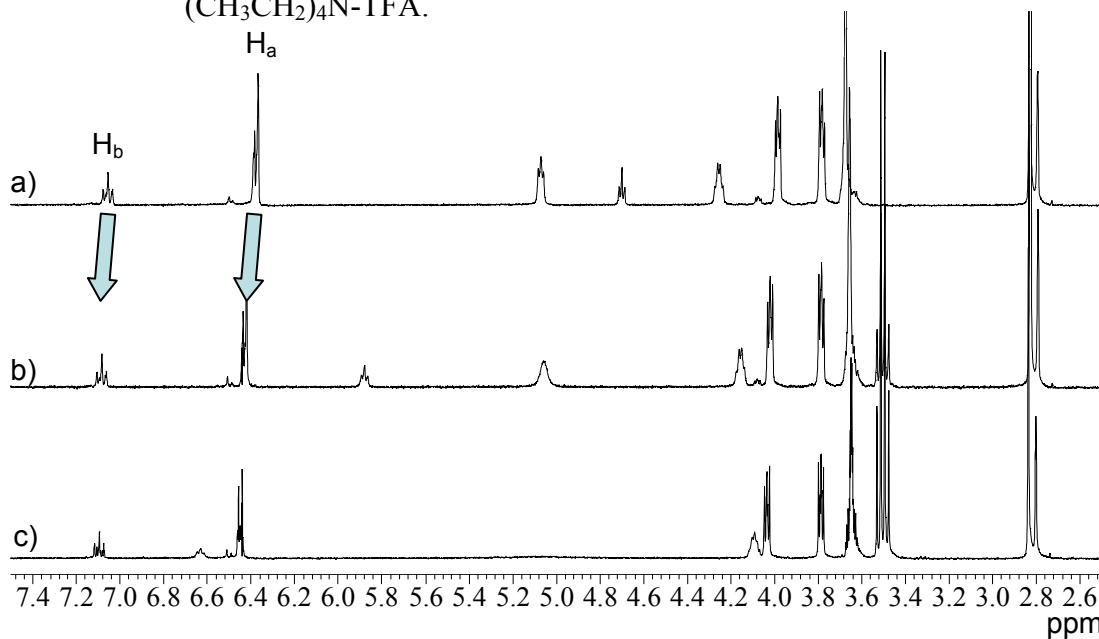


Figure V-12. ^1H NMR spectra (400 MHz, 295 K, acetone- d_6) of a) 3.00 mM **2a** + 3.00 mM **1b-2PF₆**; b) 2.00 mM **2a** + 2.00 mM **1b-2PF₆** + 2.50 mM $(\text{CH}_3\text{CH}_2)_4\text{N-TFA}$; c) 2.00 mM **2a** + 2.00 mM **1b-2PF₆** + 7.50 mM $(\text{CH}_3\text{CH}_2)_4\text{N-TFA}$.



In designing this study, we had reasoned that cooperativity would arise due to folding of **2b** by **1b-2PF₆** (or **1a-2PF₆**) into the exo- or taco-complex [14] assisted by H-bonding of the ditopic TFA ion with the crown diol functionalities, as outlined in Scheme V-1. This hypothesis was confirmed by X-ray diffraction analysis of crystals of **2b/1a-PF₆/TFA** (Figure V-13). [15] Such a counteranion interaction effectively forms a supramolecular cryptand, termed a pseudocryptand, [16] thereby stabilizing the three-component complex. In agreement with this observation, the interatomic distances between atoms C2 and C18 decrease in the order **2b/1a-2PF₆** (7.67 Å)³ > **2b/1a-PF₆/TFA** (7.65 Å) > **3/1a-2PF₆** (7.09 Å). [6]

Scheme V-1. Cartoon representation of a cooperative host/guest interaction via pseudocryptand formation.

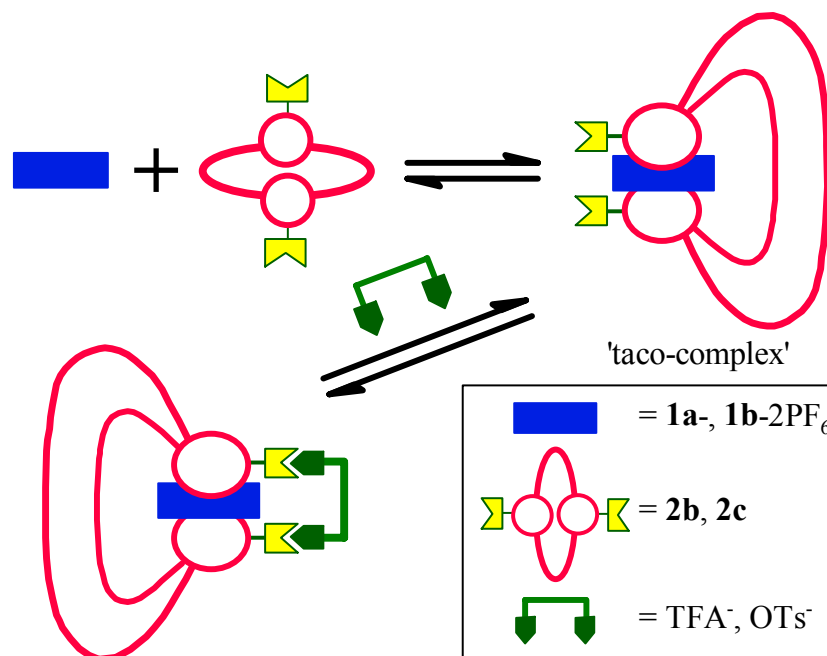
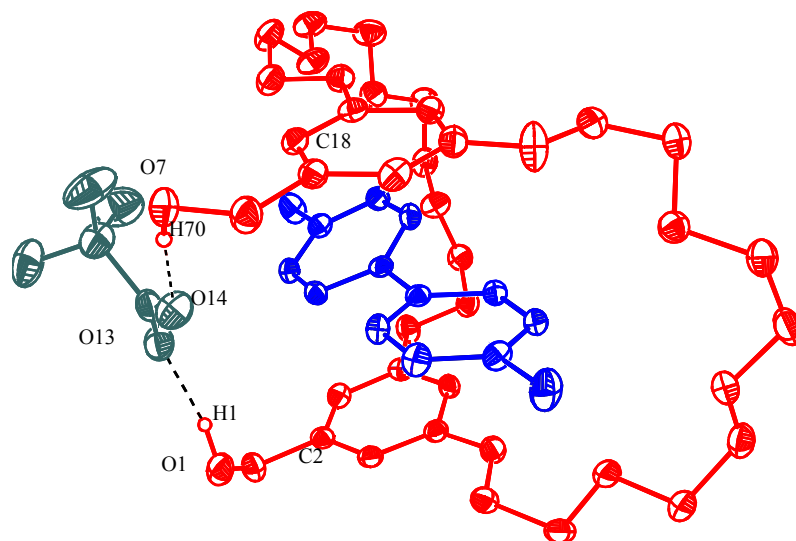


Figure V-13. ORTEP diagram of **2b/1a**-PF₆/TFA with 50% probability ellipsoids. Hydrogens and spectator PF₆ anions have been omitted for clarity. Selected interatomic distances and angles: O1⋯O13 2.73(2) Å, O1-H1 0.94(4) Å, O13⋯H1 1.80(4) Å, O1-H1⋯O13 170(4)°; O7⋯O14 2.82(3) Å, O7-H70 0.83(4) Å, O14⋯H70 1.99(4) Å, O7-H70⋯O14 170(4)°; C2⋯C18 7.65(4) Å.



V.4 Versatility of Pseudocryptands and Comparison to Covalent Cryptands

The influences of (*n*-Bu)₄N-OTs and (*n*-Bu)₄N-BF₄ on the complexation of **2b** with **1b**-2PF₆ were consistent with those described above: tridentate OTs⁻ increased $K_{a,\text{exp}} \sim 1.5$ fold ($K_{a,\text{exp}} = 920 \pm 140 \text{ M}^{-1}$, [**2b**] = 1.99 mM, [**1b**-2PF₆] = 2.00 mM, [(*n*-Bu)₄N-OTs] = 2.01 mM, Figure V-14), while the non-chelating BF₄⁻ reduced association (Figure V-15). Addition of (*n*-Bu)₄N-CF₃SO₃ also diminished $K_{a,\text{exp}}$ values, a result of the reduced basicity of triflate relative to TFA (Figure V-16). At the other extreme, addition of the more basic acetate anion via (*n*-Bu)₄N-CH₃CO₂ to **2b/1b**-2PF₆ resulted in electron transfer reactions, [17] which destroyed the guest ligand.

Figure V-14. ^1H NMR spectra (400 MHz, 295 K, acetone- d_6) of a) 2.00 mM **2b** + 2.00 mM **1b-2PF₆** and b) 2.00 mM **2b** + 2.00 mM **1b-2PF₆** + 2.50 mM (*n*-Bu) $_4$ N-OTs.

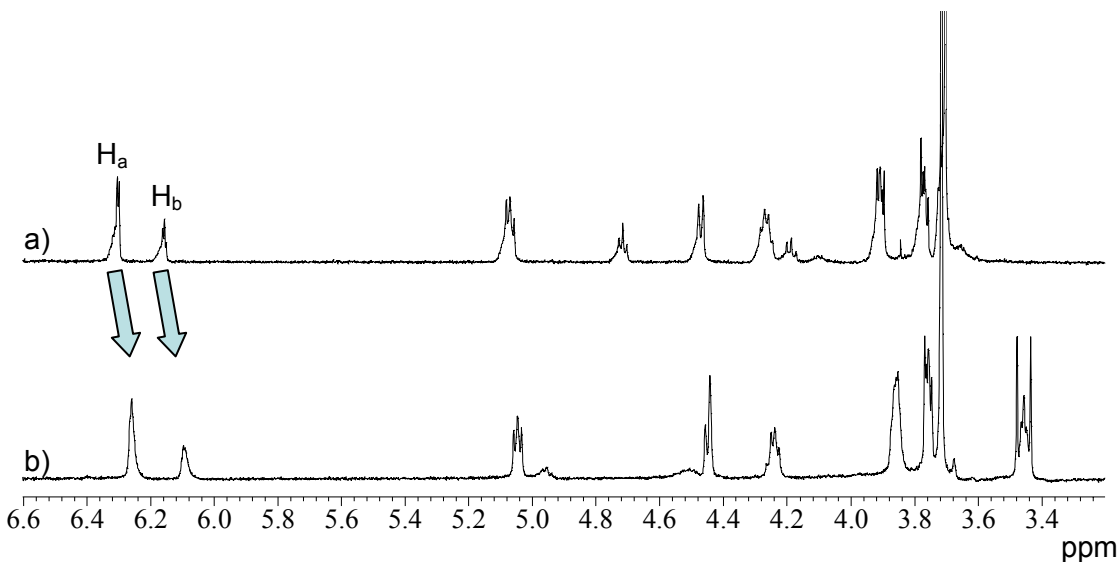


Figure V-15. ^1H NMR spectra (400 MHz, 295 K, acetone- d_6) of a) 2.00 mM **2b** + 2.00 mM **1b-2PF₆** and b) 2.00 mM **2b** + 2.00 mM **1b-2PF₆** + 4.10 mM (*n*-Bu) $_4$ N-BF $_4$.

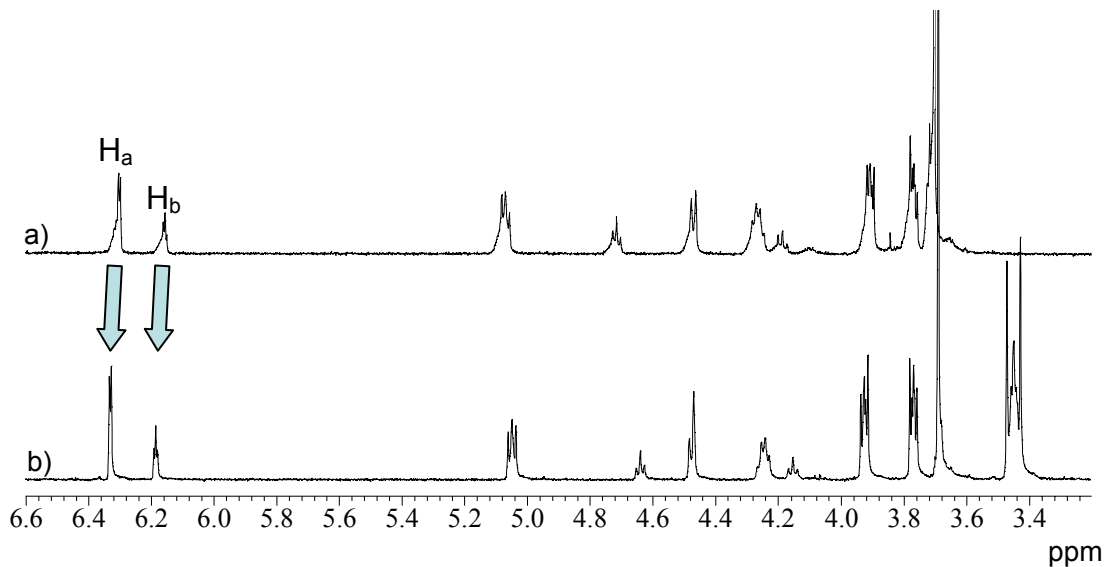
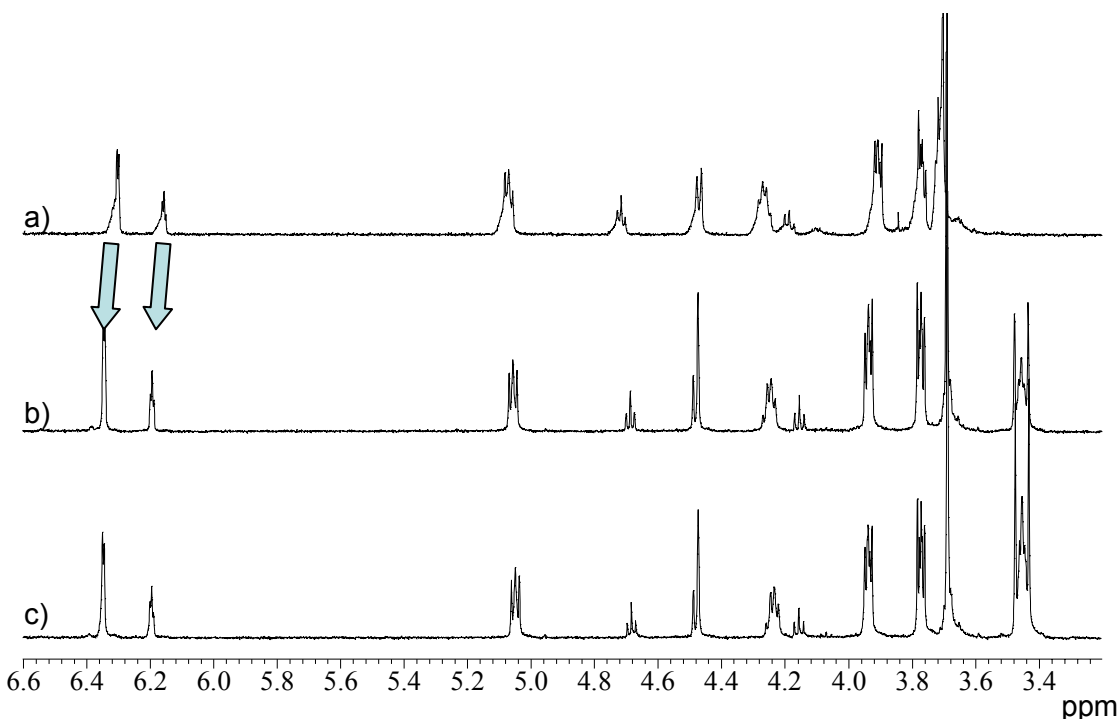
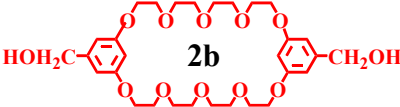
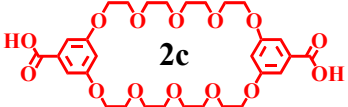
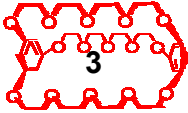


Figure V-16. ^1H NMR spectra (400 MHz, 295 K, acetone- d_6) of a) 2.00 mM **2b** + 2.00 mM **1b**-2PF $_6$; b) 2.00 mM **2b** + 2.00 mM **1b**-2PF $_6$ + 2.00 mM (*n*-Bu) $_4$ N-CF $_3$ SO $_3$; c) 2.00 mM **2b** + 2.00 mM **1b**-2PF $_6$ + 4.00 mM (*n*-Bu) $_4$ N-CF $_3$ SO $_3$.



Noting that the host **2c** should more readily H-bond to di- and tritopic anions than host **2b** due to its carboxylic acid functionality, we explored complexation of **1a**-2PF $_6$ in the presence of (CH_3CH_2) $_4$ N-TFA and found a 40 fold increase in $K_{a,\text{exp}}$ ($K_{a,\text{exp}} = (3.4 \pm 1.3) \times 10^4 \text{ M}^{-1}$, $[\mathbf{2c}] = 2.00 \text{ mM}$, $[\mathbf{1a}\text{-}2\text{PF}_6] = 2.00 \text{ mM}$, $[(\text{CH}_3\text{CH}_2)_4\text{N-TFA}] = 2.00 \text{ mM}$). [18] This finding is a significant, especially when considering that pseudocryptand **2c/1a**-PF $_6$ /TFA results in a $K_{a,\text{exp}}$ value equivalent to that determined for the covalent analog **3** (Table V-1).

Table V-1. Comparison of various pseudocryptand and cryptand systems in acetone- d_6 at 295K. Values determined from the chemical shift of H_b for each host. [18]

Host (2.00 mM)	Guest (2.00 mM)	Chelating Agent (2.00 mM)	$K_{a,exp}$ (M^{-1})	Increase in $K_{a,exp}$ (rel. to 2b)
 2b	1b -2PF ₆	none	$(8.3 \pm 1.3) \times 10^2$	---
		(<i>n</i> -Bu) ₄ N-OTs	$(1.9 \pm 0.4) \times 10^3$	2.2
		(CH ₃ CH ₂)N-TFA	$(5.6 \pm 1.5) \times 10^3$	6.8
 2c	1a -2PF ₆	(CH ₃ CH ₂)N-TFA	$(3.4 \pm 1.3) \times 10^4$	~40
 3	1a -2PF ₆	none	$(3.2 \pm 1.0) \times 10^4$	~40

$K_{a,exp}$ values being equal, the major advantage of the pseudocryptand system is in its ease of preparation: simple addition of a multitopic H-bond acceptor to a solution of host **2c** and paraquat guest results in spontaneous organization to the three component complex. Covalent cryptand **3**, on the other hand, requires multiple tedious synthetic steps and purification before it may be used in complexation studies.

V.5 *Experimental*

1a-2PF₆, [19] **1b**-2PF₆, [20] **2a**, [21] **2b**, [22] **2c**, [22] and **3** [6] were prepared as described in the literature. All other reagents were purchased from commercial suppliers and used without further purification. ¹H NMR spectra were recorded on a 400 MHz NMR spectrometer with the solvent proton signal as the reference.

For all complexation studies, precisely weighed amounts of each component were added into a 5.00 mL volumetric flask (± 0.02 mL) equipped with a ground glass stopper to make a moderately concentrated (nominally 16 mM) master solution. This solution was then sequentially diluted (no more than four sequential dilutions were performed per master solution) as needed by transferring exactly half of the higher concentration solution to a clean volumetric flask by means of to-deliver volumetric pipettes (± 0.006 mL) and diluting to the 5.00 mL mark. The fresh solutions were passed through a filter before 0.500 mL of each solution component (both host and guest) at a specified concentration was transferred via a to-deliver pipette to a 5 mm NMR tube. ¹H NMR data were collected on a temperature controlled spectrometer (400 MHz). Errors are reported by assuming a 5% variation in Δ/Δ_0 values.

Preparation of *N,N'*-dimethyl-4,4'-bipyridinium Bis(trifluoroacetate) (1a**-2TFA) and Crystallography Parameters**

X-ray quality crystals of **1a**-2TFA were crystallized out of solution through ion exchange with **1a**-2PF₆ in acetone. No further purification was necessary. X-ray data were collected with a Siemens P4/CCD diffractometer with graphite-monochromated Mo K α X-radiation ($\lambda=0.71073$ Å). The structure of **1a**-2TFA was solved by direct methods and was completed by subsequent difference Fourier syntheses and refined by full-matrix least-squares procedures. All non-hydrogen atoms were refined with anisotropic displacement coefficients. The software and sources of the scattering factors are contained in the SHELXTL NT program package. [23]

V.6 *References*

- [1] a) Cacialli, F.; Samorì, P.; Silva, C. *Mater. Today* **2004**, 24-32. b) Bosman, A. W.; Sijbesma, R. P.; Meijer, E. W. *Mater. Today* **2004**, 34-39.
- [2] Sijbesma, R. P.; Beijer, F. H.; Brunsveld, L.; Folmer, B. J. B.; Hirschberg, J. H. K. K.; Lange, R. F. M.; Lowe, J. K. L.; Meijer, E. W. *Science* **1997**, *278*, 1601-1604.
- [3] Allwood, B. L.; Shahriari-Zavareh, H.; Stoddart, J. F.; Williams, D. J. *J. Chem. Soc., Chem. Commun.* **1987**, 1058-1061.
- [4] Benesi, H.; Hildebrand, J. H. *J. Am. Chem. Soc.* **1949**, *71*, 2703-2707.
- [5] Huang, F.; Jones, J. W.; Slebodnick, C.; Gibson, H. W. *J. Am. Chem. Soc.* **2003**, *125*, 14458-14464.
- [6] Bryant, W. S.; Jones, J. W.; Mason, P. E.; Guzei, I. A.; Rheingold, A. L.; Nagvekar, D. S.; Gibson, H. W. *Org. Lett.* **1999**, *1*, 1001-1004]
- [7] The concept of preorganization traces its roots to the “lock and key” idea of Fisher [Fischer, E. *Chem. Ber.* **1894**, *27*, 2985-2993] and has been highlighted in recent Nobel Prize winning work by Cram [Cram, D. J.; Cram, J. M. *Container Molecules and Their Guests*; Royal Society of Chemistry: Cambridge, UK, 1994] and Lehn [Lehn, J.-M. *Supramolecular Chemistry*; VCH Publishers: New York, 1995].
- [8] Jones, J. W.; Bryant, W. S.; Bosman, A. W.; Janssen, R. A. J.; Meijer, E. W.; Gibson, H. W. *J. Org. Chem.* **2003**, *68*, 2385-2389.
- [9] a) Jones, J. W.; Zakharov, L. N.; Rheingold, A. L.; Gibson, H. W. *J. Am. Chem. Soc.* **2002**, *124*, 13378-13379.
- [10] a) Allwood, B. L.; Shahriari-Zavareh, H.; Stoddart, J. F.; Williams, D. J. *J. Chem. Soc., Chem. Commun.* **1987**, 1064-1066. b) Gillard, R. E.; Raymo, F. M.; Stoddart, J. F. *Chem. Eur. J.* **1997**, *3*, 1933-1940.
- [11] Savedoff, L. G. *J. Am. Chem. Soc.* **1966**, *88*, 664-667.
- [12] Gong, C.; Balanda, P. B.; Gibson, H. W. *Macromolecules* **1998**, *31*, 5278-5289. Δ_0 is defined as the average value calculated by Benesi-Hildebrand, Scatchard, and Creswell-Allred treatments.

- [13] Errors are reported by assuming a 5% variation in Δ / Δ_0 values.
- [14] Because Figure V-6 does not reveal interaction between $(\text{CH}_3\text{CH}_2)_4\text{N-TFA}$ and **2b**, it is likely that templation of **2b** by **1a-** or **2b-2PF₆** is necessary for anion chelation.
- [15] Ion-paired binding by neutral hosts to form pseudorotaxane complexes has also been shown by a) Deetz, M. J.; Shukla, R.; Smith, B. D. *Tetrahedron* **2002**, *58*, 799-805, and references therein; as well as b) Wisner, J. A.; Beer, P. D.; Drew, M. G. B. *Angew. Chem. Int. Ed. Engl.* **2001**, *40*, 3606-3609.
- [16] for a review of other known pseudocryptands see Nabeshima, T.; Akine, S.; Saiki, T. *Rev. Heteroatom Chem.* **2000**, *22*, 219-239. see also a) Huang, F.; Zakharov, L. N.; Rheingold, A. L.; Jones, J. W.; Gibson, H. W. *Chem. Comm.* **2003**, *17*, 2122-2123. b) Nabeshima, T.; Yoshihira, Y.; Saiki, T.; Akine, S.; Horn, E. *J. Am. Chem. Soc.* **2003**, *125*, 28-29. c) Katoh, A.; Kudo, H.; Saito, R. *Supra. Chem.* **2003**, *2*, 79-84. d) Heck, R.; Dumarcay, F.; Marsura, A. *Chem. Eur. J.* **2002**, *8*, 2438-2445.
- [17] Naik, D. B.; Moorthy, P. N. *J. Chem. Soc., Perkin Trans. 2* **1990**, *5*, 705-709.
- [18] All binding studies involving host **2c** were performed by Huang, F. at Virginia Tech under the guidance of Gibson, H. W.
- [19] Ashton, P. R.; Campbell, P. J.; Chrystal, E. J. T.; Glink, P. T.; Menzer, S.; Philp, D.; Spencer, N.; Stoddart, J. F.; Tasker, P. T.; Williams, D. J. *Angew. Chem., Int. Ed. Engl.* **1995**, *34*, 1865-1869.
- [20] Shen, Y. X.; Engen, P. T.; Berg, M. A. G.; Merola, J. S.; Gibson, H. W. *Macromolecules* **1992**, *25*, 2786-2788.
- [21] Delaviz, Y.; Gibson, H. W. *Polym. Commun.* **1991**, *32*, 103-105.
- [22] Gibson, H. W.; Nagvekar, D. S. *Can. J. Chem.* **1997**, *75*, 1375-1384.
- [23] Sheldrick, G. M. SHELXTL NT ver. 6.12; Bruker Analytical X-ray Systems, Inc.: Madison, WI, 2001.

Chapter VI

Conclusions and Areas of Future Work

The field of supramolecular chemistry has received considerable attention over the past few years due in large part to the identification of self-assembling nanoscale devices as viable components for future machines. On a larger scale, there is also substantial excitement over self-assembled polymers, which display vastly different properties and behaviors than their covalent counterparts. Still in its infancy, both areas are in search of recognition motifs to enable new nanotechnologies. A number of reports have singled out supramolecular complexes which incorporate charged components as potential candidates. However, current binding models were shown to inadequately describe the complexation event, leading to incomplete and often misleading results.

In this dissertation, we reported a broad equilibrium model for complexation of ionic species in low dielectric constant media that explicitly includes ion pairing for one of the components, thereby significantly advancing current host/guest descriptions. Experimental validation of our model was achieved through studies of pseudorotaxane formation between dibenzylammonium salts (DBAm-X) and dibenzo-24-crown-8 (DB24C8) in $\text{CDCl}_3:\text{CD}_3\text{CN}$ (3:2). In that particular case, we showed that fluctuations in the apparent $K_{a,\text{exp}}$ values as usually reported are attributable to ion pairing, with a dissociation constant K_{ipd} , and that the constant K_{assoc} for pseudorotaxane complexation is independent of the counterion, a result of the complex existing in solution as a free cation. Because of the concentration dependence, we also derived multiple independent theoretical treatments of the model in order to treat a wide range of experimental conditions. Future work in this area should incorporate anion specific hosts as well as non-pseudorotaxane complexation events into the model to test its generality. In addition, a technique to calculate K_{ipd} independently of complexation should also be explored; the equilibrium model would be greatly simplified if $[\text{X}^-]$ was known or capable of being determined. Future work should also include an investigation of the current Scatchard and Hill treatments, which describe binding in polytopic systems, in regard to ion pairing.

Recognizing the role of the solvent's dielectric constant on ion pairing, we probed pseudorotaxane DBAm-X/DB24C8 in a higher dielectric constant solvent than that used to verify our model, acetone- d_6 , and observed the evolution of an unanticipated, although not unexpected, byproduct. Model studies suggested the byproduct formed from the condensation of acetone with the dibenzylammonium salts to be an iminium ion, an unstable compound that was confirmed by reduction to the corresponding amine, *N,N*-dibenzylisopropylamine. Such a product was not limited to dibenzylammonium salts alone: a brief survey showed all 2° ammonium salts investigated were susceptible to condensation reactions. These observations are of particular relevance to the supramolecular literature involving 2° ammonium salts as guest ligands, as host/guest formation constants are routinely reported in acetone. They also remind us that solvents by definition are not inert species, and that careful consideration of the molecules to be studied in solution should be made before the solvent is chosen.

Finally, because a major goal of this work was to ultimately increase binding efficiency and selectivity, we explored new methods to drive complexation. We found that addition of an anion specific host to a solution of pseudorotaxane DBAm-X/DB24C8 increased the percentage of ligands bound to the host, an expected phenomenon in light of earlier model studies. In a related pseudorotaxane structure, we noted that addition of di- or tri-topic hydrogen bond accepting anions to solutions of bis(5-hydroxymethyl-1,3-phenylene)-32-crown-10 or bis(5-carboxy-1,3-phenylene)-32-crown-10 and paraquat di(hexafluorophosphate) served to significantly enhance host:guest interaction. Specifically, the addition of $\text{Et}_4\text{N}^+\text{TFA}^-$ to an acetone solution of diacid crown and paraquat 2PF_6 effectively boosted $K_{a,\text{exp}}$ 40-fold, as estimated by ^1H NMR studies. Similar increases in the apparent $K_{a,\text{exp}}$ values were observed upon the addition of *n*- $\text{Bu}_4\text{N}^+\text{OTs}^-$. Evidenced by crystal structures, the increase in association resulted from chelation of the OH moieties of the crown by the di- or tri-topic anions, forming supramolecular bicyclic macrocycles (pseudocryptands) and stabilizing the complex in a cooperative manner. The heightened extents of complexation in the pseudocryptand and cryptand versus the macrocyclic hosts will enable their use in the construction of supramolecular polymers. Future work should investigate functionalization of cryptands, followed by their incorporation into self-assembled polymers.

Appendix A
Preliminary Investigations into the Determination of K_{ipd}
For 2-X salts Based on NMR Spectroscopy

A.1 Justification for Independent Calculations

As discussed in Chapter III, Eq. A1 was used to solve for K_{ipd} and K_{assoc} at infinite dilution for pseudorotaxane **1/2-X** formation under the assumption that all of the free guest exists as the fully ion paired salt; thus $[G^+]_{observed} \approx [G^+X^-]$.

$$\frac{[H \cdot G^+]}{[G^+X^-]^{1/2}} = \frac{K_{ipd}^{1/2} K_{assoc} [H]}{\gamma_{\pm} (1 + K_{assoc} [H])^{1/2}} \quad \text{Eq. A1}$$

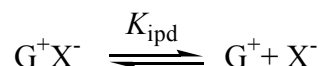
While such an assumption was shown to be approximately valid (Figure 19, Chapter 3), we acknowledged the advantage to be gained in calculating K_{ipd} independently, thereby allowing direct use of Eq. A2 at infinite dilution.

$$K_{a,exp} = \frac{K_{total}}{\gamma_{\pm}^2 [X^-]} = \frac{K_{ipd} K_{assoc}}{\gamma_{\pm}^2 [X^-]} \quad \text{Eq. A2}$$

Towards this end, a straight-forward mathematical model designed to calculate K_{ipd} based on chemical shifts will be presented below.

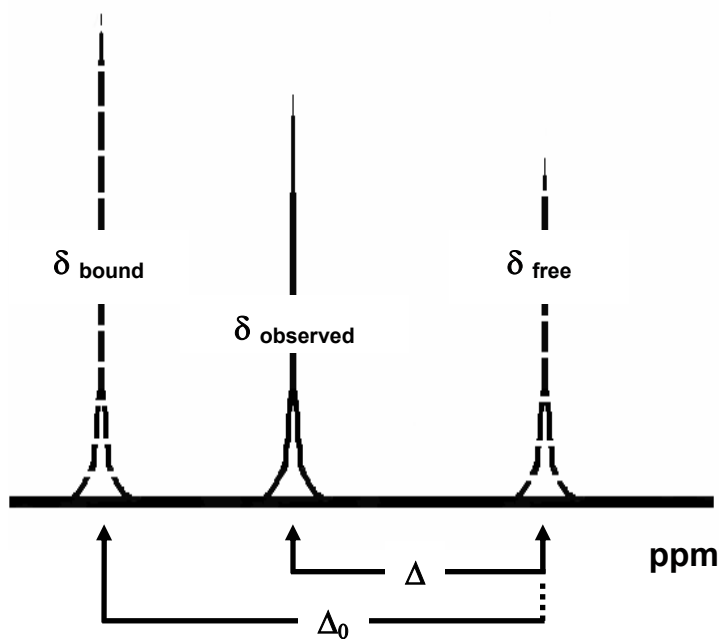
A.2 Benesi-Hildebrand Analysis and Ion Pairing

Shown in Figure II-11, H_1 of free **2-X** was found to shift with concentration. We attributed the change in chemical shift to a fast exchanging ion pairing equilibrium on the NMR time scale:



Because fast exchange events result in a time averaged signal between product and reactants (see Figure A1), it is not possible to determine K values based on the single point method. A number of mathematical treatments have thus been designed to describe binding in fast exchanged systems, including the Benesi-Hildebrand, [1] Scatchard, [2] Creswell-Allred, [3] and Rose-Drago [4] multi-point methods. Similar treatments have been described for fast exchanging ion pair equilibria. [5] We here adapt these methods to the description of ion pairing in dibenzylammonium salts (**2-X**).

Figure A1. Typical spectrum of a fast exchanged complexation event between bound and free states. The dashed resonances (δ_{bound} & δ_{free}) signify the extreme chemical shift possibilities for the resolved signal (δ_{observed}), and are not themselves typically observed in the host/guest mixture.



A.3 *Basis for Analysis of Rapidly Exchanging Events*

Consider a simple complexation equilibrium:



$$K_a = \frac{[\text{H}\cdot\text{G}]}{[\text{H}][\text{G}]}$$

For any given rapidly exchanging complexation event in which the resonance of a neutral host (or neutral guest) is followed, the three parameters of interest are δ_{bound} , δ_{free} , and δ_{observed} . δ_{free} is readily determined from a solution of the host in the absence of guest; δ_{observed} is known from experiment. Not known is the chemical shift of the fully bound state, δ_{bound} .

Because δ_{bound} is a time averaged signal, its chemical shift is proportional to the mole fraction of complexed (x_{bound}) and uncomplexed (x_{free}) species, as described by Eq. A3a

$$\delta_{\text{observed}} = x_{\text{bound}} \delta_{\text{bound}} + x_{\text{free}} \delta_{\text{free}} \quad \text{Eq. A3a}$$

x_{bound} is defined as

$$x_{\text{bound}} = \frac{[\text{Complex}]}{[\text{Free Host}] + [\text{Complex}]} \quad \text{Eq. A3b}$$

and x_{free} as

$$x_{\text{free}} = \frac{[\text{Free Host}]}{[\text{Free Host}] + [\text{Complex}]} \quad \text{Eq. A3c}$$

Accordingly, the sum of x_{bound} and x_{free} must be unity.

$$x_{\text{complex}} + x_{\text{free}} = 1 \quad \text{Eq. A3d}$$

Solving Eq. A3d for x_{free} and substituting this result along with Eq. A3b into Eq. A3a yields

$$\delta_{\text{observed}} = \delta_{\text{free}} + \frac{[\text{Complex}]}{[\text{Complex}] + [\text{Free Host}]} (\delta_{\text{complex}} - \delta_{\text{free}}) \quad \text{Eq. A3e}$$

Because the host may only exist in bound or unbound states:

$$[\text{Host}]_0 = [\text{Complex}] + [\text{Free Host}] \quad \text{Eq. A3f}$$

and Eq. A3e becomes

$$\delta_{\text{observed}} = \delta_{\text{free}} + \frac{[\text{Complex}]}{[\text{Host}]_0} (\delta_{\text{complex}} - \delta_{\text{free}}) \quad \text{Eq. A3g}$$

Solving Eq. A3g for $[\text{Complex}]$

$$[\text{Complex}] = \frac{[\text{Host}]_0 (\delta_{\text{observed}} - \delta_{\text{free}})}{(\delta_{\text{complex}} - \delta_{\text{free}})} \quad \text{Eq. A3h}$$

Returning to Figure A1, we define Δ and Δ_0 as

$$\Delta = \delta_{\text{observed}} - \delta_{\text{free}} \quad \text{Eq. A3i}$$

$$\Delta_0 = \delta_{\text{complex}} - \delta_{\text{free}} \quad \text{Eq. A3j}$$

thus, from Eq. A3h,

$$[\text{Complex}] = [\text{Host}]_0 \left(\frac{\Delta}{\Delta_0} \right) \quad \text{Eq. A3k}$$

This result is an extremely useful as the percent complexation may be directly calculated for any given fast exchange event once δ_{bound} has been determined by simply taking the ratio Δ/Δ_0 (often referred to as the saturation factor, θ).

Solving K_a for [Free Host] and substituting the result into Eq. A3f gives

$$[\text{Host}]_0 = [\text{Complex}] + \frac{[\text{Complex}]}{K_a [\text{Free Guest}]} \quad \text{Eq. A3l}$$

Rearranging,

$$\frac{[\text{Host}]_0}{[\text{Complex}]} = \left(1 + \frac{1}{K_a [\text{Free Guest}]} \right) \quad \text{Eq. A3m}$$

Which is equivalent to the result of Benesi and Hildebrand, [1] via Eq. A3k:

$$\frac{\Delta_0}{\Delta} = \frac{1}{K_a} \left(\frac{1}{[\text{Free Guest}]} \right) + 1 \quad \text{Eq. A3n}$$

Eq. A3n states that an experimental plot of Δ_0/Δ vs. $[\text{Free Guest}]^{-1}$ will yield a linear fit with a slope of K_a^{-1} and a y-intercept of unity. In order to reach this result, the concentration of free guest has traditionally been approximated by $[\text{Guest}]_0$ in systems exhibiting low association constants. [6] In this manner, inverse values of Δ are plotted versus inverse values of $[\text{Guest}]_0$ to yield a linear plot whose slope and intercept yield estimated Δ_0 and K_a^{-1} values, respectively. Previously mentioned in Chapter II, Gibson et al. have improved this approximation by using an iterative technique in which they first allow $[\text{Guest}]_0$ to approximate $[\text{Guest}]$ in order to solve Eq. A3n and then go on to use the calculated Δ_0 to refine the initial estimate of $[\text{Guest}]$. [7] This process is repeated until continued iterations result in constant Δ_0 and K_a values.

A.4 Basis for Ion Pair Dissociation Constants

To analyze the chemical shift data of fast exchange ion pairs, we define Δ and Δ_0 as follows:

$$\Delta = \delta_{\text{OBS}} - \delta_{\text{paired}}$$

$$\Delta_0 = \delta_{\text{dissociated}} - \delta_{\text{paired}}$$

and

$$\frac{\Delta}{\Delta_0} = \text{fraction } G^+X^- \text{ ionized} = \frac{[G^+]}{[G^+X^-] + [G^+]} \quad \text{Eq. A4a}$$

From K_{ipd} and because $[G^+] = [X^-]$ in the absence of other charged species,

$$[G^+] = \left(\frac{K_{\text{ipd}}[G^+X^-]}{\gamma_{\pm}^2} \right)^{1/2} \quad \text{Eq. A4b}$$

Substituting $[G^+]$ from Eq. A4b into Eq. A4a with rearrangement yields

$$\frac{\Delta}{\Delta_0} = \frac{(K_{\text{ipd}}/\gamma_{\pm}^2)^{1/2}}{[G^+X^-]^{1/2} + (K_{\text{ipd}}/\gamma_{\pm}^2)^{1/2}} \quad \text{Eq. A4c}$$

The reciprocal of the direct plot (Eq. A4c) yields Eq. A4d, which is designed to transform the direct plot into a straight line:

$$\frac{\Delta_0}{\Delta} = \frac{1}{K_{\text{ipd}}^{1/2}} \gamma_{\pm} [G^+X^-]^{1/2} + 1 \quad \text{Eq. A4d}$$

which is analogous to Eq. A3n. A plot of Δ_0/Δ versus $\gamma_{\pm}[G^+X^-]^{1/2}$ will yield a straight line with slope $K_{\text{ipd}}^{-1/2}$ and a y-intercept of 1. In the specific instance in which γ_{\pm} is not known at each concentration, a plot of Δ_0/Δ versus $[G^+X^-]^{1/2}$ will yield a straight line with a limiting slope of $K_{\text{ipd}}^{-1/2}$ and a y-intercept of 1 because γ_{\pm} approaches unity as $[G^+X^-]$ goes to zero.

A.5 *Application to 2-TFA*

We treated the fast exchange equilibrium of 2-TFA by the method of A1.4 under a broad range of concentrations (Table A1, Figure A2). The benzylic resonance displayed a continuous downfield shift with decreasing concentration until roughly 0.5 mM, at which point the signal shifted back upfield (Table A1, bold data points); this reversal in shift was confirmed by three independent experiments.

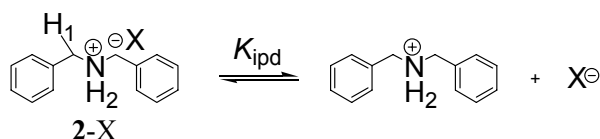
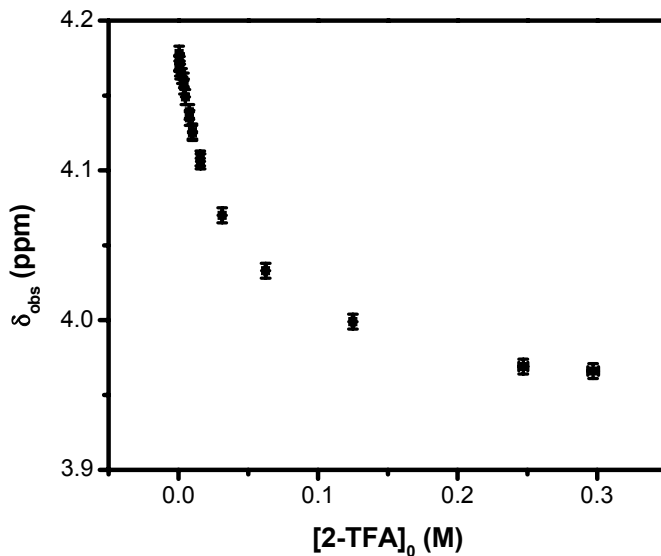


Table A1. Concentration dependence of H₁ of 2-TFA in CDCl₃:CD₃CN (3:2) at 295 K.

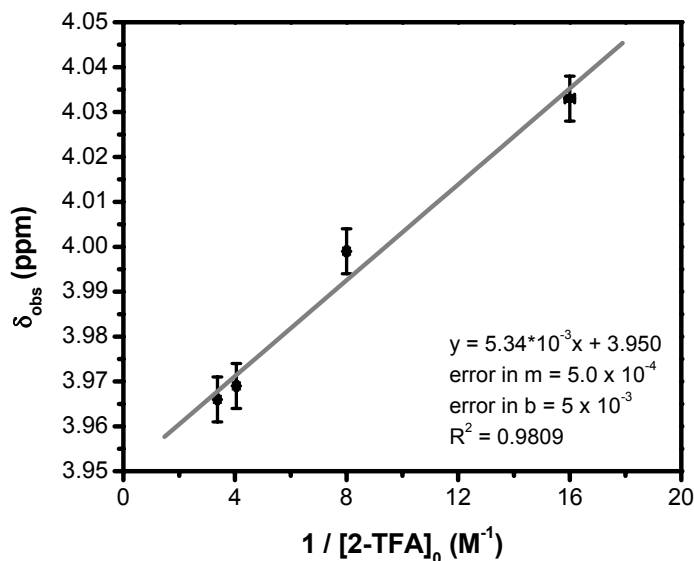
[2-TFA] (M)	δ (H1, ppm)	[2-TFA] (M)	δ (H1, ppm)
saturated	3.950	2.50E-03	4.163
2.97E-01	3.966	1.25E-03	4.166
2.47E-01	3.969	1.00E-03	4.168
1.25E-01	3.999	9.08E-04	4.171
6.25E-02	4.033	6.25E-04	4.171
3.13E-02	4.070	6.07E-04	4.172
1.58E-02	4.106	5.00E-04	4.178
1.56E-02	4.108	4.55E-04	4.171
1.00E-02	4.126	4.00E-04	4.160
1.00E-02	4.125	1.82E-04	4.152
7.91E-03	4.135	1.82E-04	4.153
7.81E-03	4.139	1.00E-04	4.125
5.00E-03	4.149	7.28E-05	4.119
3.96E-03	4.156	3.91E-05	lim. of detec.

Figure A2. Chemical shift of H₁ of **2**-TFA versus concentration ($297 \text{ mM} \geq [\mathbf{2}\text{-TFA}] \geq 0.500 \text{ mM}$) in CDCl₃:CD₃CN (3:2) at 295 K.



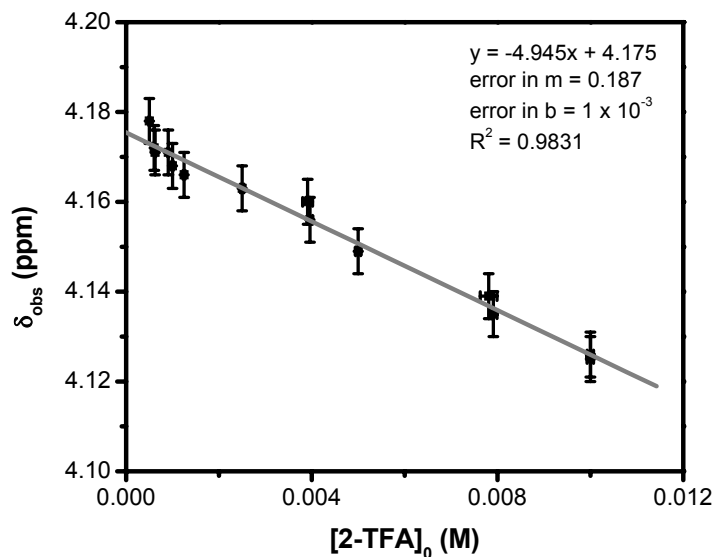
In this initial treatment, we assumed no other interaction between salts such as aggregation, triple ion formation, etc., at high concentrations (i.e., $[\mathbf{2}\text{-TFA}] \geq 100 \cdot K_{\text{ipd}}$, which yields a ratio of [ion pair] to [dissociated pair] of ~ 10). [8] Under the limit of high concentration, one expects the salt to be predominately ion paired. Thus, the chemical shift of the saturated solution described above (roughly 350 mM in **2**-TFA) is expected to approximate the chemical shift of the fully ion paired salt. To check this result, we plotted δ_{H1} versus reciprocal concentration for $[\mathbf{2}\text{-TFA}] > 60 \text{ mM}$ (Figure A3); extrapolating to infinite concentration (i.e., fully ion paired salt) yielded $\delta_{\text{paired}} = 3.950$ (± 0.005) ppm, which is reassuringly identical to that of the saturated solution.

Figure A3. Chemical shift of H₁ versus [2-TFA]₀⁻¹ ([2-TFA] > 60 mM) in CDCl₃:CD₃CN (3:2) at 295 K.



At the other extreme, under dilute conditions (i.e., [2-TFA] < 0.1 * K_{ipd} M, which yields a ratio of [dissociated pair] to [ion pair] of ~11), one expects the salt to be predominately dissociated. Focusing only on 10.0 ≥ [2-TFA] > 0.5 mM from Table A1 (thereby excluding the low concentration data points which display chemical shift reversals), we estimated the chemical shift of the fully dissociated salt by plotting the benzylic chemical shift of 2-TFA versus concentration under dilute conditions and extrapolating to infinite dilution; Figure A4 yielded a fully dissociated shift, $\delta_{\text{dissociated}}$, of 4.175 (±0.001) ppm.

Figure A4. Chemical shift of H₁ versus [2-TFA]₀ ($10.0 \geq [2-TFA] \geq 0.5$ mM) in CDCl₃:CD₃CN (3:2) at 295 K.

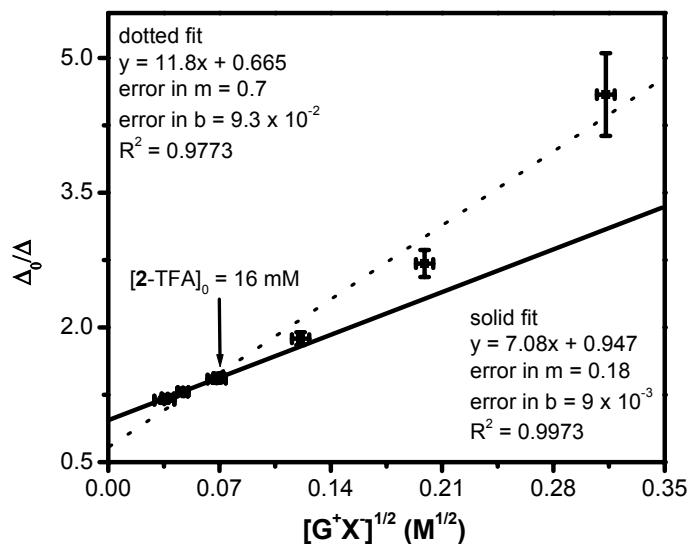


With δ_{paired} (3.950 ppm) and $\delta_{\text{dissociated}}$ in hand (4.175 ppm), we then estimated percent ionization according to Eq. A4a for $300 \geq [G^+X^-]_0 \geq 0.6$ mM, enabling the construction of Table A2. Recalling the work of Weber and Deranleau from Chapter II, [9] Figure A5 was constructed by omitting all data points outside of the 15 to 85 percent ionization range. As is evident from the dotted fit of figure A5, the plot was found to deviate from linearity at moderate $[G^+X^-]$. The deviation from linearity may signal triple ion formation. [10]

Table A2. Experimental concentrations calculated for 2-TFA in CDCl₃:CD₃CN (3:2) at 295 K, assuming $\Delta_0 = 0.225$ ppm.

[2-TFA] ₀ (M)	δ (H ₁ , ppm)	Δ ($\delta_{\text{obs}} - \delta_{\text{paired}}$)	Δ/Δ_0 (% ionized)	Δ_0/Δ	[2 ⁺] (M)	[2 ⁺ TFA] ⁻ (M)	[2 ⁺ TFA] ⁻ ^{1/2} (M ^{1/2})
0.297	3.966	1.60x10 ⁻²	7.11x10 ⁻²	14.1	2.11x10 ⁻²	0.276	0.525
0.247	3.969	1.90x10 ⁻²	8.44x10 ⁻²	11.8	2.09x10 ⁻²	0.226	0.476
0.125	3.999	4.90x10⁻²	0.218	4.59	2.72x10⁻²	9.78x10⁻²	0.313
6.25x10⁻²	4.033	8.30x10⁻²	0.369	2.71	2.31x10⁻²	3.94x10⁻²	0.199
3.13x10⁻²	4.070	0.120	0.533	1.88	1.67x10⁻²	1.46x10⁻²	0.121
1.58x10⁻²	4.106	0.156	0.693	1.44	1.10x10⁻²	4.85x10⁻³	6.96x10⁻²
1.56x10⁻²	4.108	0.158	0.702	1.42	1.10x10⁻²	4.65x10⁻³	6.82x10⁻²
1.00x10⁻²	4.126	0.176	0.782	1.28	7.82x10⁻³	2.18x10⁻³	4.67x10⁻²
1.00x10⁻²	4.125	0.175	0.778	1.29	7.78x10⁻³	2.22x10⁻³	4.71x10⁻²
7.91x10⁻³	4.135	0.185	0.822	1.22	6.50x10⁻³	1.41x10⁻³	3.75x10⁻²
7.81x10⁻³	4.139	0.189	0.840	1.19	6.56x10⁻³	1.25x10⁻³	3.53x10⁻²
5.00x10 ⁻³	4.149	0.199	0.884	1.13	4.42x10 ⁻³	5.78x10 ⁻⁴	2.40x10 ⁻²
3.96x10 ⁻³	4.156	0.206	0.916	1.09	3.63x10 ⁻³	3.34x10 ⁻⁴	1.83x10 ⁻²
3.91x10 ⁻³	4.160	0.210	0.933	1.07	3.65x10 ⁻³	2.61x10 ⁻⁴	1.61x10 ⁻²
2.50x10 ⁻³	4.163	0.213	0.947	1.06	2.37x10 ⁻³	1.33x10 ⁻⁴	1.15x10 ⁻²
1.25x10 ⁻³	4.166	0.216	0.960	1.04	1.20x10 ⁻³	5.00x10 ⁻⁵	7.07x10 ⁻³
1.00x10 ⁻³	4.168	0.218	0.969	1.03	9.69x10 ⁻⁴	3.11x10 ⁻⁵	5.58x10 ⁻³
9.08x10 ⁻⁴	4.171	0.221	0.982	1.02	8.92x10 ⁻⁴	1.61x10 ⁻⁵	4.02x10 ⁻³
6.25x10 ⁻⁴	4.171	0.221	0.982	1.02	6.14x10 ⁻⁴	1.11x10 ⁻⁵	3.33x10 ⁻³
6.07x10 ⁻⁴	4.172	0.222	0.987	1.01	5.99x10 ⁻⁴	8.09x10 ⁻⁶	2.84x10 ⁻³

Figure A5. Limiting plot of Eq. A4d for a) all data points between 15 and 85 percent ionization (dotted fit) and b) $16 \text{ mM} > [\mathbf{2-TFA}]_0 > 5 \text{ mM}$ (solid fit) in $\text{CDCl}_3:\text{CD}_3\text{CN}$ (3:2) at 295 K.



Hence, we refit the data from Figure A5 to include only those points which do not deviate from linearity, i.e., $16 \text{ mM} > [\mathbf{2-TFA}] > 5 \text{ mM}$, assuming that all observed changes in the chemical shift result solely from ion pair dissociation. [11] The resulting treatment (Figure A5, solid fit) yielded a limiting K_{ipd} of $(2.0 \pm 0.1) \times 10^{-2} \text{ M}$. This value represents a significant difference from those calculated in Chapter II according to the pseudorotaxane model, in which K_{ipd} was found to range from 1.9 to $8.3 \times 10^{-4} \text{ M}$. In light of the omission of activity coefficients, the gross overestimation of K_{ipd} from Figure A5 is not unexpected (Eq. A4d).

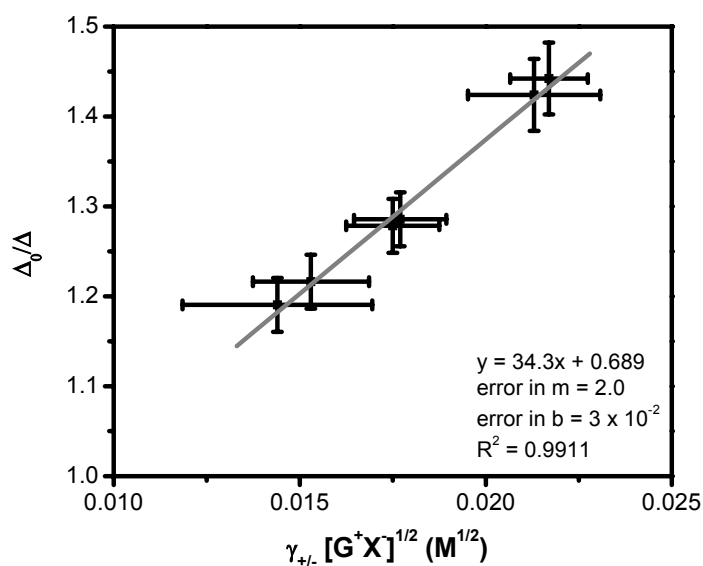
To correct for this omission, we estimated γ_{\pm} according to Eq. 3 [12] from the experimental data of Table A2 under the assumption $\epsilon_{\text{mixture}} \approx (3/5)\epsilon_{\text{CDCl}_3} + (2/5)\epsilon_{\text{CD}_3\text{CN}} = 17.5$ (Table A3). Figure A6 was thus constructed, yielding a K_{ipd} of $(8.5 \pm 1.1) \times 10^{-4} \text{ M}$, which is reassuringly in line with that calculated in Chapter 2. However, the y-intercept of Figure A6 does not result in unity within experimental error, as expected according to Eq. A4d. This may be the result of assuming $\epsilon_{\text{mixture}}$ to be the weighted average of the mixture components CDCl_3 and CD_3CN ; if the cosolvents display intermolecular interactions, $\epsilon_{\text{mixture}}$ will not obey the additive function. [13] Future work should

investigate conductance of the **2**-X salts under identical conditions for validation. Similarly, the systems should also be followed by vapor phase osmometry.

Table A3. γ_{\pm} for 16 mM > [2-TFA] > 5 mM calculated according to Eq. 3 [13] from experimental concentrations of 2^{+} in $\text{CDCl}_3:\text{CD}_3\text{CN}$ (3:2) at 295 K, assuming $\epsilon_{\text{mixture}} \approx 17.5$.

[2-TFA] ₀ (M)	Δ/Δ_0 (% ionized)	Δ_0/Δ	[2 ⁺] (M)	[2 ⁺ TFA ⁻] (M)	γ_{\pm} ($\epsilon_{\text{mixture}} \approx 17.5$)	$\gamma_{\pm} [2^{+}\text{TFA}^{-}]^{1/2}$ (M ^{1/2})
1.58x10 ⁻²	0.693	1.44	1.10x10 ⁻²	4.85x10 ⁻³	0.31	2.17x10 ⁻²
1.56x10 ⁻²	0.702	1.42	1.10x10 ⁻²	4.65x10 ⁻³	0.31	2.13x10 ⁻²
1.00x10 ⁻²	0.782	1.28	7.82x10 ⁻³	2.18x10 ⁻³	0.37	1.75x10 ⁻²
1.00x10 ⁻²	0.778	1.29	7.78x10 ⁻³	2.22x10 ⁻³	0.38	1.77x10 ⁻²
7.91x10 ⁻³	0.822	1.22	6.50x10 ⁻³	1.41x10 ⁻³	0.41	1.53x10 ⁻²
7.81x10 ⁻³	0.840	1.19	6.56x10 ⁻³	1.25x10 ⁻³	0.41	1.44x10 ⁻²

Figure A6. Plot of Eq. A4d for 16 mM > [2-TFA]₀ ≥ 5 mM) in $\text{CDCl}_3:\text{CD}_3\text{CN}$ (3:2) at 295 K, assuming $\epsilon_{\text{mixture}} \approx 17.5$.



A.6 *References*

- [1] Benesi, H.; Hildebrand, J. H. *J. Am. Chem. Soc.* **1949**, *71*, 2703-2707.
- [2] Scatchard, G. *Ann. N.Y. Acad. Sci.* **1949**, *51*, 660-672.
- [3] Cresswell, C. J.; Allred, M. L. *J. Phys. Chem.* **1962**, *66*, 1469-1472.
- [4] Rose, N. J.; Drago, R. S. *J. Am. Chem. Soc.* **1959**, *81*, 798-799.
- [5] a) Haque, R.; Coshov, W. R.; Johnson, L. F. *J. Am. Chem. Soc.* **1969**, *91*, 3822-3827. b) Neuman, R. C., Jr.; Jonas, V. *J. Phys. Chem.* **1971**, *75*, 3550-3554. c) Lim, Y. -Y.; Drago, R. S. *J. Am. Chem. Soc.* **1972**, *94*, 84-90. d) Haake, P.; Prigodich, R. V. *Inorg. Chem.* **1984**, *23*, 457-462.
- [6] Tsukube, H.; Furuta, H.; Odani, A.; Takeda, Y.; Kudo, Y.; Inoue, Y.; Liu, Y.; Sakamoto, H.; Kimura, K. *Comprehensive Supramolecular Chemistry*; Davies, J. E. D.; Ripmeester, J. A.; Eds. Pergamon: Oxford, UK, 1997, Vol. 8, 425.
- [7] Gong, C.; Balanda, P. B.; Gibson, H. W. *Macromolecules* **1998**, *31*, 5278-5289.
- [8] Calculated according to the following, allowing $[G]_0=0.01$ M and $K_{ipd}=10^{-4}$ M:

$$K_{ipd} = \frac{[G^+][X^-]}{[G^+X^-]} = \frac{x^2}{[G]_0 - x}$$

and from the quadratic formula:

$$x = [G^+] = [X^-] = \frac{-K_{ipd} + \sqrt{K_{ipd}^2 + 4K_{ipd}[G]_0}}{2}$$

- [9] a) Weber, G. *Molecular Biophysics*. Pullman, B.; Weissbluth, M., Eds. Academic Press: New York, NY, 1965, 369-367. b) Deranleau, D. A. *J. Am. Chem. Soc.* **1969**, *91*, 4044-4049.
- [10] Fuoss, R. M.; Kraus, C. A. *J. Am. Chem. Soc.* **1933**, *55*, 2387-2399.
- [11] This same conclusion was reached by Dye et al., who correlated ion pairing of Cs^+X^- to chemical shift changes in ^{133}Cs NMR spectra. [Khazaeli, S.; Popov, A. I.; Dye, J. L. *J. Phys. Chem.* **1982**, *86*, 4238-4244] In their studies, Dye et al. performed a fit of chemical shift versus $[G^+X^-]$ directly (i.e., Figure A2) to derive K_{ipd}^{-1} and noted that their treatment required a sharp change in chemical shift at low concentrations followed by a flat portion at high concentrations. Although this description is similar to what we observed in Figure A2, the systems

investigated by Dye et al. did not indicate leveling off of δ at high concentration. From this, they concluded that description of their system by a simple model which considers ion pairing only and not higher ordered species such as triple ions was incomplete. Nonetheless, it was emphasized that *most* of the changes in chemical shift with concentration resulted from ion pairing alone, and that influence by triple ions was negligible.

[12] From Eq. 3:
$$\log \gamma_{\pm av} = -1.823 \times 10^6 \frac{z_i^2}{(\epsilon T)^{\frac{3}{2}}} \sqrt{\mu}$$

[13] Jouyban, A.; Soltanpour, S.; Chan, H. -K *Int. J. Pharm.* **2004**, *269*, 252-360.